

Summer 2005

The Role of Geomorphic Features and Hydrologic Processes on Sediment Clusters in Gravel-Bed Rivers, Washington: A Field-Based Approach

Ross Richard Hendrick
Central Washington University

Follow this and additional works at: <https://digitalcommons.cwu.edu/etd>



Part of the [Geomorphology Commons](#), [Hydrology Commons](#), and the [Sedimentology Commons](#)

Recommended Citation

Hendrick, Ross Richard, "The Role of Geomorphic Features and Hydrologic Processes on Sediment Clusters in Gravel-Bed Rivers, Washington: A Field-Based Approach" (2005). *All Master's Theses*. 1471.
<https://digitalcommons.cwu.edu/etd/1471>

This Thesis is brought to you for free and open access by the Master's Theses at ScholarWorks@CWU. It has been accepted for inclusion in All Master's Theses by an authorized administrator of ScholarWorks@CWU. For more information, please contact scholarworks@cwu.edu.

THE ROLE OF GEOMORPHIC FEATURES AND HYDROLOGIC
PROCESSES ON SEDIMENT CLUSTERS IN GRAVEL-BED
RIVERS, WASHINGTON: A FIELD-BASED
APPROACH

A Thesis
Presented to
The Graduate Faculty
Central Washington University

In Partial Fulfillment
of the Requirements for the Degree
Master of Science
Geology

by
Ross Richard Hendrick
August 2005

ABSTRACT

THE ROLE OF GEOMORPHIC FEATURES AND HYDROLOGIC PROCESSES ON SEDIMENT CLUSTERS IN GRAVEL-BED RIVERS, WASHINGTON: A FIELD-BASED APPROACH

by

Ross Richard Hendrick

August 2005

This project investigated the movement and evolution of sediment clusters after four separate flood events at two geomorphically different sites along the Entiat River, Washington. Clusters are defined as an obstacle or anchor clast(s) that impede the progress of two or more sediment particles, and are believed to be an important characteristic of the variable bed topography of gravel-bed rivers. Detailed field descriptions and digital photographs of clusters were used to determine the characteristics of clusters at chosen locations on gravel bars regularly covered by high flow events. Data were collected during low-flow conditions, and clusters were re-examined and re-photographed after each flow event. Clusters were examined to determine whether they changed form, remained stable or were completely destroyed. Individual particles within clusters were also tracked, and the velocity and critical shear stress required to entrain particles were calculated to determine the possible effects of

clusters on the entrainment of sediment. An improved understanding of how clusters develop, evolve and affect the entrainment of sediment under various hydrologic processes will aid in assessment of sediment transport processes, bed stability, and in-stream habitat conditions.

ACKNOWLEDGMENTS

I would like to thank those who helped make this a rewarding, fulfilling, and complete project. First to my wife, Molly, who supported me throughout this entire process, stood by me when others said I was crazy, and was always there to pull me out of the office for a “quick” trip to store. Her understanding, patience, and perseverance over this last two years have been amazing. To my kids, Kyle and Travis, who will never know how important and supportive they have been, as they helped me remember what is truly important and have been and always will be my inspiration. Special thanks to my parents for their words of encouragement, prayers, guidance, and for always believing in me; also to my brothers, Brett and Brian, for helping in the field and at home with my kids. I am also indebted to my in-laws, for their support and for housing my family while I was out chasing rivers or working long hours in the office. Thanks also to my extended family, grandparents, aunts and uncles, and friends for their support and for helping with the kids while Molly and I were in the field.

I want to acknowledge those who have been instrumental in my professional development these last few years. First to my committee chair, Lisa Ely, for her continued support and knowledge during my development as a scientist, for helping me gain an appreciation of the field of fluvial geomorphology, and for always having an “open-door-policy.” Thanks also to Jeffery Lee, Morris Uebelacker, and Anthony Gabriel for serving as committee members during this project. I am grateful to John Monahan, who will always be my “Jedi-Master,” for providing me with invaluable

experience, guidance, and friendship during my internship at the Washington State Department of Ecology, and for encouraging me to pursue a master's degree. Thanks to Sarah Walker and Kurt Hosman of the Chelan County Conservation District, for offering words of encouragement, advice, and for providing me with background data and maps of the Entiat River.

I am indebted to all those who volunteered their time to help collect field data: Janielle Marcell helped collect field data and provided valuable analysis and results from the American River, which will be compared with results from this study. Deron Carter and Stephen Slaughter collected early survey data and helped install hydrologic recording equipment along the American River. My brother Brett, Tarin Kendrick, Kurt Hosman, and Cooper Brossey also volunteered their time and effort in the field. Thanks also to fellow graduate students for their support, friendship, and laughter. They made long office days and class time enjoyable and memorable. Thanks also to Craig Scriver for his technical support during the formatting and printing of this document.

A very special acknowledgment and thanks to Phil, Kim, and "Mac-the-Dog" Archibald, for without their support this project would not have been possible in the Entiat River. Phil, a fishery biologist with the U.S. Forest Service, Entiat Ranger District, and resident along the Entiat River within my study area, provided biologic, hydrologic, and location expertise that was invaluable in helping choose and access study sites, knowing what the weather and river were doing before making a two-hr drive over there, and knowing where to find clusters! Thanks also to Phil for his

friendly review of this document. The Archibalds always made me feel welcome and are true stewards of the Entiat River, and I will always appreciate the professional and personal relationship that I gained with them.

Thanks also to Dr. Athanasios Papanicolaou and Kyle Strom from the Institute of Hydraulic Research-Hydroscience and Engineering, University of Iowa, for their collaboration on this project, and their infinite knowledge and understanding of hydrologic and sediment transport processes, laboratory flume experiments, and critical shear stress equations. Thanks to Kyle and Jodi Strom for providing food and housing while I visited this superb research institute.

This work was made possible by the Chelan Douglass Land Trust, Bob and Casey Bockoven, and the Archibalds for allowing me accessibility to my study area in this beautiful section of the Entiat River. This project was funded by the U.S. Geological Survey, Water Resources Grant no. 2002WA12G awarded to Dr. Lisa Ely and Dr. Athanasios Papanicolaou, the Geological Society of America, Sigma Xi, Central Washington University Puget Sound Energy Graduate Fellowship, and the Central Washington University Office of Graduate Studies.

TABLE OF CONTENTS

Chapter	Page
I. INTRODUCTION.....	1
Purpose	1
Cluster Definition	4
Project Significance.....	7
Geographic Settings.....	8
II. GEOMORPHIC SETTINGS.....	14
Methods	14
Results and Discussion	18
Summary.....	24
III. CLUSTER EVOLUTION	26
Methods	28
Results and Discussion	42
Summary.....	76
IV. CLUSTER CHARACTERISTICS.....	80
Methods	80
Results and Discussion	81
Summary.....	90
V. SUMMARY AND CONCLUSIONS.....	92
Future Work.....	96
REFERENCES CITED	98
APPENDIXES.....	103
Appendix A–Entrained Isolated and Clustered Particle Data	103
Appendix B–Cluster Characteristic Data	105
Appendix C–Compilation of Previous Cluster Characteristic Data	116

LIST OF TABLES

Table	Page
1. Entiat River Flow Characteristics.....	12
2. Geomorphic Features of Cluster Bars vs. Non-Cluster Bars.....	19
3. Hydrologic Model Outputs.....	45
4. Median Diameter of Particle Sizes Entrained by a Given Flow Event	59
5. Dimensionless Critical Shear Stress for Particle Entrainment	65
6. Critical Shear Stress Values Reported by Reid et al. (1992).....	71
7. Critical Shear Stress Values Based on Minimum and Maximum Flow Depths.....	75
8. Cluster Strength Classification Criteria.....	81
9. Cluster Density	84
10. Mean Cluster Characteristics for Entiat River.....	84
11. Cluster Strength Classifications	86
A1. Five Largest Entrained Isolated and Clustered Particle Sizes at Site 1, Plot 1	103
A2. Five Largest Entrained Isolated and Clustered Particle Sizes at Site 1, Plot 2	103
A3. Five Largest Entrained Isolated and Clustered Particle Sizes at Site 1, Plot 3	104
A4. Five Largest Entrained Isolated and Clustered Particle Sizes at Site 2, Plot 1	104
B1. Cluster Characteristics at Site 1, Entiat River	105
B2. Cluster Characteristics at Site 2, Entiat River	110
C1. Previous Field-Based Studies Featuring Cluster Characteristics	116

LIST OF FIGURES

Figure	Page
1. Sketch of typical sediment cluster	2
2. Photograph of typical upstream triangle cluster found along Entiat River	6
3. Typical cluster geometries found along Entiat River	6
4. Location of Entiat River watershed within Washington State	9
5. Longitudinal profile of lower 55 Rkm (34 RM) of Entiat River as measured from confluence with Columbia River.....	11
6. Mean monthly discharge of Entiat River within study area	13
7. Longitudinal profile of study reach and locations of cluster bars and non-cluster bars	18
8. Digitized U.S. Geological Survey (USGS) quadrangle showing geomorphic settings of cluster bars and non-cluster bars within study reach.....	20
9. Geomorphic constriction between sites 1 and 2	22
10. Sediment-size distribution at sites 1 (A) and 2 (B)	23
11. Photograph of sediment at sites 1 (A) and 2 (B)	23
12. Spawning salmon adjacent to cluster bar along Entiat River	25
13. Spatial positions of cross sections at sites 1 (A) and 2 (B)	39
14. Channel geometry at site 1	40
15. Channel geometry at site 2	41
16. Daily maximum discharge values during period of study.....	43
17. Cluster evolution for site 1 (all plots).....	47
18. Cluster evolution for site 2 (all plots).....	48

LIST OF FIGURES (continued)

Figure	Page
19. Spatial distribution of cluster morphologies at site 1	50
20. Cross-sectional profile data from plots 1 and 2 at site 1	50
21. Cross-sectional profile data from plot 3 at site 1	51
22. Spatial distribution of cluster morphologies at site 2	51
23. Cross-sectional profile data from plot 1 at site 2.....	52
24. Cluster evolution as observed in laboratory flume experiments	56
25. Median diameter of largest isolated and clustered particles entrained by each flow event at site 1	60
26. Median diameter of largest isolated and clustered particles entrained by each flow event at sites 1 and 2	61
27. Critical shear stress values for largest isolated and clustered particles entrained by each flow event.....	66
28. Critical shear stress values for largest isolated and clustered particles entrained by each flow event.....	67
29. Annual peak flow values between sites 1 and 2 since 1958.....	77
30. Number of each cluster type within detailed cluster plots at sites 1 (A) and 2 (B).....	82
31. Spatial distribution of cluster morphologies for all plots at sites 1 (A) and 2 (B)	83
32. Average size of each cluster type within detailed cluster plots at sites 1 (A) and 2 (B)	85
33. Number of each cluster type within each detailed plot at sites 1 (A) and 2 (B)	87

CHAPTER I

INTRODUCTION

Purpose

The purpose of this study was to quantify the effects of sediment clusters on the entrainment and transport of sediment particles along the Entiat River, a gravel-bed river located in central Washington State, and to examine the geomorphic conditions affecting sediment cluster formation and evolution. The range of flows that maintain and destroy sediment clusters were determined, and an extensive database of sediment cluster characteristics was developed as part of this project. Finally, the results of this study were compared with laboratory flume experiments conducted by colleagues at the University of Iowa.

Channel-bed topography in gravel-bed rivers can consist of large-scale bedform features ranging from pools and riffles, step-pool systems, and antidunes (Maxwell and Papanicolaou, 2001) to small-scale features known as cluster microforms, or sediment clusters (Brayshaw, 1984; Billi, 1988; Church et al., 1998; Strom et al., 2004b). Sediment clusters are groups of two or more sediment particles that are impeded by a third, often larger, obstacle clast on the surface of a gravel-bed river (Figure 1). The effects of sediment clusters (clusters) on sediment transport and bed stability have been widely studied in controlled laboratory flume experiments (Hassan and Reid, 1990; Papanicolaou et al., 2003; Strom et al., 2004b). Other studies have attempted to determine the effects of clusters on aquatic habitat (Biggs et al. 1997; Boelman and Stein, 1997). However, as Strom et al. (2004a) has noted, there is a lack of extensive

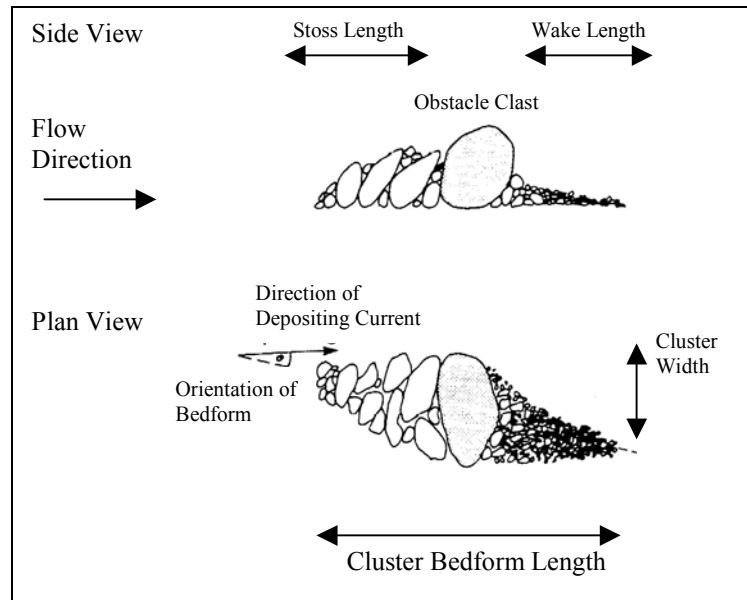


Figure 1. Sketch of typical sediment cluster. Adapted from Brayshaw (1984).

field-based data that provide detailed, field-based, characterizations of clusters. Limited field-based cluster data is given by Teisseyre (1977) and Brayshaw (1984), while studies by Billi (1988), de Jong (1991) and Wittenberg (2002) have also provided valuable field-based cluster characteristic data; however, these studies did not cumulatively address different cluster morphologies, sizes, densities, and geomorphic settings of cluster formation. Detailed field data on clusters, such as cluster size, morphology, and density are needed to support laboratory studies that simulate cluster formation and investigate the effect of clusters on hydrologic and sediment transport parameters. Most field-based cluster studies describe only broad location and site descriptions, but do not describe reference specific geomorphic features, such as those that affect sediment supply (and thus cluster size), large-scale bedforms (e.g., pools and

riffles), and channel slope under which the clusters form or do not form (Brayshaw, 1984; De Jong, 1991; Reid et al., 1992; Church et al., 1998).

This study consisted of three major components. The first characterized where clusters form within a reference specific reach of the Entiat River, the geomorphic features surrounding their formation, such as large-scale bedforms, sediment supply, sediment-size distribution, and channel slope and how these features might influence cluster formation, characteristics (e.g., size, morphology, and density), and stabilization.

The second component of this study determined how clusters evolved during four separate flow events of various intensities and durations, and quantified the range of discharges, velocities, and shear stresses required to maintain and destroy clusters in the Entiat River. This component also tested the hypothesis that clusters delay the entrainment and transport of sediment by requiring higher shear stress values to entrain sediment in clusters than isolated sediment particles. This hypothesis was tested by documenting the movement of clustered and isolated sediment particles and calculating the critical shear stress required to move them. Results from this component were compared to those of Strom (2002) and Papanicolaou et al. (2003), colleagues from the Iowa Institute of Hydraulic Research (IIHR)-Hydroscience and Engineering, a research center at the University of Iowa and one of the nation's premier and oldest fluids research and engineering laboratories. Recent laboratory flume experiments conducted by Strom (2002) and Papanicolaou et al. (2003) characterized cluster formation, evolution, and associated critical shear stress values based on varying factors such as the specific gravity of sediment and sediment availability (Papanicolaou and Schuyler,

2003; Papanicolaou et al., 2003; Strom et al., 2004b). Strom et al. (2004b) also determined the range of shear stress values for cluster formation and destruction and showed that clusters delay sediment transport and thus contribute to the pulsating nature of bed-load transport.

The third and final component of this study described in detailed the cluster characteristics at two geomorphically different sites, adding to the limited data on cluster characteristics.

Cluster Definition

Brayshaw (1984) defined clusters as a group of particles typically formed around a larger obstacle clast (also referred to as an anchor clast) on the surface of a gravel-bed river (Figure 1). Clusters are believed to form during the recession of a high flow event capable of transporting and depositing particles large enough to form an anchor clast that begins to impede smaller particles during waning stages of the flow event and/or during subsequent flow events (Dal Cin, 1968; Brayshaw, 1984; De Jong, 1991; Reid et al., 1992; Church et al., 1998). Clusters are typically formed as individual discrete structures, often protruding above the gravel bed surface (Brayshaw, 1984; Reid et al., 1992); however, other studies have shown that clusters form as interconnected structures in a reticulate pattern (Church et al., 1998; Hassan and Church, 2000). Experimental flume studies have typically characterized clusters as consisting of two or more particles (Papanicolaou and Schuyler, 2003; Strom et al., 2004b). However, using this definition would prove very difficult in the field because most sediment particles on the bed are interlocked with at least one other particle, and

would thus require nearly all of the particles to be defined as clustered. Therefore, for the purpose of this study clusters were defined as an anchor clast(s) that impedes the progress of *two* or more sediment particles. In addition, due to the irregular microscale topography of the gravel bars examined for this study, clusters were also defined as those protruding above the normal gravel bed surface (greater than 2-3 cm) of the immediate surrounding area (within an approximately 50-cm radius of the cluster) to be defined as a cluster (Figure 2). For the purpose of this project, microscale clusters were not considered and only those clusters with anchor clasts larger than 5 cm were defined as clusters.

Clusters can form in various sizes and morphologies (Figure 3). The naming scheme for the different cluster geometries varies by study (Brayshaw, 1984; Wittenberg, 2002; Papanicolaou and Schuyler, 2003; Strom et al., 2004a; Strom et al., 2004b), but in general refers to a similar set of cluster forms. The naming scheme used in this study is as follows:

- Upstream triangle: one or more anchor clasts that trap particles on the stoss, or upstream, side of the anchor, with minimal particles (usually sand sized) in the wake, or downstream, side of the anchor.
- Downstream triangle: one or more anchor clasts that trap particles on the wake side of the anchor, with minimal particles on the stoss side.
- Diamond: one or more anchor clasts that trap particles on both the stoss and wake sides of the anchor clast(s).

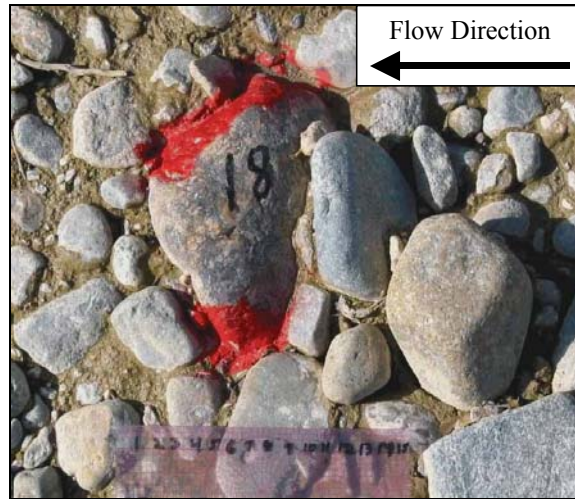


Figure 2. Photograph of typical upstream triangle cluster found along Entiat River. Note that the numbered particle is the anchor clast that trapped the smaller particles in the stoss. Scale bar is 15 cm.

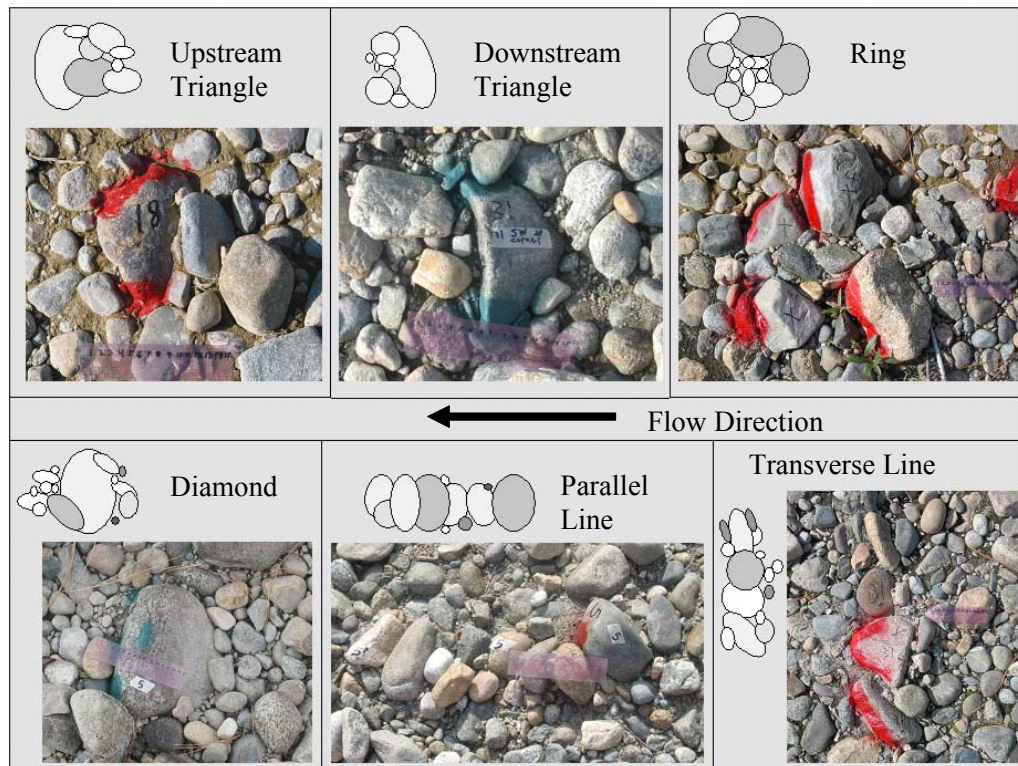


Figure 3. Typical cluster geometries found along Entiat River. Channel position is at the top of the sketch or photograph with flow direction from right to left.

- Ring: rounded formation of anchor clasts that trap particles in the center; typically does not have a wake or stoss.
- Parallel line: particles (typically of similar size) that form in a line parallel to flow direction.
- Transverse line: particles (typically of similar size) that form in a line perpendicular to flow direction.

Project Significance

Results from this project will improve our overall understanding of sediment transport processes, considered by Phil Archibald, a biologist for the U.S. Forest Service, Entiat Ranger district, to be an important component of instream water quality and habitat (Archibald, personal communication, October 18, 2004). In addition, results from this project documented some of the geomorphic settings that favor cluster formation, and how geomorphic settings and hydrologic processes affect the size, shape, and density of clusters.

Given the importance of clusters on the physical, and possibly biological, components of gravel-bed rivers (Brayshaw, 1985; Biggs et al., 1997; Church et al., 1998), and the recent efforts to determine adequate channel maintenance flows in regulated rivers (Andrews and Nankervis, 1995; Kondolf, 1995), results from this study could have practical applications for managers of regulated rivers. These applications include aiding river managers in determining where and how clusters form, and what peak discharges and average bed shear stresses are needed to maintain them. Furthermore, due to an increased interest by Pacific Northwest conservation groups to

utilize hydraulic structures to increase aquatic habitat diversity, results from this study will provide information on the hydraulic parameters necessary to maintain clusters, which can then be factored into the design of such structures. Such data will allow assessment of the benefits and feasibility of placing/preserving structures similar to clusters in areas lacking quality aquatic habitat. Finally, the reach of the Entiat River chosen for study is located within an unregulated and mostly undisturbed portion of the Entiat River, which will remain so as part of the recently purchased Chelan-Douglas Land Trust Stormy Preserve property. This reach of the river supports abundant aquatic and terrestrial wildlife, and is considered prime salmon spawning biologic habitat (Archibald, personal communication, October 18, 2004). Therefore, results from this pristine portion of the river, with abundant aquatic habitat, could be applied to river restoration projects that aim to improve aquatic habitat by enhancing our overall understanding of how a natural and healthy river functions.

Geographic Settings

Location

The Entiat River Watershed is located in Chelan County in north-central Washington State (Figure 4). The Entiat River flows southeasterly approximately 69 km from an elevation of approximately 2819 m in the Cascade Mountains to an elevation of approximately 217 m at its confluence with the Columbia River near the town of Entiat. The watershed drains an area of approximately 1232 km² and varies from 8 to 24 km in width. The North Fork Entiat River and the Mad River are the two main tributaries joining the Entiat River at river-kilometers (Rkm) 53 and 16 (river-miles [RM] 33 and

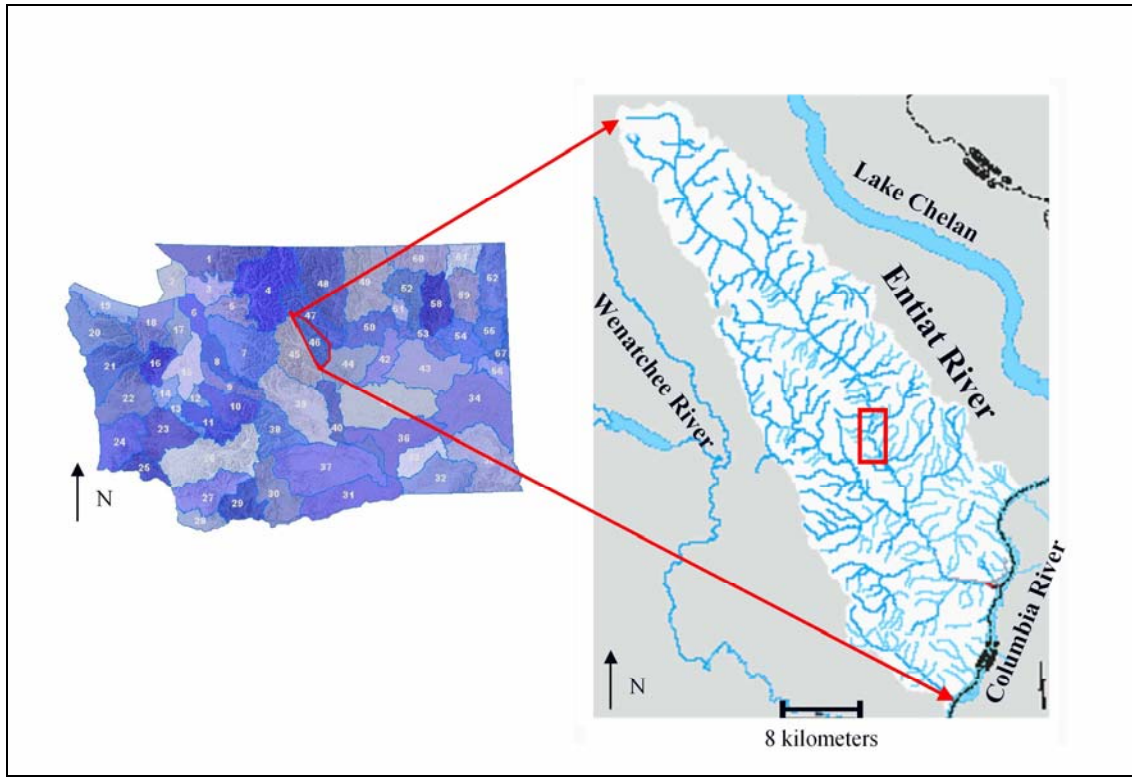


Figure 4. Location of Entiat River watershed within Washington State. Red box shows location of study area. Maps adapted from Washington State Department of Ecology (2005).

10), respectively, measured from the confluence with the Columbia River. Numerous small tributaries and springs also join the Entiat River along its length. The study area of this project was located near the middle of the watershed between Rkm 27 and Rkm 30 (RM 17-19) (Figure 4). Two main sites, chosen based on criteria explained in chapter II, are located within the study area near Rkm 29 (RM 18). These two sites are less than 0.5 km apart and are separated by a real-time streamflow gaging station operated by the U.S. Geological Survey (USGS, 2005).

Topography

The upper Entiat River Watershed is highly glaciated with a steeply side-sloped “U-shaped” valley from the headwaters down to the terminal moraine near Rkm 26 (RM 16). The middle watershed is heavily influenced by this terminal glacial moraine, and is distinguished by a relatively wide valley bottom of low slope, while the lower watershed is characterized by steep topography and narrowly cut canyons until the lowermost section of the watershed, which has rolling hills and a gentle slope (Chelan County Conservation District [CCCD], 2004). Figure 5 shows the longitudinal profile of the lower 55 Rkm (34 RM) of the Entiat River that illustrates the changes in slope throughout this section of the river. An obvious break in slope along the river’s longitudinal profile at Rkm 42 (RM 26) marks the beginning of a depositional zone of sediments within the Entiat River (CCCD, 2004).

Geology

The geology of the Entiat River watershed is characterized by intrusive granodiorite, quartz diorite, and metamorphic schist and gneiss (CCCD, 2004). The rugged peaks of quartz diorite and granodiorite dominate the Chelan and Entiat Mountain ranges; metamorphic rocks and a few rhyolite dikes are also exposed within the watershed (CCCD, 2004). Geologic formations include the Swakane Gneiss, Chiwaukum Schist, and Mt. Stuart Granodiorite, with the Swakane Gneiss being the oldest formation (CCCD, 2004). The Swakane Formation consists of medium-grained gneiss, coarse amphibolite schist, and some pegmatite and mylonite stringers (CCCD,

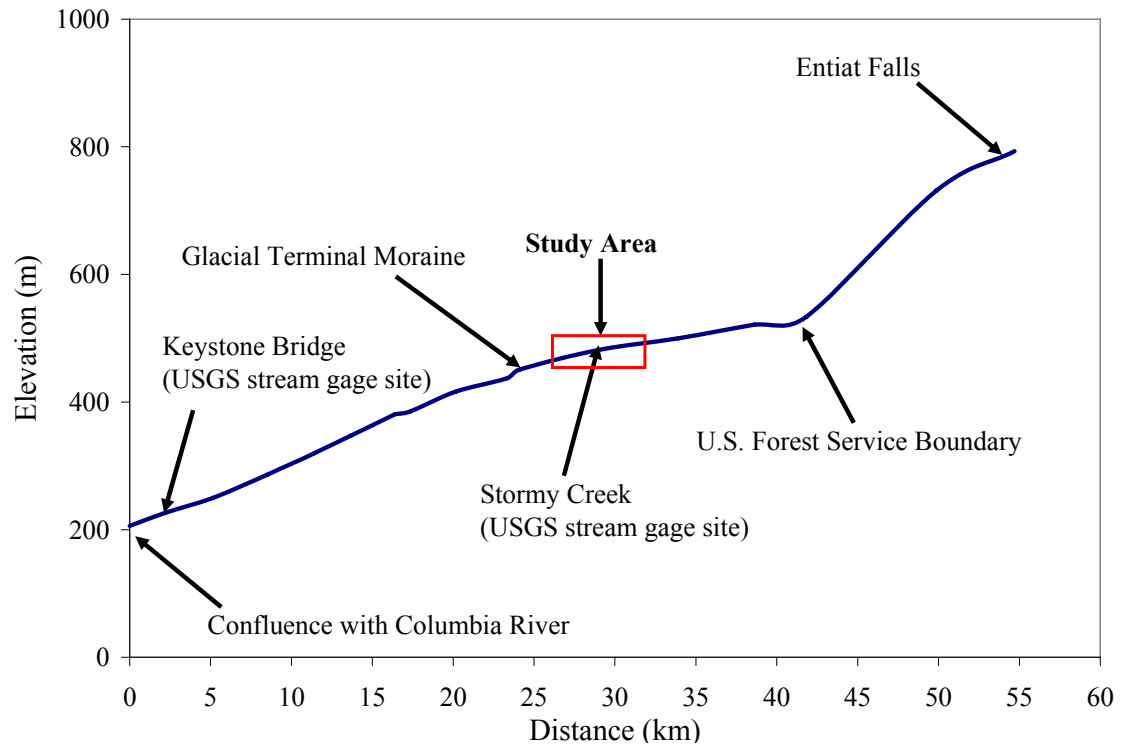


Figure 5. Longitudinal profile of lower 55 Rkm (34 RM) of Entiat River as measured from confluence with Columbia River. USGS = U.S. Geological Survey. Box indicates study area. Data courtesy Chelan County Conservation District (2004).

2004). The Chiwaukum Formation consists of foliated rocks ranging from phyllite to fine-grained gneiss.

The Mt. Stuart granodiorite formation consists of medium- to coarse-grained gray granodiorite containing abundant biotite and some hornblende; this formation is usually highly weathered (CCCD, 2004). The Entiat watershed also contains minor amounts of Columbia River Basalt, and some Glacier Peak volcanic ash deposits (CCCD, 2004). All of the above mentioned geologic formations were represented in the

river gravel within the study area for this project, with the exception of the Glacier Peak volcanic ash and Columbia River Basalt downstream of the study area.

Climate and River Discharge

Climate within the watershed varies from warm to hot summer temperatures (32°C-38°C) to sub-zero temperatures in the winter, with mean annual temperatures of approximately 10°C in the middle watershed (CCCD, 2004). Most precipitation occurs in the winter in the form of snow, and in the spring in the form of rain, with a mean annual precipitation of approximately 38 cm in the middle watershed. The summer months produce some light to heavy thundershowers and can produce flash flooding (CCCD, 2004). Table 1 and Figure 6 show the general streamflow characteristics for the Entiat River based on USGS (2005) streamflow gage no. 12452800 located near Rkm 29 (RM 18).

TABLE 1. ENTIAT RIVER FLOW CHARACTERISTICS

Flow parameter	Flow range (m ³ s ⁻¹)	Flow range (ft ³ s ⁻¹)
Mean annual flow range	5-18	175-621
Peak annual flow range	26-193	900-6800
7-day mean low flow range	1-3	36-90

Note: Data courtesy Chelan County Conservation District (2004).

Streamflows are typically lowest in the late summer months (August-September) and highest in the late spring to early summer in this snowmelt-based river system (CCCD, 2004). The majority of the high flow events, and typically the annual peak-flow event are produced by snowmelt-runoff from the Cascade Mountains. These high flow events are typically gradual, long in duration, and do most of the “work”

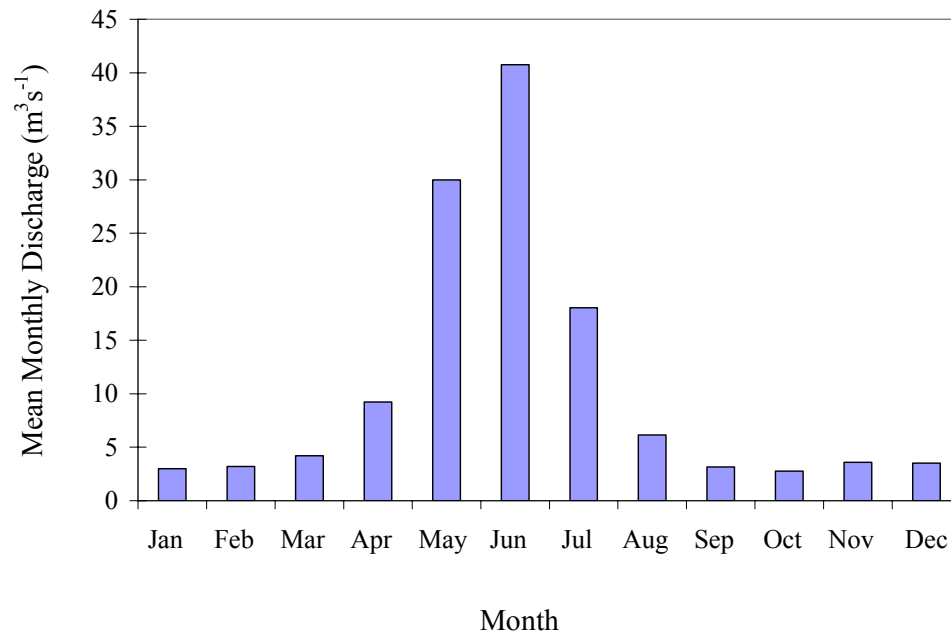


Figure 6. Mean monthly discharge of Entiat River within study area. Values based on 47-year record given by U.S. Geological Survey (2005) streamflow gage no. 12452800 located at Rkm 29 (RM 18).

within the river channel. However, the Entiat watershed also experiences rain-on-snow events and intense summer thunderstorms that can produce flash floods exhibiting rapid, short duration increases in streamflow.

CHAPTER II

GEOMORPHIC SETTINGS

Investigations of sediment clusters have focused on their effect on sediment transport (as will be discussed in chapter IV), their relative spacing on a gravel bar and geometric characteristics (Brayshaw, 1985; Church et al., 1998; Papanicolaou and Schuyler, 2003; Strom et al., 2004b), and their effect on benthic populations by providing refuge during high flow events (Biggs et al., 1997; Boelman and Stein, 1997). However, limited study has focused on the geomorphic settings under which clusters form (e.g., Strom et al., 2004a). Because clusters are an important component of gravel-bed rivers (as discussed in chapter I), it is useful to know where clusters are likely to form in gravel-bed rivers, and what geomorphic features may have the greatest influence on the characteristics of cluster formation. This chapter will outline the geomorphic conditions under which clusters form within a 3-km reach of the Entiat River and detail variations in cluster formation between two sites that are less than 1 km apart.

Methods

The geomorphic features surrounding cluster formation were identified at each gravel bar within a 3-km reach of the Entiat River (Rkm 27-30; RMs 17.5-18.5), which will be referred to as the “study reach,” located on the Chelan-Douglas Land Trust Stormy Preserve property. For the purpose of this project, the geomorphic features noted at each gravel bar were as follows:

- Presence or absence of clusters on gravel bars (defined either as a cluster bar

or non-cluster bar)

- Location of gravel bar within river, such as adjacent to a pool or riffle bedform or along straight or curved reach
- Sediment-size distribution
- Approximate slope of water surface
- General description of the surrounding geomorphology (presence of alluvial fans, bank characteristics, basic vegetation description, and other significant features)

Another important attribute that was noted was the presence of spawning salmon, as September through October is a peak spawning season for late-run Chinook salmon within this reach (Archibald, personal communication, October 18, 2004).

To determine the geomorphic features that favor cluster formation, the entire study reach was walked during the low flow season (September-October). Each gravel bar was located, identified, and given a classification of either having clusters (cluster bar) or being devoid of clusters (non-cluster bar). An attempt was also made to check for the presence of clusters within the low-flow channel at each site, so that it could be determined if the descriptions of the gravel bar characteristics, such as presence of clusters and sediment-size distributions, could be applied to the low-flow channel. Establishing a protocol for identifying a cluster bar from a non-cluster bar was difficult, since the definition of a cluster is fairly subjective, and the accepted methods for classifying a gravel bar as containing clusters are limited in the literature. Furthermore, even gravel bars that did not exhibit clusters easily visible to the eye likely exhibited

clusters on a smaller scale. However, for the purpose of this project, clusters are defined as having an anchor clast that traps two or more particles, protrudes above the normal gravel-bed surface greater than 2-3 cm (within a 50-cm radius) and contains anchor clasts larger than 5 cm. Therefore, microscale cluster formations were not considered clusters for this study. A cluster bar was defined as exhibiting clusters that met the criteria described above and accounted for at least 15% of the bar. In general, these criteria were met if one cluster was visible within 360° viewing distance every 2 to 3 m.

After gravel bars were located, identified, and given a cluster bar or non-cluster bar classification, the location of the bar was marked on the Tye Mountain U.S. Geological Survey (USGS) quadrangle map. Other key geomorphic features, such as pools, riffles, presence of alluvial fans and terraces, and bedrock outcrops were also noted and placed on the map. These features were then digitized onto a scanned Tye Mountain USGS quadrangle map using ArcGIS. Digital photographs of each gravel bar and surrounding geomorphic conditions, such as riffles, pools, alluvial fans, and general gravel bar position within the channel, were taken. Photographs of the sediment at each bar were taken at approximately the same scale and orientation to the river (with the channel position toward the top of the photograph with flow from right to left) and with the same metric ruler in each photograph (40 cm), so that the relative variations in sediment-size distribution could be determined. An attempt was made to photograph a section of the gravel bar that best represented the grain-size distribution, and if the gravel bar was a cluster bar, the most prominent clusters were included in the photograph. Sediment pebble counts were conducted at each bar using the Wolman

(1954) method. Thirty to forty random samples were taken at each bar, and the long, intermediate, and short axes were measured and recorded with a standard metric ruler (values were limited to $\frac{1}{2}$ cm increments). In addition to the pebble counts, the five largest particles from each bar were measured and averaged to obtain the D_{100} of the bar (largest particle on the bar). The D_{100} yields a better comparison of the sediment sorting differences between each bar because it gives a maximum value, which is commonly lost when values are averaged.

Water-surface slope values along the study reach were measured along the water's edge with a standard clinometer, which allows one person to sight to another person standing downstream and determine the percent slope value. These measurements were taken in 50-m increments or at obvious breaks in slope along the length of pools, riffles, and gravel bars.

In addition to describing the general geomorphology of cluster bars vs. non-cluster bars for the entire study reach, as explained above, two sites were selected for detailed examination based on their proximity to the USGS real-time streamflow gage and to each other (less than 1 km apart), and the different geomorphic features and cluster characteristics at each site. Additional components of the detailed study of sites 1 and 2 included identifying, describing, and photographing clusters before and after peak flow events in order to document their movement and evolution with varying discharges and associated velocities and average bed shear stress values. Further discussion of this component can be found in chapter III.

Results and Discussion

Figure 7 shows the longitudinal profile of the study area based on the water-surface slope values collected with the clinometer, as well as the locations of cluster and non-cluster bars along the study area and channel constriction between sites 1 and 2.

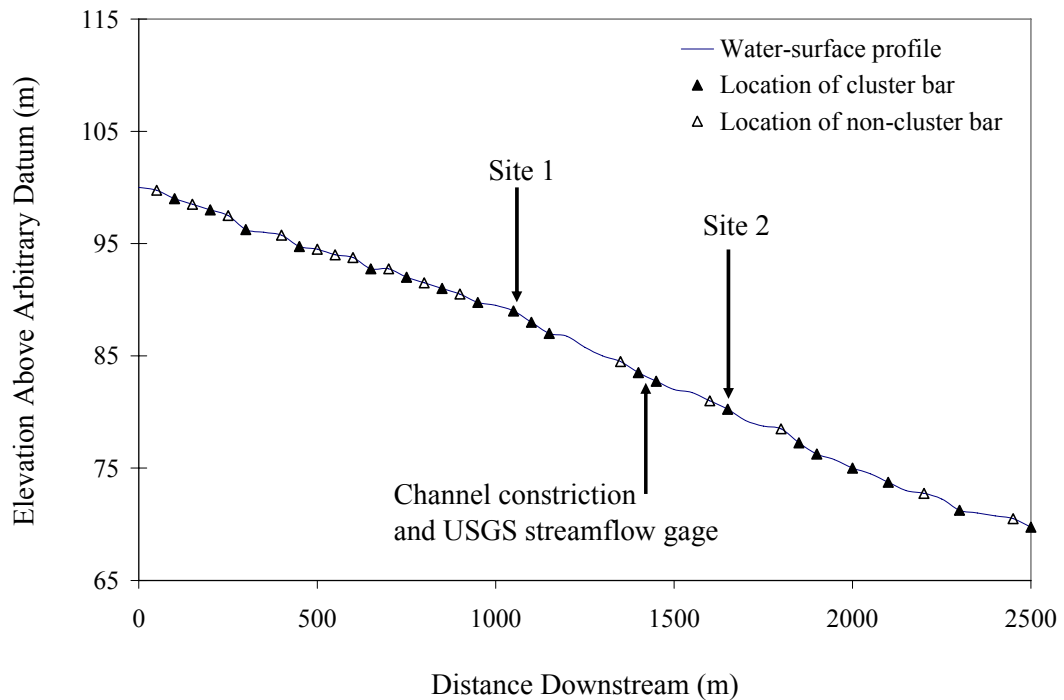


Figure 7. Longitudinal profile of study reach and locations of cluster bars and non-cluster bars. USGS = U.S. Geological Survey.

Most cluster bars occurred adjacent to riffles with higher water-surface slopes ($\geq 1\%$), where sediment sorting was typically poor, the average particle size (D_{50}) was within the range of 3-9 cm and the maximum particle size (D_{100}) was in the range of 9.5-26 cm (Table 2). Gravel bars that had smaller sediment sizes (D_{50} ranging from sand to 4.5 cm; D_{100} from 6 to 14.5 cm), were adjacent to pools, had a more uniform sediment-size

TABLE 2. GEOMORPHIC FEATURES OF CLUSTER BARS VS.
NON-CLUSTER BARS

Gravel bar no.	Geomorphic feature	D_{50} (cm)	D_{100} (cm)	Sediment sorting	Slope (%)
<u>Cluster bars</u>					
1	Riffle	3.6	10.0	Moderate-poor	1.0
2	Riffle	6.0	23.6	Poor	2.0
3	Riffle	9.1	20.0	Poor	2.0
4	Riffle	2.9	10.5	Moderate-poor	2.0
5	Riffle	3.9	9.5	Moderate-poor	2.5
6	Pool	4.4	12.8	Poor	1.0
7	Riffle	4.4	11.0	Moderate-poor	1.5
8	Riffle	3.9	10.8	Moderate-poor	1.5
9	Riffle	4.2	11.3	Moderate-poor	1.5
10	Riffle	4.4	11.4	Poor	2.0
11	Riffle	4.0	20.5	Moderate-poor	1.5
12	Riffle	N.D.	N.D.	Poor	2.0
13	Riffle	5.8	26.2	Poor	1.5
14	Riffle	4.5	13.8	Moderate-poor	2.5
15	Riffle	5.0	13.0	Moderate-poor	1.5
16	Riffle	4.9	12.8	Moderate-poor	1.0
17	Riffle	4.9	12.4	Moderate-poor	2.0
18	Riffle	3.8	11.6	Moderate-poor	1.5
<u>Non-cluster bars</u>					
19	Pool	3.7	10.4	Moderate-well	0.5
20	Pool	4.4	11.0	Moderate-well	0.5
21	Pool	Sand	Sand	Well	0.5
22	Pool	Sand	Sand	Well	1.5
23	Pool	2.4	5.8	Well	1.0
24	Pool	4.8	11.6	Moderate-well	0.5
25	Pool	2.0	7.4	Well	0.5
26	Pool	2.0	6.9	Well	1.0
27	Pool	Sand	Sand	Well	1.0
28	Pool	2.2	9.6	Well	0.5
29	Pool	4.4	14.4	Moderate-well	0.5

Note: Sand-sized particles are typically smaller than 0.01 cm. N.D. = no data.

distribution, or had water-surface slopes less than 1% did not exhibit clusters as defined for this project (Table 2). The digitized geomorphic map with the locations of cluster

bars, non-cluster bars, pools, riffles, alluvial fans, and other geomorphic features illustrates the occurrence of cluster bars adjacent to riffles (Figure 8).

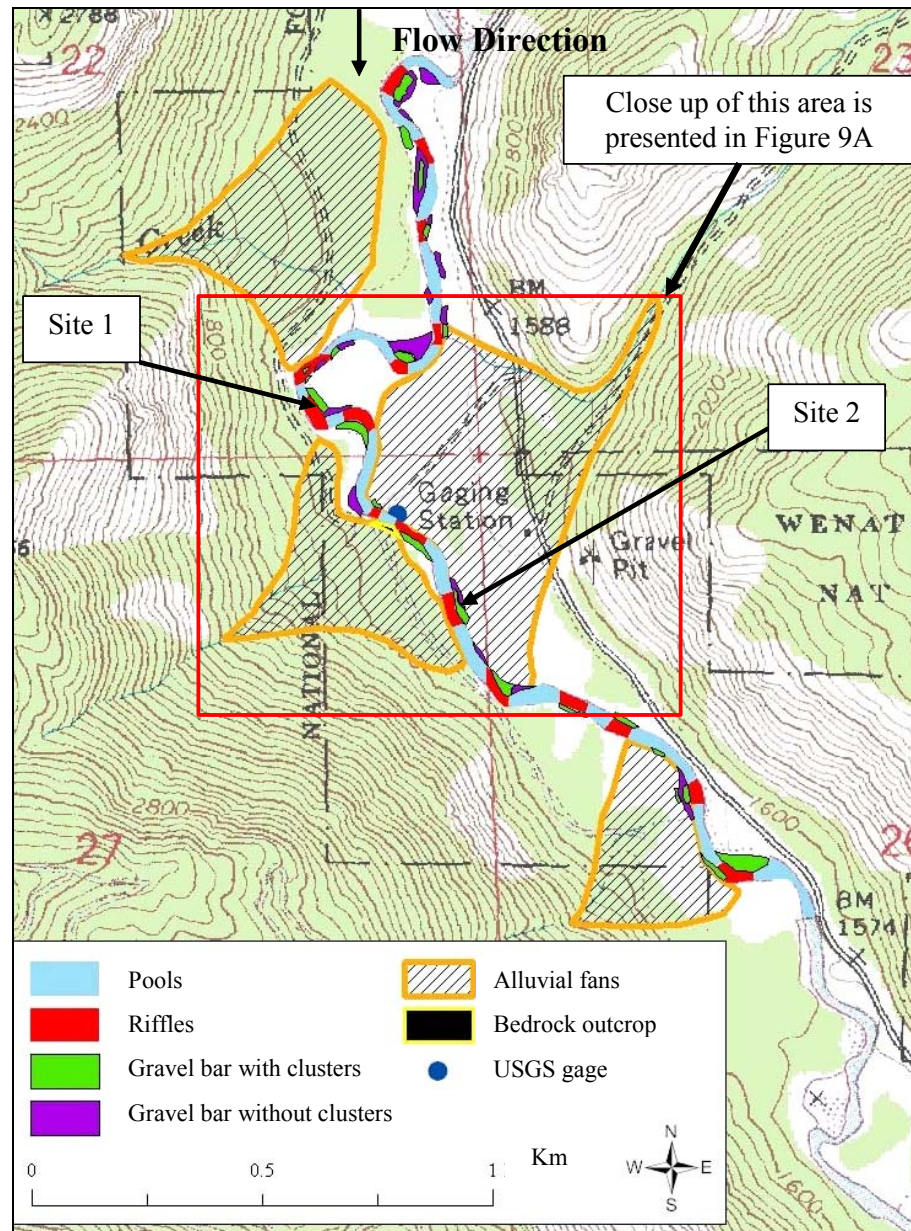


Figure 8. Digitized U.S. Geological Survey (USGS) quadrangle showing geomorphic settings of cluster bars and non-cluster bars within study reach.

There are four major alluvial fans within the study reach; the middle two along with a small bedrock outcrop constrict the channel near the USGS gaging station (Figure 9A). This constriction likely has major effects on the channel's sediment supply, carrying capacity, and downstream cluster characteristics. Visual inspection of the two fans and the bedrock outcrop indicated that they are supplying the channel with larger particles, some as large as 1 m in diameter. The two alluvial fans create steep banks, which are greater than 3 m high on both sides of the channel (Figure 9B). Therefore, as high flow events increase in velocity through this constriction, they entrain and transport the larger-sized particles downstream, depositing them as the channel widens and velocities decrease. These large particles then serve as anchor clasts for cluster formation at site 2, downstream of the constriction. These geomorphic and sediment size differences lead to a significant difference in the sediment-size distribution, cluster formation, and cluster stability at sites 1 and 2.

Figure 10 shows the differences in the sediment-size distribution based on Wolman (1954) pebble counts between site 1 (above constriction) and site 2 (below constriction). Figure 11 shows a comparison of the sediment sizes at each site using digital photographs. Site 1 has a nearly uniform distribution, with one major grouping of particles ranging from 0 to 12 cm; site 2 has a bimodal distribution, with one group of particles in the 0-10 cm range. These differences in sediment-size distribution caused significant variations in cluster formation characteristics, evolution, and stability at these two sites, which will be discussed in chapters IV and V.

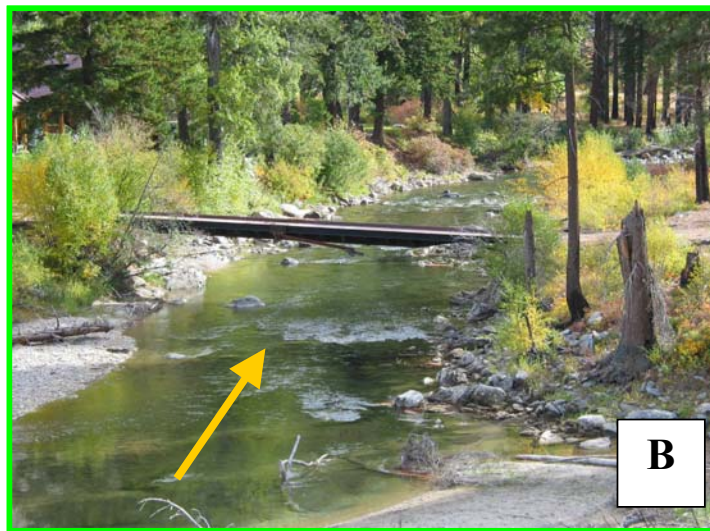
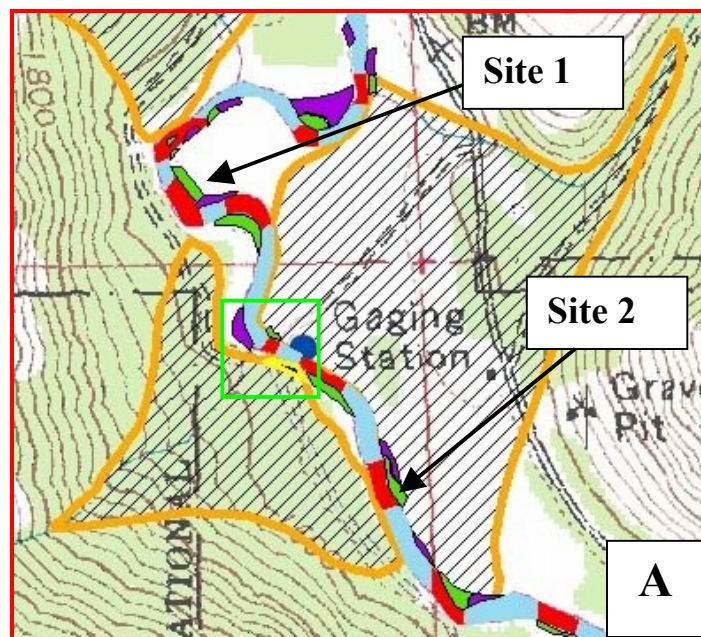


Figure 9. Geomorphic constriction between sites 1 and 2. (A) Close up view of geomorphic settings map (from Figure 8) showing river constriction at the U.S. Geological Survey streamflow gage. Legend is same as Figure 8, flow direction is toward the bottom of the page, and the green box shows location of the photograph shown in part B. (B) Photograph of constriction; banks are approximately 3 m high (yellow arrow denotes flow direction).

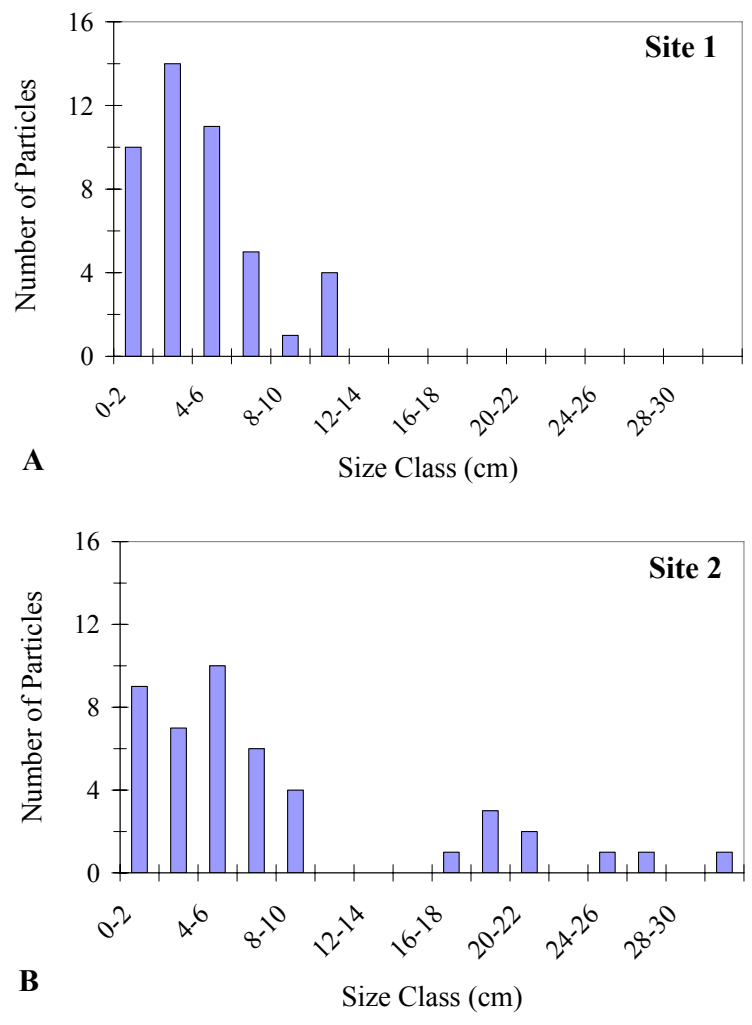


Figure 10. Sediment-size distribution at sites 1 (A) and 2 (B). $n = 40$.

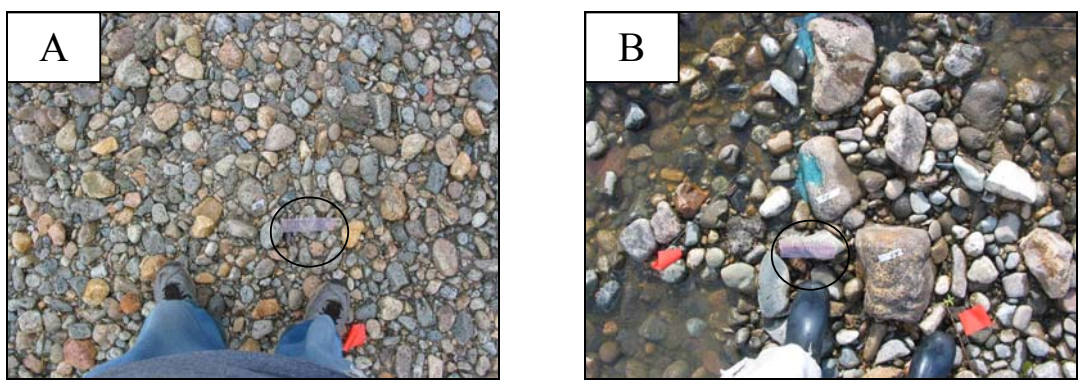


Figure 11. Photograph of sediment at sites 1 (A) and 2 (B). Circled object is 15-cm scale bar.

Summary

Geomorphic analysis of the study reach showed that clusters in the Entiat River formed within or adjacent to riffles with water surface gradients equal to or greater than 1%. Sediment was typically moderate-to-poorly sorted, with D_{50} values ranging from 3 to 9 cm and D_{100} values ranging from 9.5 to 26 cm. In general, the greater the sediment-size distribution, the more prominent the clusters appeared to be. These variations in sediment-size distribution can be attributed at least in part to geomorphic conditions. Between sites 1 and 2, two alluvial fans and a bedrock outcrop (Figures 8 and 9) supply the river with large-sized particles and also constrict the channel so that these large-sized particles are transported downstream to site 2. The following chapters will discuss in detail the characteristics of cluster formation and evolution at sites 1 and 2 based on the above discussion, and their effect on sediment transport.

Active salmon spawning was also noted within the channel adjacent to almost every cluster bar (Figure 12), while many of the pools served as resting areas for the salmon (Archibald, personal communication, October 18, 2004). Although at this time there is no evidence that clusters improve salmon habitat, observations from this project suggest that excellent salmon spawning habitat is found in the Entiat River within the study reach of this project and within areas where clusters are located. Future work is needed to thoroughly test this observation and to determine the role of clusters in salmon habitat.



Figure 12. Spawning salmon adjacent to cluster bar along Entiat River.

CHAPTER III

CLUSTER EVOLUTION

This study quantified the importance of clusters on sediment transport processes based on field observations. Some previous studies have found clusters to have a delaying effect on sediment transport (Brayshaw et al., 1983; Brayshaw, 1984; Naden and Brayshaw, 1987; Church et al., 1998; Strom et al., 2004b), while other studies consider clusters to be an insignificant factor in sediment transport (Billi, 1988; De Jong, 1991). Brayshaw (1984) showed that clusters delay sediment entrainment and that anchor clasts must be mobilized before a cluster is destroyed, thus suggesting the particles within clusters are “trapped” until flows are large enough to mobilize the anchor clast. This idea was challenged by de Jong (1991) who looked at mobilization of clusters in a partially braided river in Scotland after minor flood events, and noted that particles were entrained and transported downstream without prior mobilization of the obstacle clast, and that, in general, the obstacle clast remained stable while the particles initially impeded by the obstacle clast were entrained by relatively weak flow events. This, according to de Jong (1991, p. 737), suggests that obstacle clasts “probably form a less significant delay to sediment entrainment than previously assumed.” In contrast, Church et al. (1998, p. 3174) studied clusters in both a natural setting and laboratory flume and found that clusters “improve the overall stability of gravel bars and play an important role in decreasing sediment transport rates.” Church et al. (1998) based their conclusions on experimental results that showed reduced transport rates after initial removal of fine-grained material with increased flow velocities. They attributed this

reduction in sediment transport to cluster formation and impediment of smaller particles, which remained constant until larger flow values were introduced into the flume, thus destroying the clusters, at approximately two times the normal shear stress required to entrain isolated particles. Their field investigations yielded cluster formations similar to those created in the flume experiments, from which Church et al. (1998) concluded that results from the flume could be applied in the field. A more recent laboratory flume experiment also showed that clusters were destroyed at two times the critical shear stress required to entrain isolated particles (Strom et al., 2004b).

Studying sediment transport by flowing water in nature is a difficult and complicated process, and trying to determine the effects of clusters on these processes can be even more difficult. Bed evolution occurs during flow events too large to study directly, and observations of sediment transport must be made after the flow event that caused the movement. Many laboratory flume experiments have allowed for detailed examination of the effects of clusters on sediment transport during the transporting flow event (Hassan and Reid, 1990; Church et al., 1998; Lawless and Robert, 2001; Papanicolaou and Schuyler, 2003; Papanicolaou et al., 2003; Dey, 2004; Strom et al., 2004b). However, natural processes are often much more complex than laboratory flumes, and accompanying field data are needed to validate and compare with laboratory studies. Cluster studies that have included field components have been limited; Brayshaw et al. (1983) used an experimental flume study to show decreases in the lift and drag forces acting on particles within the wake and stoss of clusters compared with isolated particles in the open plane-bed. This data was combined with

field data, in which “seeded” particles were tracked after a high flow event. Results from this field data showed that 46% of the seeded clustered particles were entrained compared to 87% of the seeded isolated particles. Furthermore, results from the Brayshaw et al. (1983) study showed that cluster particles that were entrained were transported shorter distances, suggesting earlier and longer entrainment of isolated particles, which had higher transport distances during the same flood event. In another field-based cluster study, Reid et al. (1992) used electromagnetic particle tracing sensors to determine “moment of initial entrainment,” which was used with flow, grain size, and density data to determine the dimensionless critical shear stresses (based on that critical velocity and basic Shields equation) associated with the movement of the tracer particles. Selected results from these studies will be compared with those found in this study.

Methods

Tracking Cluster Movement

During the initial period of this study, two gravel bars were selected to determine how clusters evolved with various flow events. Sites 1 and 2 were selected based on the following criteria:

- Sites must have gravel bars that are regularly inundated by high flows and exhibit cluster formations.
- Sites must be accessible year-round with permission from the appropriate governmental agency or private party.

- Sites must be located on a mostly unregulated stream, so that high flow events and inundation periods occur naturally and are not altered by human influences or structures.
- Sites are preferably near a real-time streamflow station that is accessible online (such as a USGS real-time recording station), which allows for careful observation and documentation of flow patterns near each site, so that the precise date, time, and duration of high flow events can be known. The drop in discharge that provides access to the gravel bar can also be monitored so that the effects of high flow events can be documented soon after the high flows recede.

Sites 1 and 2 were also selected based on their differences in sediment-size distribution and geomorphic features (as explained in chapter I) in order to determine how these factors may affect cluster evolution.

At each site 5-m x 5-m square plots were measured and marked on the gravel bars, three at site 1 and one at site 2 (more plots were planned for site 2, but a high flow event occurred before the additional plots could be marked and described (see Results and Discussion section of this chapter)). Once cluster plots were measured and marked, a baseline data set was compiled, and the most prominent 15 clusters within each plot were identified (site 2 had 16). Each identified cluster was marked with numbers written on masking tape and on the anchor clasts using permanent markers. Small colored paint marks were also applied to each anchor clast, so that clusters would stand out when trying to find them after high flow events. These paint marks were subtle enough so that

the clusters were not too obvious to hikers, fishermen, and other recreational enthusiasts who might walk by and disturb the clusters. Each cluster description included a classification of the cluster identification number, geometry, and orientation to flow direction. The number of anchors and size of the largest anchor within each cluster (long, short, and intermediate axis) was recorded, as was the overall length, width, and the total number and average size of particles greater than 3 cm being impeded by the anchor(s). After each cluster was marked and described, it was photographed using a digital camera. Two photographs of each cluster were taken, the first using the widest angle setting on the camera from a consistent height so that a similar scale for all the clusters could be documented, and a close-up photograph of the cluster, which yielded a more detailed documentation of the cluster with varying scales for different sized clusters. Each photograph included a 15-cm scale and the masking tape number of the cluster, although this was not always possible for submerged clusters. Each photograph was taken with the photographer standing above the cluster, facing the stream with flow direction from right to left.

Of the initial 45 clusters that were identified, described, and photographed in September 2003 at site 1, 8 were eliminated after further review because they did not meet the pre-defined criteria for clusters as described in chapter I. Therefore, a total of 37 baseline clusters were tracked at site 1, and 16 at site 2. Shortly after the clusters were marked, described, and photographed, the first and highest flow event occurred on October 21, 2003, caused by consecutive days of light to heavy rain throughout the watershed (see also the High Flow Events section of this chapter). This event eliminated

the opportunity to mark and describe additional clusters at site 2 for tracking, and thus caused the uneven sample size between sites.

After each high flow event that inundated the gravel bars, the clusters were again identified, described, and photographed, to assess the evolution of the clusters with varying flow events, velocities, and shear stress values. The digital photographs of the clusters before and after the high flow events were compared using digital imaging software to determine whether they remained stable, changed morphologies, or were destroyed. Photographs and the scale bar were used to measure the sizes of particles that remained in place, moved, or were removed from the stoss or wake of the cluster. The wide-view photographs were used to track the movement of individual, isolated particles that did not appear to be impeded by any other particles and were essentially “perched” atop the gravel bed. The sizes of these particles were also estimated using the scale bar in the digital photographs. These sizes, in addition to the size of particles that moved within clusters, provided input variables for determining the critical shear stress value associated with particle entrainment during each flow event, as described in the following section. Horizontal and vertical lens distortion was calibrated in the laboratory to the edge of the wide-angled photographs by measuring an object of known length across the entire photograph. Maximum distortion was 3%, which was within the measurement error of the particle sizes. These measurements were rounded to the nearest 0.5 cm. Measurements near the edge of the photographs were up to 3% smaller than those in the center. Because the photographs were consistently centered on the clusters, size estimates for the surrounding isolated particles were slightly

underestimated if they were located near the edge of the photograph. Thus, the size differential between isolated and clustered particles that moved during a particular flow event may have been greater in some cases.

Shear Stress Equations

As water flows downstream in a river, the force of the water exerted on the streambed is referred to as the bed shear stress (Knighton, 1998). Shear stress is one of the many variables that contribute to the entrainment of sediment, which also includes the force of gravity; the mass, shape and packing of the particles; and the overall channel roughness. The shear stress that is required to initiate movement of sediment particles is referred to as the critical shear stress of incipient motion (Knighton, 1998). Shields developed one of the first equations for determining the dimensionless critical shear stress, also referred to as the Shields Parameter (τ^*_{cri}), required to entrain sediment particles of a given size and density (Buffington and Montgomery, 1997). The Shields equation is given by:

$$\tau^*_{\text{cri}} = \tau_{\text{cri}} / (\rho_s - \rho)gD_i \quad \text{Equation 1}$$

where τ_{cri} is the mean shear stress in Newtons per meter squared (N/m^2) at initial motion of the grain size of interest D_i (mm), ρ_s equals the density of sediment (g/cm^3), ρ equals the density of water (g/cm^3), and g equals the acceleration of gravity (m/s^2). The mean shear stress value (τ_{cri}) was estimated from water-surface elevations, mean flow depths, and the specific weight of water given by a hydrologic model and the Dubois

equation (Chow, 1959). For this study the grain size of interest (D_i) was the mean intermediate axis diameter of the five largest particles that were entrained by a given flow event (either isolated or clustered particles).

Using the Shields equation allowed for estimations of the critical shear stress required to entrain both individual, “isolated” particles sitting atop the gravel bed and those trapped in clusters, regardless of other variables. The Shields equation was chosen for this study for two reasons, the first being that it was developed for determining the shear stress required to entrain individual particles atop a layer of uniform sediment. Although the sediment is not uniform in the Entiat River, some of the particles are sitting on top of the bed, and are assumed to be isolated from hiding effects of the larger sized particles. The second reason the Shields equation was chosen is that it can be used to determine the effects of clusters on the entrainment of individual particles without introducing some of the complex modifications and additions to the basic critical shear stress equation. The more elaborate equations account for various parameters affecting sediment entrainment to determine the average critical shear stress for the entire bed (Buffington and Montgomery, 1997), whereas the purpose of this study was to estimate the critical shear stress for individual particles. Therefore, although the use of the bed shear stress to model sediment entrainment is limited because of above-mentioned simplifying assumptions, it is useful as a comparison of clustered vs. non-clustered particles that are adjacent to each other on the same gravel bed. This eliminates or reduces some of the complex factors of other shear stress equations such as effects of channel shape on large-scale turbulence, general degrees of sediment packing,

sediment-size distribution, sediment shape, pivot angles, degree of sorting, and microscale flow velocities around individual particles (Knighton, 1998).

Although the Shields equation provides a simple means to compare the critical shear stresses required to entrain particles sitting alone on the bed to those trapped by clusters, it has been extensively debated and modified in the literature since its publication (Buffington and Montgomery, 1997). This debate is due mainly to the assumptions of the Shields equation, which include uniform grain sizes, spherical grains, general degrees of packing, and a planar-bed surface; these assumptions are not common in a natural streams, particularly gravel-bed streams. In addition, the Shields equation does not account for the hiding effects and relative protrusion of larger-sized particles on flow (Komar and Zhenlin, 1986; Komar, 1989; Papanicolaou et al., 2004; Papanicolaou, personal communication, January 25, 2005). Therefore, an equation given by Komar (1989), which accounts for larger particle size fractions in a non-uniform sediment-size distribution, was also used to compare the critical shear stress values for isolated vs. clustered particles. The Komar equation provides a general and simplistic equation for selective-entrainment of varying particle size fractions in a non-uniform sediment-size distribution, and is given by:

$$\tau^*_{\text{cri}} = a(D_i / D_{50})^b \quad \text{Equation 2}$$

where τ^*_{cri} is the critical shear stress required to entrain particles (dimensionless; similar to the Shields Parameter), a and b are coefficients (-0.045 and -0.65 ,

respectively). The a and b coefficients were developed by Komar (1989) based on comparisons of previous selective entrainment data, each of which was developed using field-based methods (Milhous, 1973; Carling, 1983; Hammond et al., 1984). The D_i in Equation 2 represents the mean b-axis diameter of the five largest isolated or clustered particles that were entrained by a given flow event, with respect to the average grain size of the bed (D_{50}).

Using both the Shields and Komar equations allowed for the testing of one of the main hypotheses of this study: that entrainment of particles within clusters will require a higher critical shear stress than entrainment of isolated particles, thus reducing sediment transport during high flow events. Of course, the use of any empirical equation in a field-based study comes with assumptions. The main assumptions of the Shields equation include uniform grain size that is spherical in shape, a limited degree of bed packing, and a planar bed surface. These assumptions are considered acceptable given the advantage of using this simplistic, basic shear stress equation to determine the differences in critical shear stress values for individual particles isolated on the bed compared to those in clusters. The Komar equation also has assumptions, one of which is that the standardized coefficients can be applied to the Entiat River, and can account for many of the factors that affect average bed shear stress. However, for the purpose of this study these two equations will provide estimates of the actual critical shear stress values required to entrain isolated and clustered particles, as well as the differences between them (isolated vs. clustered particles). Potential errors in the actual critical shears stress values, including under and/or over estimations, are acceptable if they are

systematic for both isolated and clustered particles because it was the difference of these values that was of interest for this study.

Hydrologic Engineering Center River Analysis System

To determine the effect of clusters on sediment entrainment, comparisons were made between the critical shear stress required to entrain isolated particles vs. those in clusters. The velocities and flow depths associated with each high flow event were calculated using the U.S. Army Corps of Engineers' Hydrologic Engineering Center (HEC, 2002) River Analysis System (HEC-RAS) one-dimensional water-surface profile model. The HEC-RAS model and gaged flow record were used to determine the discharge required to completely inundate the gravel bars containing clusters, how frequently clusters are inundated (based on historical discharge records), and the velocities and associated average bed shear stresses of each flow event required to maintain and destroy clusters. These average bed shear stress values yielded minimum critical shear stress values necessary for input into the dimensionless critical shear stress equations. Modeling methods were necessary for this study since velocity and shear stress measurements required to calculate critical shear stress are very difficult to obtain in the field, especially during high flow events when the gravel bars are inaccessible, and are often inaccurate (Biron et al., 1998).

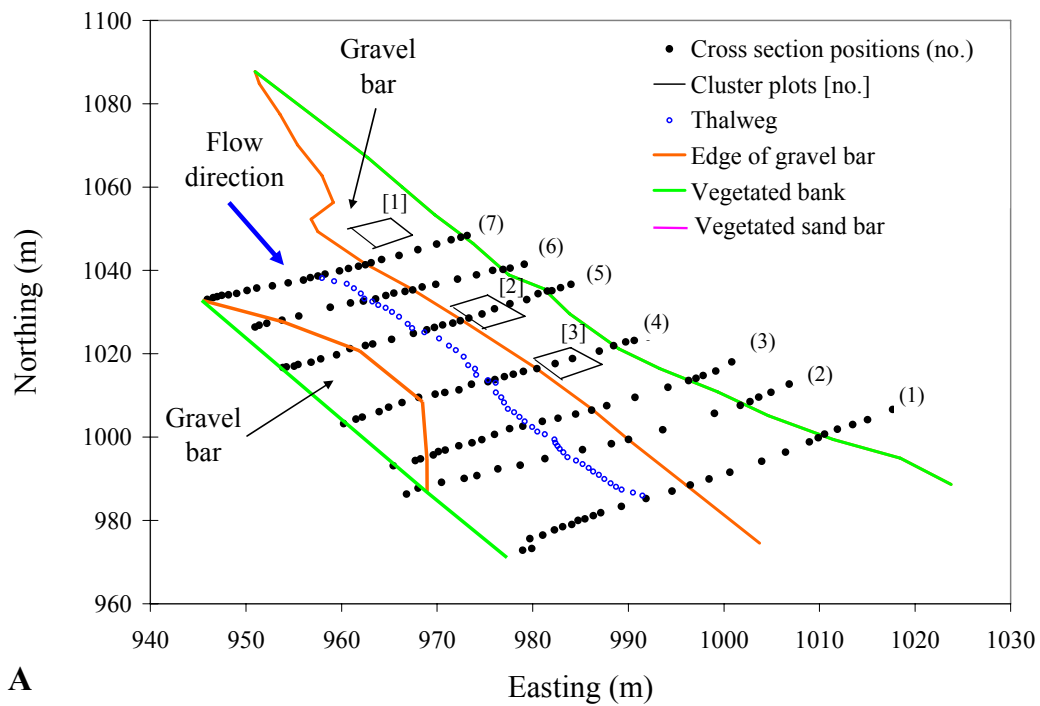
HEC-RAS uses step-backwater calculations to estimate water-surface elevations, streamflow depths, and other hydraulic conditions in river channels and adjacent flood plains (Feldman, 1981; O'Connor, 1993; Elliott, 2002; HEC, 2002). The step-backwater calculations are based on the principle of conservation of energy

between channel cross sections, minus the energy loss due to friction (Feldman, 1981; HEC, 2002). The flow-modeling component of this study used uniform streamflow, which assumes velocity is constant in both magnitude and direction through the reach, and steady-state flow conditions, which assumes that there is a continuity of discharge along the reach. These conditions are relatively standard and provide the simplest means for modeling water-surface elevations using HEC-RAS (O'Connor, 1993; Elliott, 2002; HEC, 2002). HEC-RAS uses channel and overbank cross-sectional geometry data, reach lengths between cross sections in both channel and overbank areas, estimates of hydraulic roughness (Manning's roughness coefficient), expansion/contraction frictional loss coefficients, flow regime, starting water surface elevations, and specified discharges as input variables (O'Connor, 1993; Hosman, 2001; HEC, 2002).

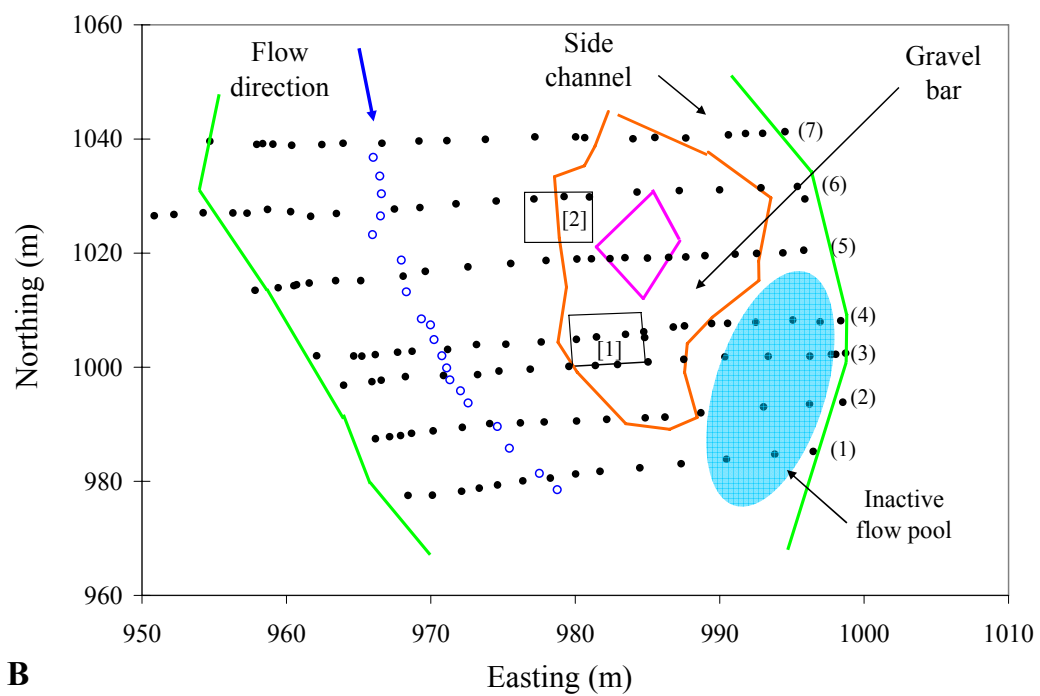
Channel geometry and specified discharge values are the most sensitive input variables of the HEC-RAS model (O'Connor and Webb, 1988; Hosman, 2001; HEC, 2002). Channel cross sections must be fairly equally spaced and within a relatively straight reach of the river, as HEC-RAS loses its ability to accurately determine the energy losses resulting from special variations in channel geometry and roughness, each of which were confidently measured or known for this study (O'Connor, 1993; Elliott, 2002; HEC, 2002). In the Entiat River, 14 channel cross sections were surveyed at sites 1 and 2 (seven at each site) using a Total-Station laser theodolite surveying instrument. The cross sections were positioned at short intervals and were relatively evenly spaced along straight reaches of the river, so that they characterized the flow capacity of the

channel and its floodplains while providing fairly simple channel geometry for input into HEC-RAS. Survey points were taken from a consistent position, or survey station, from terraces above the gravel bars so that control points used for setting up the survey station could be relocated for future studies. In general, survey points were collected every 2-3 m along the cross section, or whenever there was a notable change in channel geometry. Additional survey data were collected to represent the spatial position of the gravel bar, water surface elevations, and position of the thalweg for the day of the surveys. Figure 13 shows the spatial distribution of the cross sections in relation to the gravel bars and cluster plots at sites 1 and 2, while Figures 14 and 15 show the geometry of each cross section at both sites.

Discharge values were obtained from the USGS's (2005) real-time streamflow gage no. 12452800, Entiat River near Ardenvoir. This gage is located approximately 0.5 km downstream of site 1 and 0.5 km upstream of site 2, with no major tributary additions in between, and therefore similar hydrologic processes can be assumed at sites 1 and 2. Therefore discharge values from the USGS gage were used to calibrate the HEC-RAS variables to determine if the calculated water-surface elevations given by HEC-RAS matched known water-surface elevations recorded while surveying channel cross sections. A consistent roughness coefficient of 0.035 was used for the HEC-RAS modeling at both sites, calibrated with known discharge and water-surface elevations. The water-surface elevations and flow depths provided by HEC-RAS were used to calculate the average bed shear stress values using the relationship between boundary



A



B

Figure 13. Spatial positions of cross sections at sites 1 (A) and 2 (B). Legend for part A also applies to part B.

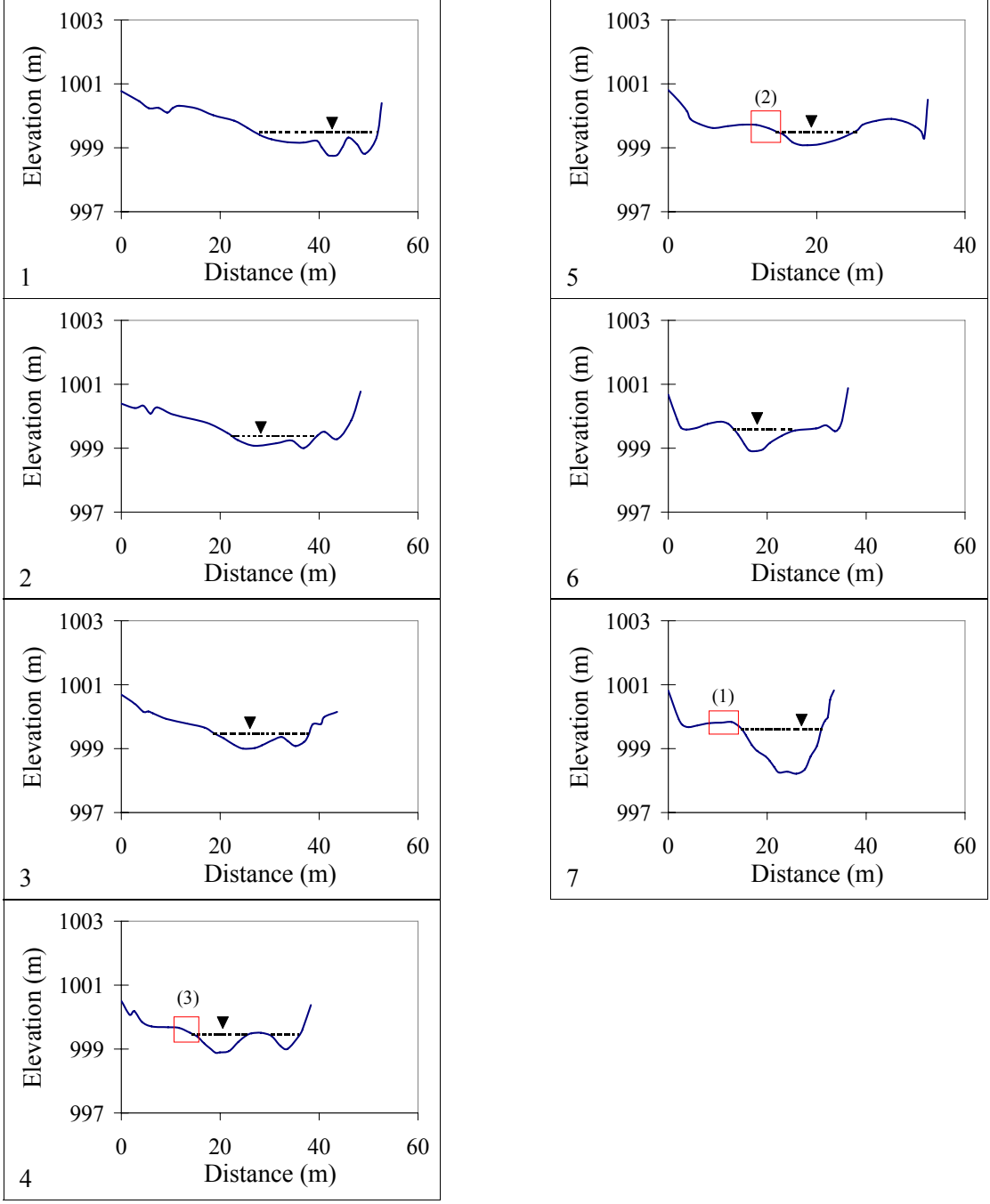


Figure 14. Channel geometry at site 1. Cross section numbers (1-7) are given in lower left corner of each plot. Dashed lines denote low-flow water surface ($3.5 \text{ m}^3 \text{ s}^{-1}$). Boxes indicate location of cluster plot (with plot number in parenthesis). Pointed triangle represents approximate thalweg.

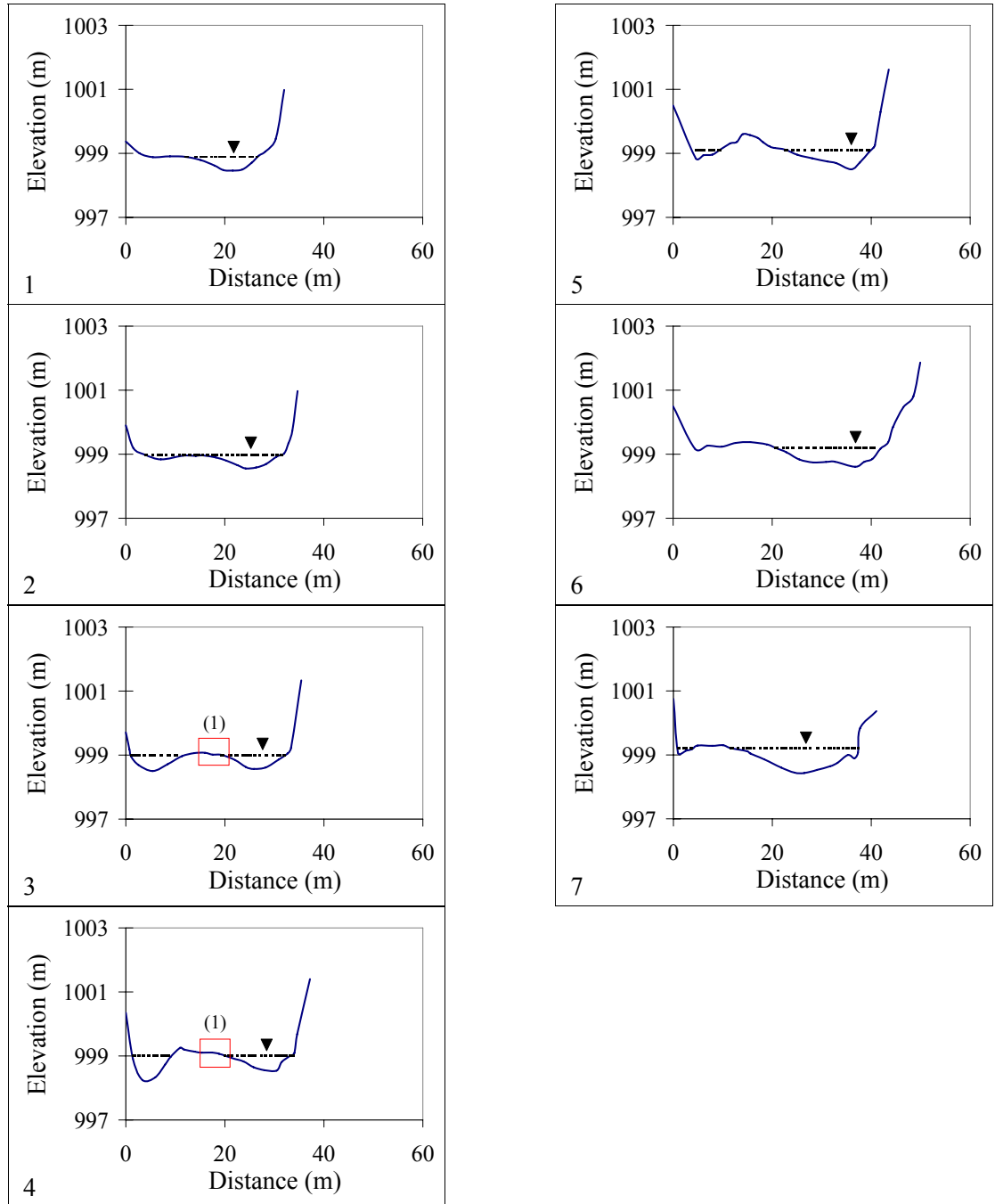


Figure 15. Channel geometry at site 2. Cross section numbers (1-7) are given in lower left corner of each plot. Dashed lines denote low-flow water surface ($3.5 \text{ m}^3 \text{ s}^{-1}$). Boxes indicate location of cluster plot (with plot number in parenthesis; plot 1 is bordered by cross sections 3 and 4). Pointed triangle represents approximate thalweg.

shear stress, flow depth, and energy gradient given by the Duboys equation (Chow 1959):

$$\tau_o = \gamma DS \quad \text{Equation 3}$$

where τ_o equals the mean boundary shear stress (N/m^2), γ equals the specific weight of water (9807 N/m^3), D equals the mean flow depth (meters), and S equals the energy gradient (dimensionless) (water-surface slope is often used as a substitute). The assumptions for using the HEC-RAS hydrologic model (Elliott, 2002) are as follows: (1) the channel cross section has a regular, or trapezoidal, shape and width at least 10 times greater than its depth; (2) streamflow is steady; and (3) stream flow is uniform. Although the channel geometry for the both sites along the Entiat River is not trapezoidal, most cross sections have a single, dominant channel that conveys most of the streamflow, with the exception of cross sections 1-4 at site 2. These sections contain a small side channel that drains into an inactive flow pool (see Figure 13B and Figure 15). That could cause average bed shear stress values to be underestimated, as discussed in the following section.

Results and Discussion

High Flow Events

During the period of this study (September 2003-March 2005), there were 4 high flow events that inundated both sites (hereafter referred to as events 1-4) ranging

from 13 to $57.4 \text{ m}^3\text{s}^{-1}$ at the USGS (2005) streamflow gage. Figure 16 shows the daily maximum discharge values during the time period of this study and associated high flow events that inundated both sites, as well as the mean annual peak flow value ($80 \text{ m}^3\text{s}^{-1}$) based on 46 years of record (USGS, 2005). The dates of each successive photograph set, in which clusters were again photographed and described, are also shown. It should be noted that at site 2 the gravel bar was inundated and not accessible until after high flow event 3, and it was therefore assumed that any particle and/or cluster movement was caused by the largest of the three events (event 1; $57 \text{ m}^3\text{s}^{-1}$).

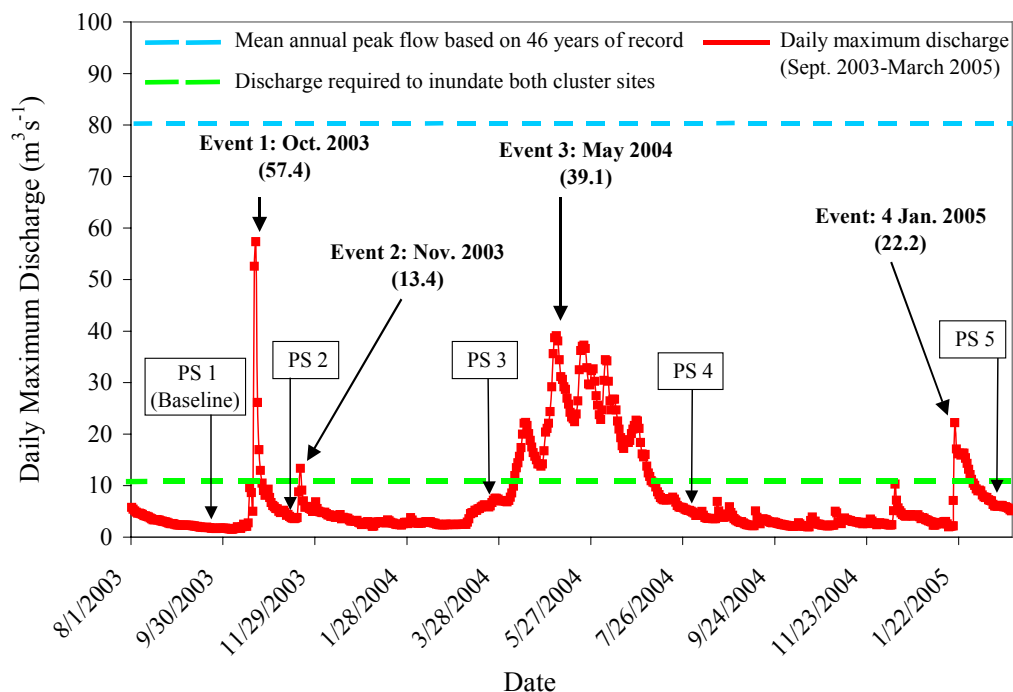


Figure 16. Daily maximum discharge values during period of study. PS = photograph set. Discharge data obtained from U.S. Geological Survey (2005) streamflow gage located at Rkm 29 (RM 18), between sites 1 and 2.

Table 3 shows that the calculated shear stress values over the cluster plots ranged from 10 N/m^2 during the smallest flow event (event 2, site 1/plot 2) to 145 N/m^2 during the largest flow event (event 1, site 1/plot 3). Velocity values over the cluster plots ranged from 2.0 m/s (event 1, site 1/plot 1) to 0.2 m/s (event 2, site 1/plot 3). It should be noted that at site 1 the highest values for shear stress and velocity were not at the same plot for a given flow event. These disagreements in velocity and shear stress values between plots may suggest an error in the velocity calculations and/or shear stress equations. A possible explanation for this discrepancy could be the simplistic nature of the equations from which the values were calculated. Recall from the Methods section of this chapter that velocity values were calculated by HEC-RAS based on discharge, channel geometry (specifically channel width), and flow depth, while shear stress values were calculated using the Duboys equation (Chow, 1959), based on water-surface gradient and flow depth (both of which are determined from the HEC-RAS model) and the specific weight of water. For plot 3, the water-surface gradients and flow depths were slightly larger compared with plots 1 and 2, which would produce higher shear stress values based on the Duboys equation. However, at plot 2 the channel was narrower than at plots 1 and 3, and given the same discharge and flow depth, would produce higher velocity values. Furthermore, the inability of the model to accurately calculate the small-scale, near-bed velocities and shear stress values created by the microscale topography of gravel-bed rivers is another source of uncertainty.

HEC-RAS is also limited by assumptions, such as uniform and steady streamflow and simplistic channel geometry. However, discharge values, the most

TABLE 3. HYDROLOGIC MODEL OUTPUTS

Event and site/plot no.	Discharge at USGS gage (m^3s^{-1})	Average flow depth over cluster plot (m)*	Calculated velocity over cluster plot (m/s)*	Calculated shear stress over cluster plot (N/m^2) [†]
<u>Event 1</u>				
Site 1/plot 1	57	0.79	0.9	62
Site 1/plot 2	57	0.68	2.0	61
Site 1/plot 3	57	0.79	1.4	145
Site 2/plot 1	57	0.90	1.3	54
<u>Event 2</u>				
Site 1/plot 1	13	0.20	0.2	12
Site 1/plot 2	13	0.11	0.7	10
Site 1/plot 3	13	0.14	0.4	14
Site 2/plot 1	13	0.27	0.5	110
<u>Event 3</u>				
Site 1/plot 1	39	0.58	0.7	57
Site 1/plot 2	39	0.50	1.6	45
Site 1/plot 3	39	0.51	1.1	103
Site 2/plot 1	39	0.67	1.1	34
<u>Event 4</u>				
Site 1/plot 1	22	0.35	0.4	27
Site 1/plot 2	22	0.31	1.3	22
Site 1/plot 3	22	0.31	0.7	46
Site 2/plot 1	22	0.43	0.7	21

Note: USGS gage = U.S. Geological Survey real-time streamflow gage.

*Calculated by Hydrologic Engineering Center River Analysis System (Hydrologic Engineering Center, 2002).

[†]Calculated using the Dubois equation.

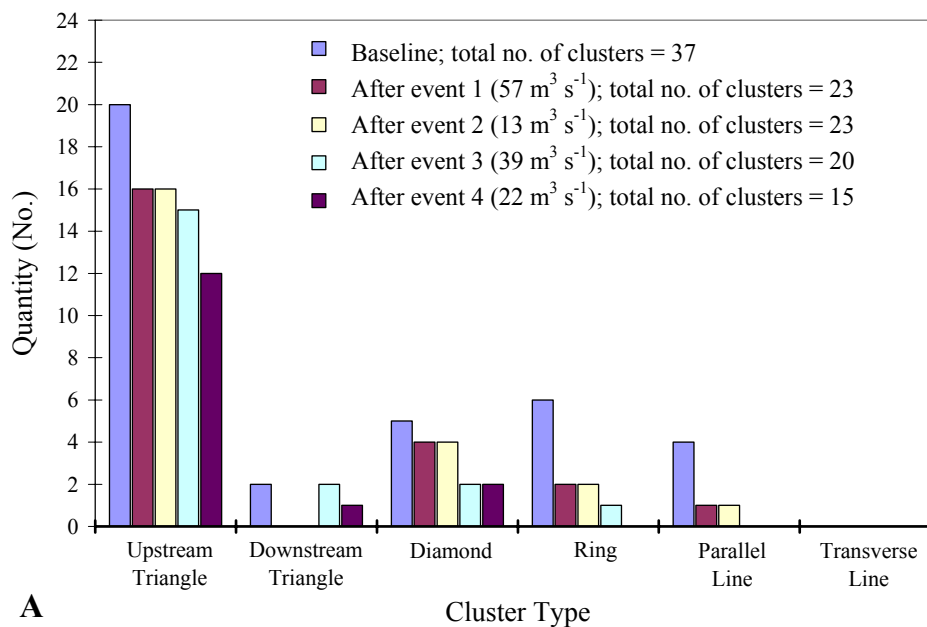
sensitive and important input variable (O'Connor and Webb, 1988; Hosman, 2001; HEC, 2002), were collected by the USGS (2005) streamflow gage and therefore considered accurate, and attempts were made to assure simplistic and accurate channel geometry by surveying evenly spaced channel cross sections within relatively straight reaches of the river. Finally, the use of the mean flow depth over each plot (as calculated by HEC-RAS), and not accounting for variations of flow depth due to the

side slope of the bar and possible variations in the protrusion of each cluster, is another possible source of error in the Dubois (1959) equation used to calculate shear stress. The maximum variations in flow depths at each plot, and the difference in shear stress calculated from the minimum and maximum flow depths, are presented in the following section.

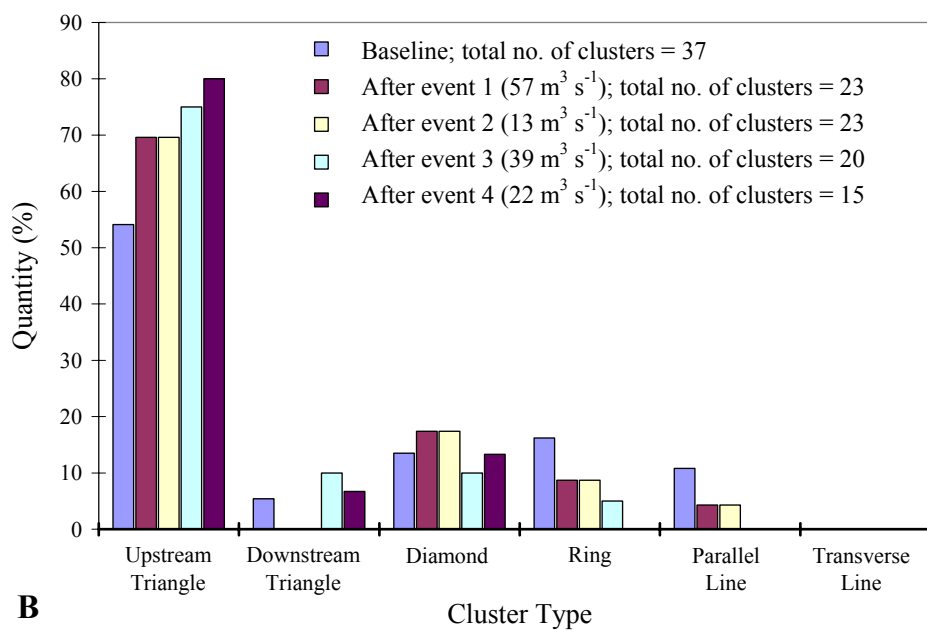
Cluster Evolution

Figures 17 and 18 show how the clusters evolved with each flow event, which cluster type was the most stable, and which cluster morphology was the most abundant at each site. It should be noted that this section describes the evolution of clusters at sites 1 and 2 during 4 observed flow events, and in general, shows that the original number of clusters tagged for tracking decreased with each flow event. However, these results do not suggest that the total number of clusters on the bar (that were not tagged for tracking) decreased with each flow event. In fact, both general observation of the gravel bar after each flow event and detailed examination of the plots after event 3 (see chapter IV) showed that many new clusters formed after each event. However, for the purpose of this chapter only the original tagged clusters and their evolution and/or destruction after each flow event are discussed, and no newly formed clusters were added to the original dataset used for tracking cluster evolution.

Possible uncertainties associated with tracking cluster evolution are anthropogenic or biologic disturbances. Clusters could have been disturbed, displaced, or removed by people walking along the gravel bar and/or terrestrial or aquatic species,



A



B

Figure 17. Cluster evolution for site 1 (all plots). (A) Number of each cluster morphology that were marked for the baseline dataset and relocated after each observed flow event during period of study. (B) Percentage of each cluster type out of the total number of clusters for the baseline dataset and after each observed flow event during period of study.

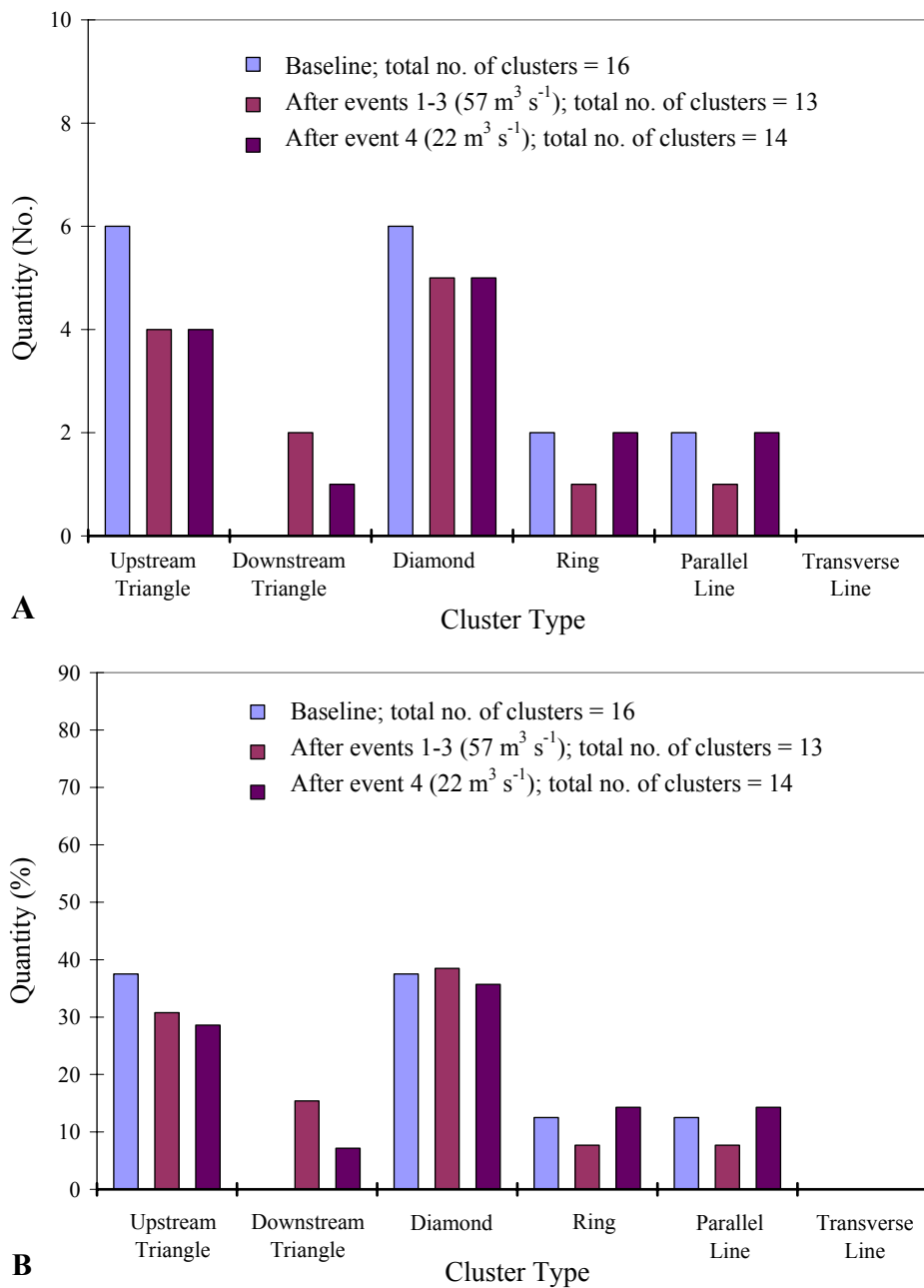


Figure 18. Cluster evolution for site 2 (all plots). (A) Number of each cluster morphology that were marked for the baseline dataset and relocated after each observed flow event during period of study. (B) Percentage of each cluster type out of the total number of clusters for the baseline dataset and after each observed flow event during period of study.

such as spawning salmonids. Anthropogenic disturbances are unlikely because of the relative seclusion of this site and the lack of evidence, such as large holes where clusters should have been or concentrated areas of cluster disturbance. Of greater concern are the isolated particles, which were sitting atop the bed and would be harder to determine if they were removed by flow or by other actions. These uncertainties were accounted for, in part, by using the mean of the five largest clustered and isolated particles that moved, so that if one were moved by something other than streamflow, it was averaged out.

No pattern was observed in the location of that clusters were destroyed within each plot, suggesting that at sites 1 and 2 the location of clusters on the bar was not an important factor in the stability of the cluster (Figures 19-23). Furthermore, no relationship could be determined between the flow depth over each cluster and whether the cluster was destroyed (Figures 19-23) or between the relative protrusion, or elevation, of each cluster morphology and its stability, as the elevation differences among the cluster morphologies were not statistically significant.

Cluster Evolution at Site 1

High-flow event 1. Of the original 37 clusters identified at site 1, 17 were destroyed by event 1 ($57 \text{ m}^3\text{s}^{-1}$). Three discounted “clusters” (see Methods section of this chapter) trapped additional particles and thus “reformed” into a diamond and 2 upstream triangles. Therefore, 23 clusters remained after event 1. Four clusters evolved into different cluster morphologies during event 1; a parallel line evolved into an upstream triangle, 2 diamond clusters evolved into upstream triangles, and 2 upstream

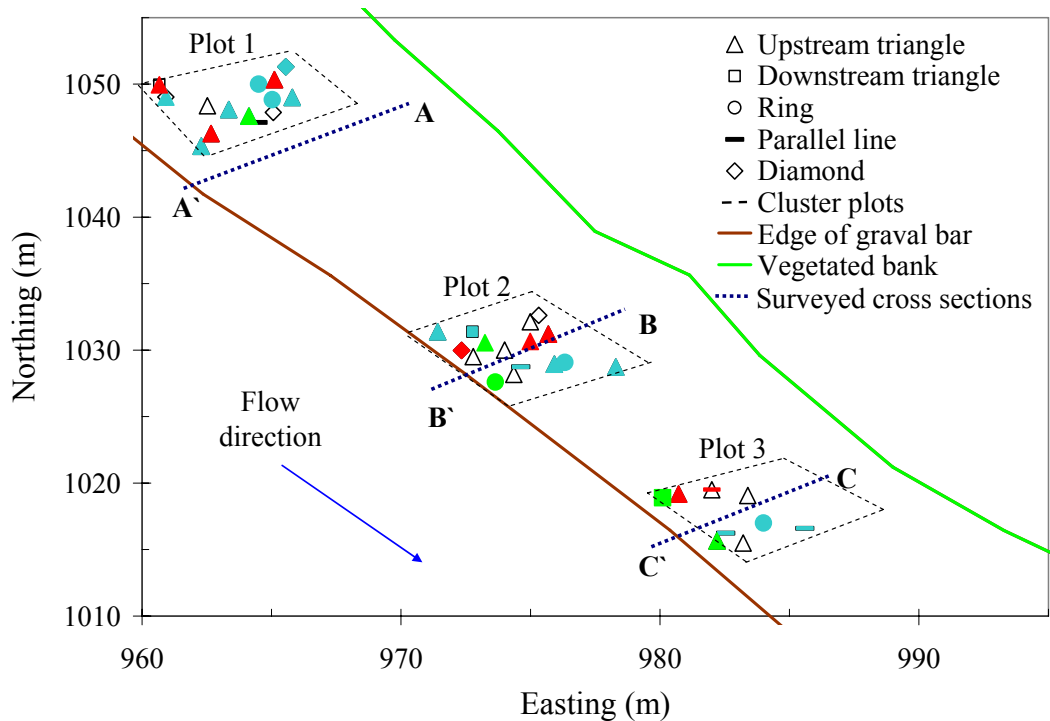


Figure 19. Spatial distribution of cluster morphologies at site 1. Colored symbols represent cluster morphologies that were destroyed by a given flow event: aqua = event 1, red = event 3, green = event 4. Letters represent cross-sectional profile data presented in Figures 20 and 21.

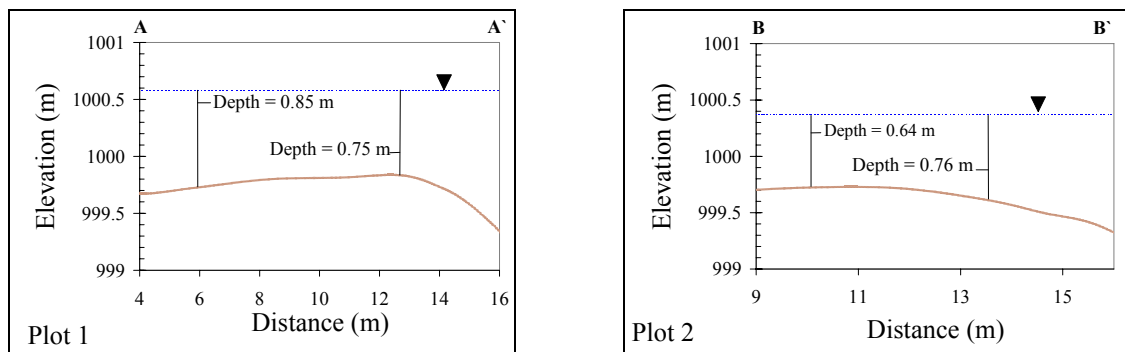


Figure 20. Cross-sectional profile data from plots 1 and 2 at site 1. Brown line represents ground surface, dashed-blue line represents water-surface elevation during event 1.

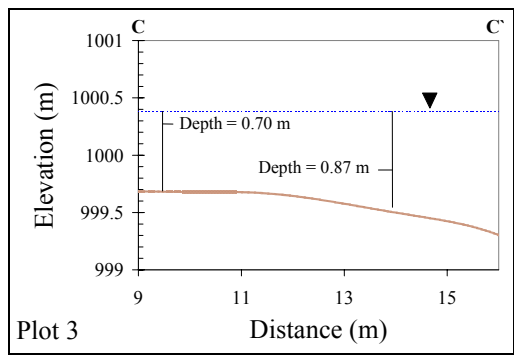


Figure 21. Cross-sectional profile data from plot 3 at site 1. Letters represent position of cross-section lines on Figure 19. Brown line represents ground surface, dashed-blue line represents water-surface elevation during event 1.

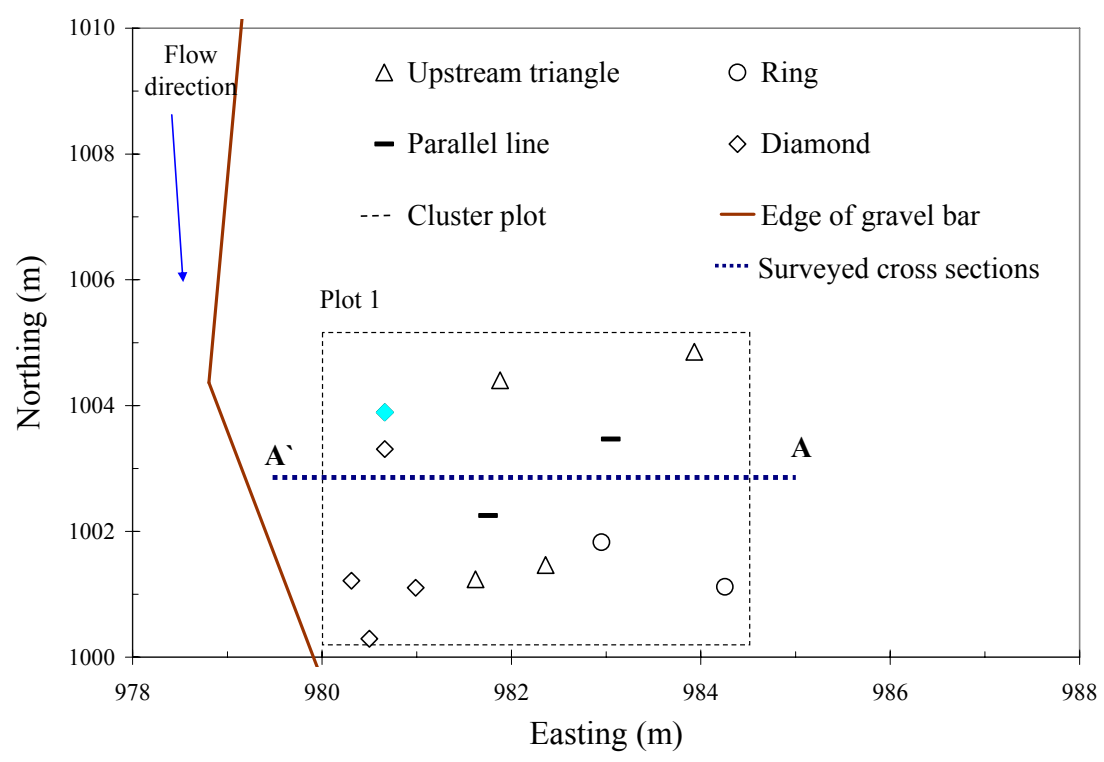


Figure 22. Spatial distribution of cluster morphologies at site 2. Aqua-colored symbol represents cluster morphology that was destroyed by flow event 1. Letters represent cross-sectional profile data presented in Figure 23.

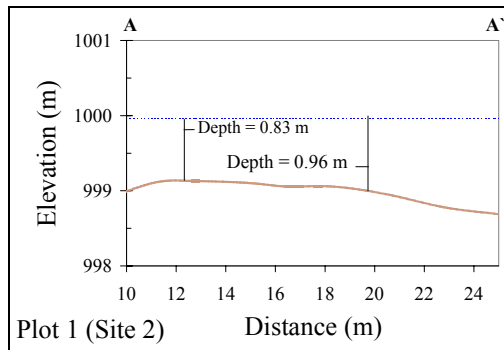


Figure 23. Cross-sectional profile data from plot 1 at site 2. Letters represent position of cross-section lines on Figure 22. Brown line represents ground surface, dashed-blue line represents water-surface elevation during event 1.

triangles evolved into a ring and parallel line, respectively. In general, the clusters that remained stable experienced some particle removal, and then deposition (likely during the waning stages of the event), which suggests that event 1, while producing flows large enough to mobilize particles within clusters, was also large enough to supply the bar with new sediment from upstream.

High-flow event 2. The clusters remained stable during event 2 ($13 \text{ m}^3 \text{ s}^{-1}$), as did isolated particles that could be seen in the wide-angle photographs, suggesting that a flow event equal to or less than $13 \text{ m}^3 \text{ s}^{-1}$ will not mobilize clustered or isolated particles at site 1.

High-flow event 3. Event 3 ($39 \text{ m}^3 \text{ s}^{-1}$) destroyed 9 clusters, while 5 clusters that were either destroyed by event 1 or discounted from the original dataset reformed, one in a new location, so the total number of clusters remaining after event 3 equaled 19. Numerous particle additions to remaining clusters were also noted, suggesting that although event 3 was the second largest of the observed flow events (see Figure 16)

destroying 9 of the remaining 23 clusters, it also appears to have been a depositing event, supplying new particles that were trapped by some of the remaining anchor clasts. One possible reason that event 3 was a depositing event was its duration. This event represented the spring runoff of 3-months duration and, therefore, the longest lasting observed event and had the longest waning period (see Figure 16). It is during the waning stages of a flood event that most gravel-cobble-sized particles are deposited (Brayshaw, 1984; Knighton, 1998). Two clusters evolved into different cluster morphologies during event 3: a diamond evolved into a downstream triangle and an upstream triangle evolved into a diamond. All 5 clusters that reformed did so into upstream triangles. This observation, combined with the observation that the upstream triangle was the most abundant cluster type at site 1, suggests that the upstream triangle may be the initial cluster morphology to form during the evolutionary cycle of a cluster. For a more detailed discussion of the evolutionary cycle of clusters see the Comparison with Previous Work section of this chapter.

High-flow event 4. Five clusters were destroyed during event 4 ($22 \text{ m}^3\text{s}^{-1}$), while one previously discounted (from the baseline dataset, as explained earlier in this chapter) reformed into an upstream triangle. This left only 15 of the original 37 clusters remaining at site 1. One downstream triangle cluster evolved into a diamond type, while an upstream triangle reformed into a diamond.

Cluster Evolution at Site 2

At site 2, the diamond and upstream triangle were the most abundant cluster morphologies (Figure 18), each accounting for 37% (6 of 16 total clusters) of the

original baseline dataset. In general, all the clusters remained stable during all four flow events at site 2, with the total number of clusters decreasing by only 2, from 16 to 14. However, there was particle movement and deposition within the clusters, as explained below.

High-flow events 1-3. During events 1-3 (recall that site 2 was not accessible until after event 3, as explained earlier), 3 clusters were destroyed, 2 clusters evolved from a diamond to a downstream triangle, and another changed from a ring to a diamond. Furthermore, some of the clusters experienced particle removal, but either did not lose enough particles to be destroyed or the anchor trapped new particles during waning stages of event 3.

High-flow event 4. No clusters were destroyed during event 4 ($22 \text{ m}^3 \text{ s}^{-1}$). One anchor particle that was displaced by events 1-3 trapped new particles and reformed into a parallel line cluster in a different location, and another remnant anchor clast was displaced downstream and joined two other anchor particles to form a large ring cluster.

Comparison with Previous Work

At site 1, nearly half of all clusters that were destroyed during the period of study were destroyed by complete cluster mobilization (anchor clast and particles entrained and transported downstream): 8 of 17 during event 1, 3 of 9 during event 3, and 3 of 5 during event 4. The other clusters were destroyed by mobilization of only the clustered particles while the anchor clast remained in place. There was also complete mobilization, and then reformation in a new location, of one cluster during event 3. At

site 2 only 3 clusters were destroyed during the period of study, each by complete mobilization of the cluster, including the anchor clast.

Brayshaw (1985) and Reid et al. (1992) suggested that mobilization of anchor clasts must occur prior to cluster destruction, while de Jong (1991) and Billi (1988) suggested clustered particles could be removed without anchor clast mobilization. Results from the Entiat River indicate that at site 1, with nearly uniform sediment-size distribution, both methods of cluster destruction occurred. However, results from site 2, with a bi-modal sediment-size distribution, suggest that anchor clast mobilization must occur prior to cluster destruction, supporting the results of Brayshaw (1985) and Reid et al. (1992). Therefore, while both hypotheses of cluster destruction appear to be correct, results from the present study indicate that sediment-size distribution is a major controlling factor in the method of cluster destruction. Other factors, including particle size, shape, density, packing, and flow conditions are also likely to affect the method of cluster destruction.

Laboratory flume experiments conducted by Strom (2002) and Papanicolaou et al. (2003) showed the following evolutionary cycle of cluster morphologies under increasing flows: no cluster → two-particle cluster → comet → triangle → rhomboid → cluster break-up (Figure 24). This cycle was indicated by two particles that come in contact during low flow forming an “inline” cluster (Strom, 2002; Papanicolaou et al., 2003). As flow strength increases, this two-particle cluster captures incoming particles either in its wake or stoss and forms a comet cluster, described as a “loosely-packed” cluster that does not require particle-to-particle contact to influence flow. As flow

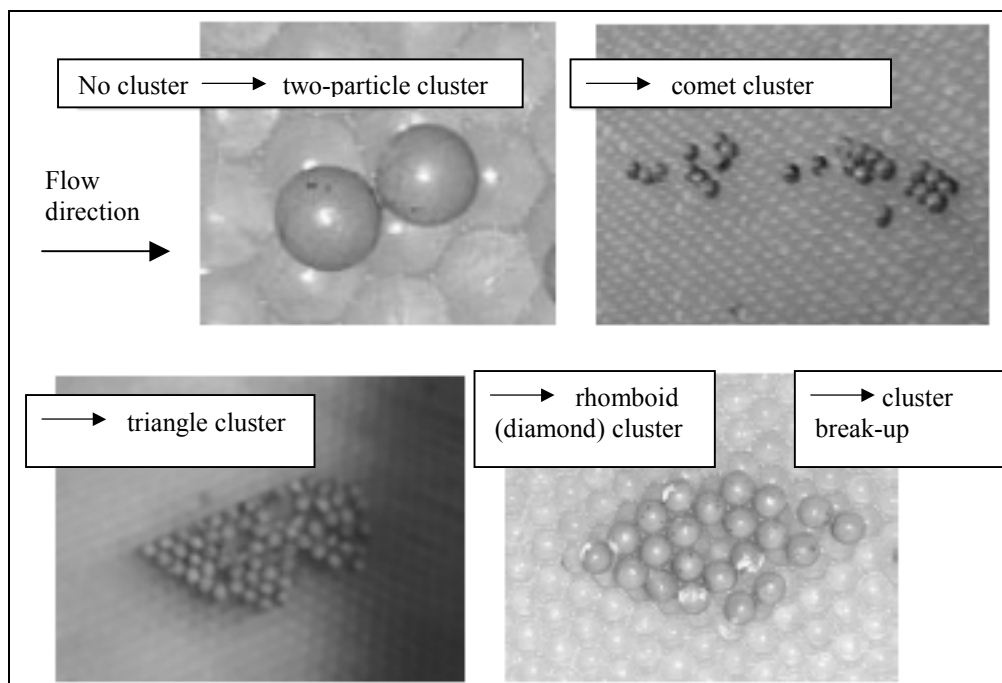


Figure 24. Cluster evolution as observed in laboratory flume experiments. Glass spheres were used in place of sediment. Evolutionary cycle, under increasing flows, is no cluster → two-particle cluster → comet cluster → triangle cluster → rhomboid (diamond) cluster → cluster break-up. Photographs are from Papanicolaou et al. (2003).

strength continues to increase, the cluster begins to form into upstream or downstream triangles. Finally, as more particles are captured by the cluster at the highest flow strengths, it forms a rhomboid morphology. The rhomboid cluster, which is the same shape as the diamond cluster described in the present study, is thought to be the most stable cluster morphology due to its hydrodynamic shape, which produces the lowest drag forces acting on the cluster (Strom, 2002; Papanicolaou et al., 2003).

In the Entiat River there were 17 clusters that evolved from one cluster morphology to another during the 4 high flow events observed during this study, but no consistent evolutionary pattern was observed and only one upstream triangle evolved

into a diamond cluster type. This lack of an apparent evolutionary cycle may be due to the order of the flow events observed during this study, with the largest event first, followed by the smallest event, a mid-sized event, and then another small event (see Figure 16). These flow patterns are different from the experimentally generated smallest-to-largest flow conditions produced by Strom (2002) and Papanicolaou et al. (2003), and may have disrupted the evolutionary cycle of the clusters in the field. Further complicating the field-based evolutionary patterns of clusters is the fact that many clusters were destroyed at site 1 during flow events 1, 2, and 3, which may have “reset” the cluster cycle after each flow event. If the upstream triangle represents the initial cluster morphology after two-particle and comet clusters, which were not considered during this study (see below), the resetting of the cluster cycle may explain why the upstream triangle is the most abundant cluster morphology in the Entiat River.

Although no evolutionary pattern could be found for clusters, the initial formation morphologies of clusters in the Entiat River may be similar to those found by Strom (2002) and Papanicolaou et al. (2003). Although two-particle “clusters” were not defined as clusters in the Entiat River, two-particle clusters were noted, some of which were originally defined as clusters but then discounted after initial reevaluation (see Methods section of this chapter). In addition, some clusters that were destroyed (without anchor mobilization) by a previous flow event remained as a two-particle cluster, and were still tracked before and after each subsequent event. During the period of this study, 6 two-particle clusters reformed into upstream triangles (one formed into a diamond). These results suggest that it is likely that two-particle clusters are

predecessors of cluster formation, especially triangle clusters, supporting the results found by Strom (2002) and Papanicolaou et al. (2003).

Results from flume experiments conducted by Strom (2002) and Papanicolaou et al. (2003) also showed that the rhomboid, or diamond, cluster was the most stable morphology, which has also been shown in other field and laboratory studies (Reid et al., 1992). Results from the Entiat River showed that the upstream triangle was the most abundant cluster morphology at site 1 and that many clusters were unstable. At site 2 the diamond and upstream triangle were the most abundant cluster morphologies, and clusters remained fairly stable over the entire study period compared to site 1, where grain sizes were smaller and there were fewer diamond clusters. These results from site 2 suggest that the diamond may be the most stable cluster morphology in the Entiat River at site 2, which supports the laboratory flume results Strom (2002) and Papanicolaou et al. (2003). At site 1, although the absolute number of diamond clusters decreased, their percentage of the total number of clusters remained relatively consistent compared with the other cluster morphologies (see Figure 17).

Effects on Sediment Transport

Particle Size

In order to determine the effects of clusters on sediment transport, the sizes of isolated and clustered particles that were entrained during a given high flow event were compared (Table 4 and Figures 25 and 26). The clustered particles included those particles that were anchor clasts if the entire cluster was mobilized. It is recognized that larger isolated particles may have been entrained that were not observable in the before-

TABLE 4. MEDIAN DIAMETER OF PARTICLE SIZES ENTRAINED BY A GIVEN FLOW EVENT

Event and site/plot no.	Median diameter (b-axis) of five largest isolated particles that were entrained (cm)	Median diameter (b-axis) of five largest clustered particles that were entrained (cm)	Difference* (%)
<u>Event 1 ($57 \text{ m}^3\text{s}^{-1}$)</u>			
Site 1 (Plot 1)	6.4	5.4	19
Site 1 (Plot 2)	8.0	6.7	19
Site 1 (Plot 3)	7.2	6.3	14
Site 2 (Plot 1)	8.2	7.0	17
<u>Event 2 ($13 \text{ m}^3\text{s}^{-1}$)</u>			
Site 1 (Plot 1)	No observed movement	No observed movement	Not applicable
Site 1 (Plot 2)	No observed movement	No observed movement	Not applicable
Site 1 (Plot 3)	No observed movement	No observed movement	Not applicable
Site 2 (Plot 1)	No data	No data	Not applicable
<u>Event 3 ($39 \text{ m}^3\text{s}^{-1}$)</u>			
Site 1 (Plot 1)	7.4	4.1	80
Site 1 (Plot 2)	6.5	6.1	7
Site 1 (Plot 3)	6.6	4.1	61
Site 2 (Plot 1)	No data	No data	Not applicable
<u>Event 4 ($22 \text{ m}^3\text{s}^{-1}$)</u>			
Site 1 (Plot 1)	6.8	3.6	89
Site 1 (Plot 2)	5.8	5.8	0
Site 1 (Plot 3)	6.5	2.2	19
Site 2 (Plot 1)	8.7	5.3	64
<p><i>Note:</i> The median b-axis diameter (D_{50}) for the entire gravel bar at site 1 is 3.8 cm. The D_{50} for the entire gravel bar at site 2 is 5.9 cm. The median b-axis diameter of the five largest particles on the entire bar (D_{100}) is 10 cm at site 1. The D_{100} at site 2 is 23.5 cm.</p> <p>*Differences for all plots and all flow events were statistically significant with a P value of 0.0034.</p>			

and-after photographs used to track cluster evolution (see Methods section of this chapter). There also may have been larger particles entrained within other clusters outside of the cluster plots that were not part of the original clusters tracked during the period of this study.

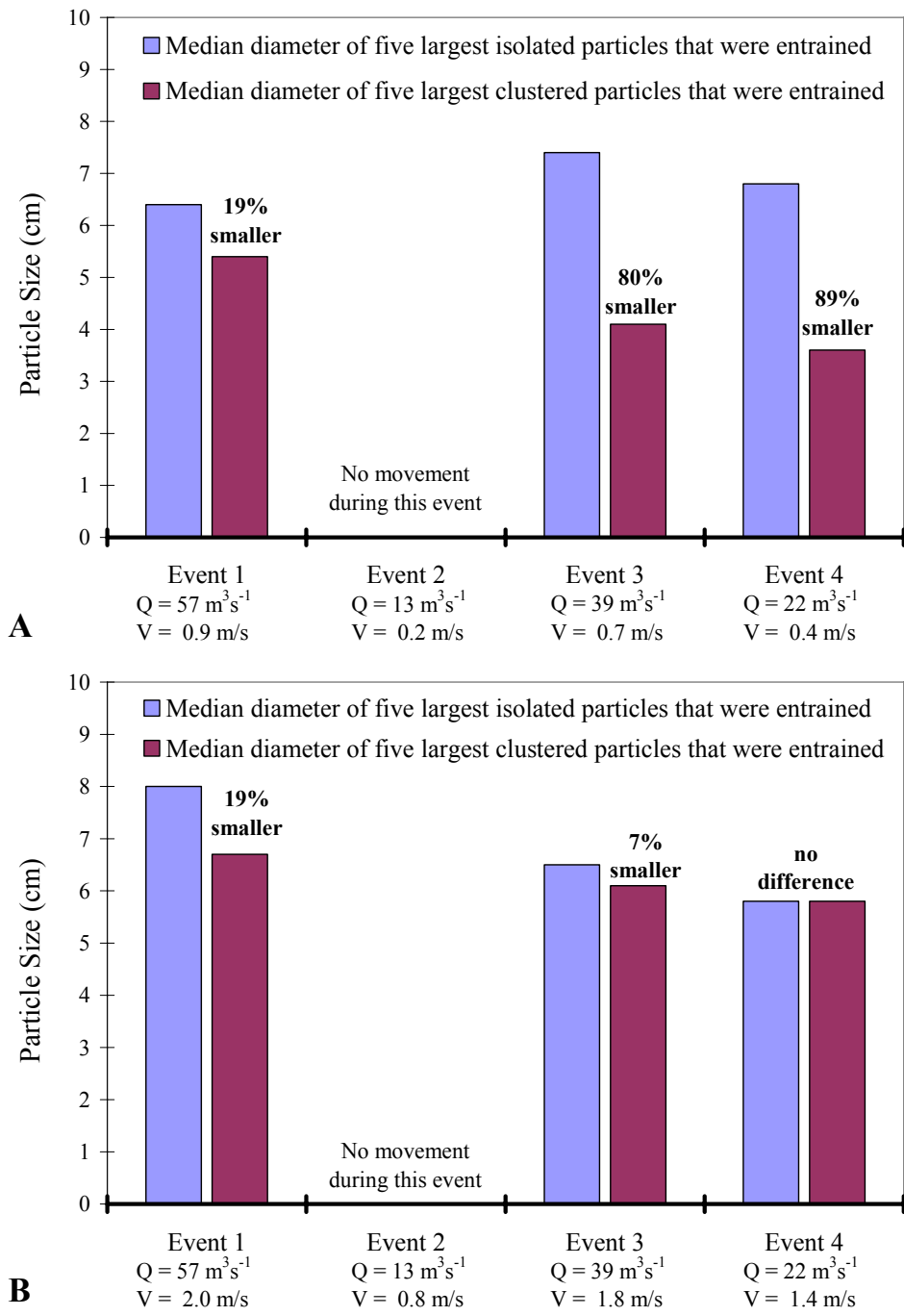


Figure 25. Median diameter of largest isolated and clustered particles entrained by each flow event at site 1. Figure shows site 1, plots 1 (A) and 2 (B). Percentage smaller represents the percentage difference between the size of isolated and clustered particles. Differences were statistically significant with a *P* value of 0.0034.

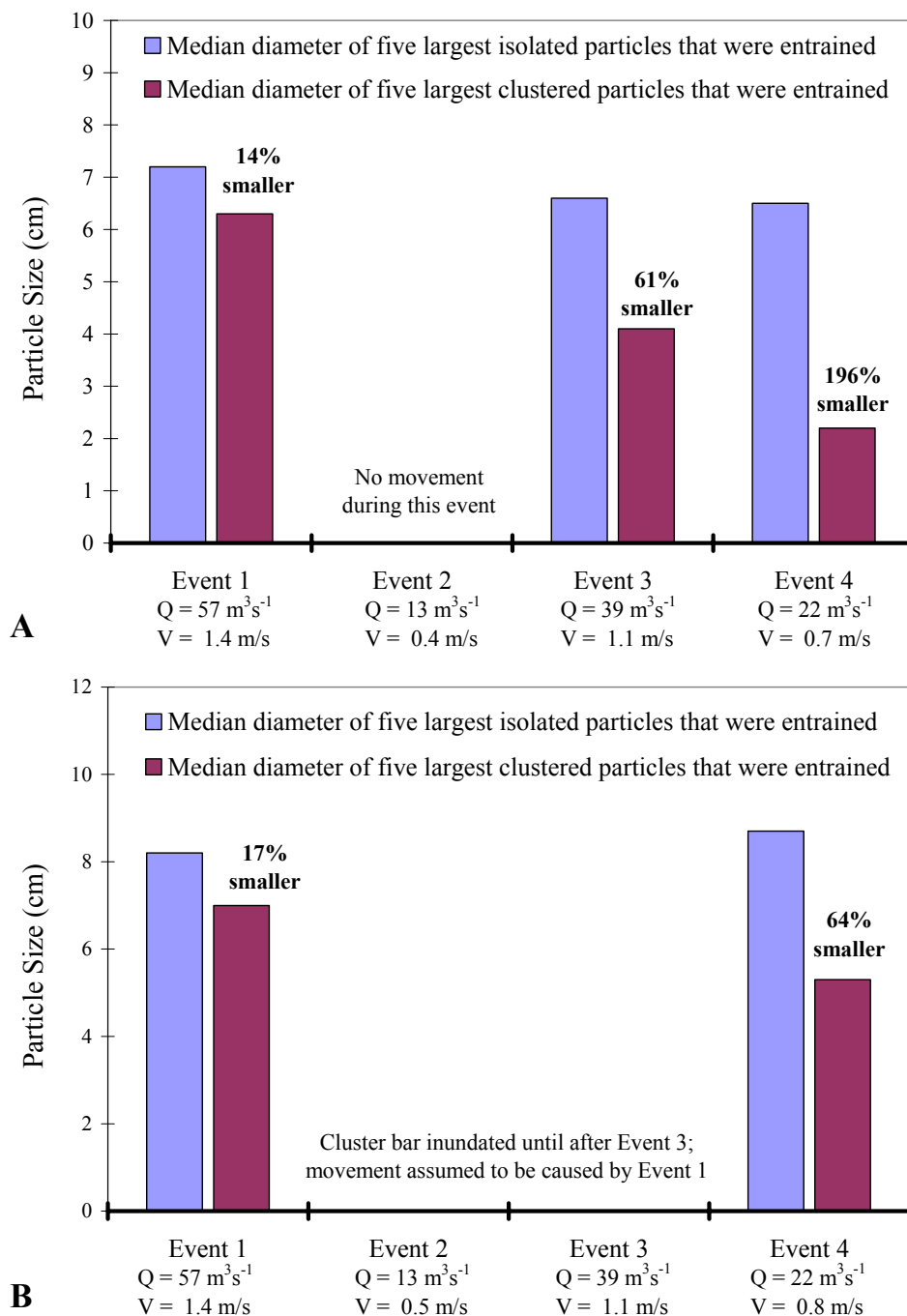


Figure 26. Median diameter of largest isolated and clustered particles entrained by each flow event at sites 1 and 2. Figure shows site 1, plots 3 (A) and site 2, plot 1 (B). Percentage smaller represents the percentage difference between the size of isolated and clustered particles. Differences were statistically significant with a P value of 0.0034.

At site 1, mean particle size for the entire gravel bar (D_{50}) was 3.8 cm, while the mean b-axis diameter of the five largest particles on the gravel bar (D_{100}) was 10 cm (Table 4). At site 2 the D_{50} was 5.9 cm while the D_{100} was 23.5 cm (Table 4). In general, both D_{50} - and D_{100} -sized particles were observed as isolated and clustered, meaning that there was sufficient opportunity for isolated and clustered particles of similar sizes to be entrained and there was no bias of the results because only smaller-sized particles were present within clusters. This suggests that flow hydraulics, such as bed shear stress, surrounding the clustered particles is limiting entrainment and not the limited availability of larger particle sizes within clusters.

Statistical analyses of the differences in the sizes of isolated and clustered particles that were entrained during each flow event were run using the Wilcoxon Rank Sum test (Wilcoxon, 1945; Mann and Whitney, 1947). Results from this test showed that clustered particles were significantly smaller than isolated particles, with a P value of 0.0034. Appendix A shows the five largest entrained clustered and isolated particles used to determine the mean values discussed in this chapter.

In general, isolated and cluster particle sizes entrained by event 1 were similar at both sites, with the clustered particles between 17% and 19% smaller than isolated particles. These results suggest that for flows equal to or greater than event 1 ($57 \text{ m}^3 \text{ s}^{-1}$, with a range of velocities ranging from 0.9 to 2.0 m/s over the gravel bar based on HEC-RAS calculations), clusters may have only moderate effects in delaying sediment transport. No movement was observed during event 2 ($13 \text{ m}^3 \text{ s}^{-1}$, with velocities ranging from 0.2 to 0.7 m/s), as discussed earlier, suggesting that all sediment particles,

clustered or isolated, remain stable at flows less than $13 \text{ m}^3\text{s}^{-1}$. This observation provides an estimate of the lower flow limit for cluster and general gravel-bed mobilization at site 1. During event 3 ($39 \text{ m}^3\text{s}^{-1}$, with velocities ranging from 0.7 to 1.6 m/s), entrained clustered particles were between 7% and 81% smaller than the entrained isolated particles at site 1. Recall that no observation was made for site 2 until after event 3, and isolated and cluster movement was assumed to be caused by event 1 because it was the largest event. Event 4 ($22 \text{ m}^3\text{s}^{-1}$, with velocities ranging from 0.4 to 1.3 m/s) produced the largest range of differences in isolated vs. clustered particles that were entrained, with clustered particles between 0% and 196% smaller than isolated particles. The large size difference (196%) occurred at plot 3 (Figure 26A) and likely resulted from limited clustered particle sample size, because many of the remaining clusters at this plot were destroyed by events 1 and 3.

There is a large range in the sizes of isolated and clustered particles entrained during events 3 and 4 (Table 4). The low values in these ranges were caused by the relatively small difference between the five largest entrained isolated and clustered particles at plot 2 of site 1 during events 3 and 4 (Table 4). During event 3, two clusters that were completely mobilized (including anchor) had larger particles, causing the mean of the five largest clustered particles to be larger (Table 4). During event 4, a ring cluster that included an anchor clast 10 cm in diameter was completely mobilized, causing the mean of the five largest clustered particles entrained to be 5.8 cm (Table 4). Omitting this larger anchor clast would reduce the mean of the five largest clustered particles entrained to 4 cm during event 4. It is unclear why this large ring cluster

remained stable during events 1 and 3, both larger events, but was mobilized during event 4. One possible explanation is that there was a large amount of snow and ice on the gravel bar at site 1 during event 4 (Archibald, personal communication, October 18, 2004). This ice may have caused higher velocities and shear stresses on the bar as water moved around the ice during the flow-event, which would not be detected by the HEC-RAS model. Other possible explanations include human or biologic disturbances or variations in near-bed flow conditions, such as velocity bursts or turbulence that cannot be accounted for in the field by equations or models used in this study. Finally, particles at plot 2, both clustered and isolated, may be entrained at lower shear stress values compared to plots 1 and 3 at site 1. However, the effect of clusters on sediment transport was clear during events 3 and 4 at plots 1 and 3 (Table 4, Figures 25 and 26).

Also worth noting in Figure 25A is the larger size of isolated particles that were entrained during events 3 and 4 compared to the size of the isolated particles that were entrained during event 1 (a larger flow event) within plot 1 at site 1. A possible explanation for this is that either there were larger particles that moved during event 1 that were not observed (due to the limitation of the area photographed), or that larger isolated particles, possibly transported from upstream and deposited during the waning stages of event 1, were available during events 3 and 4. These particles would likely have been entrained during event 1 as well, but were not available.

From the above discussions it can be seen that there are uncertainties involved in determining the size differences between isolated and clustered particles, such as observable area imposed by the area of the bar photographed, limited sample sizes, etc.

However, in spite of these uncertainties the effect of clusters is clear; they impede entrainment of clustered particles while particles of similar or greater size that are isolated on the bed are being entrained.

Critical Shear Stress

An additional approach to determining the effects of clusters on sediment transport, the critical shear stress required to entrain the isolated and clustered particles, was calculated using the Shields and Komar equations (Table 5 and Figures 27 and 28).

TABLE 5. DIMENSIONLESS CRITICAL SHEAR STRESS FOR PARTICLE ENTRAINMENT

Event and site/plot no.	Critical shear stress at entrainment of particles as calculated by Shields equation		Difference* (%)	Critical shear stress at entrainment of particles as calculated by Komar equation		Difference† (%)
	Isolated	Clustered		Isolated	Clustered	
	<u>Event 1</u>					
Site 1/plot 1	0.052	0.062	19	0.032	0.036	12
Site 1/plot 2	0.046	0.055	19	0.028	0.031	12
Site 1/plot 3	0.114	0.130	14	0.030	0.032	9
Site 2/plot 1	0.037	0.044	17	0.027	0.030	11
<u>Event 2</u>						
Site 1/plot 1	N.A.	N.A.	N.A.	N.A.	N.A.	N.A.
Site 1/plot 2	N.A.	N.A.	N.A.	N.A.	N.A.	N.A.
Site 1/plot 3	N.A.	N.A.	N.A.	N.A.	N.A.	N.A.
Site 2/plot 1	N.D.	N.D.	N.D.	N.D.	N.D.	N.D.
<u>Event 3</u>						
Site 1/plot 1	0.044	0.079	80	0.029	0.043	47
Site 1/plot 2	0.042	0.045	7	0.032	0.033	4
Site 1/plot 3	0.088	0.142	61	0.031	0.043	36
Site 2/plot 1	N.D.	N.D.	N.D.	N.D.	N.D.	N.D.
<u>Event 4</u>						
Site 1/plot 1	0.023	0.043	89	0.031	0.047	51
Site 1/plot 2	0.036	0.036	0	0.034	0.034	0
Site 1/plot 3	0.040	0.119	195	0.032	0.064	102
Site 2/plot 1	0.014	0.022	64	0.026	0.036	38

Note: N.A. = not applicable; N.D. = no data.

*Differences were statistically significant with a P value of 0.0299.

† Differences were statistically significant with a P value of 0.0125.

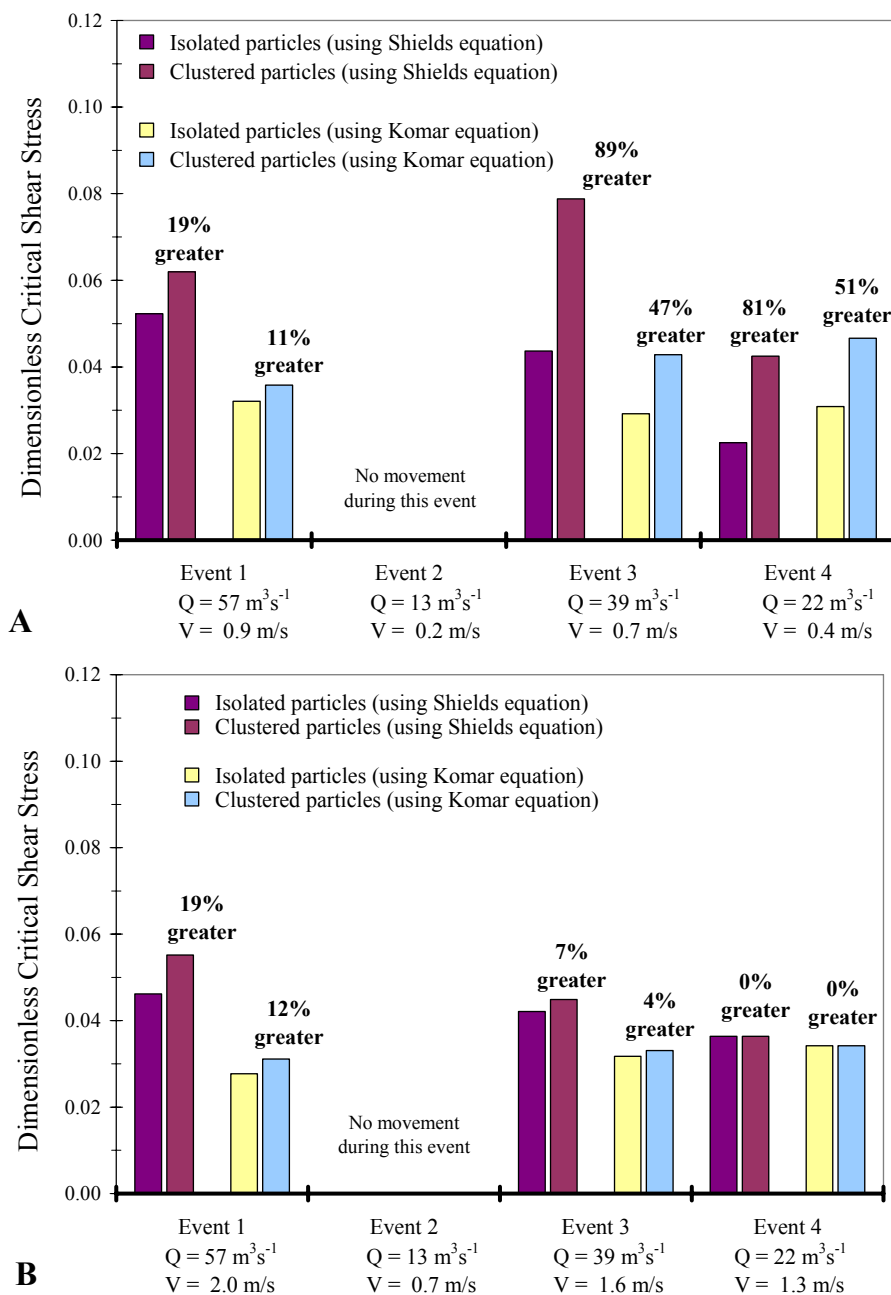


Figure 27. Critical shear stress values for largest isolated and clustered particles entrained by each flow event. Values are for site 1, plots 1 (A) and 2 (B). Percentage greater represents the percentage difference between the critical shear stress required to entrain the isolated and clustered particles. Differences were statistically significant with P values of 0.0299 using the Shields equation and 0.0125 using the Komar equation.

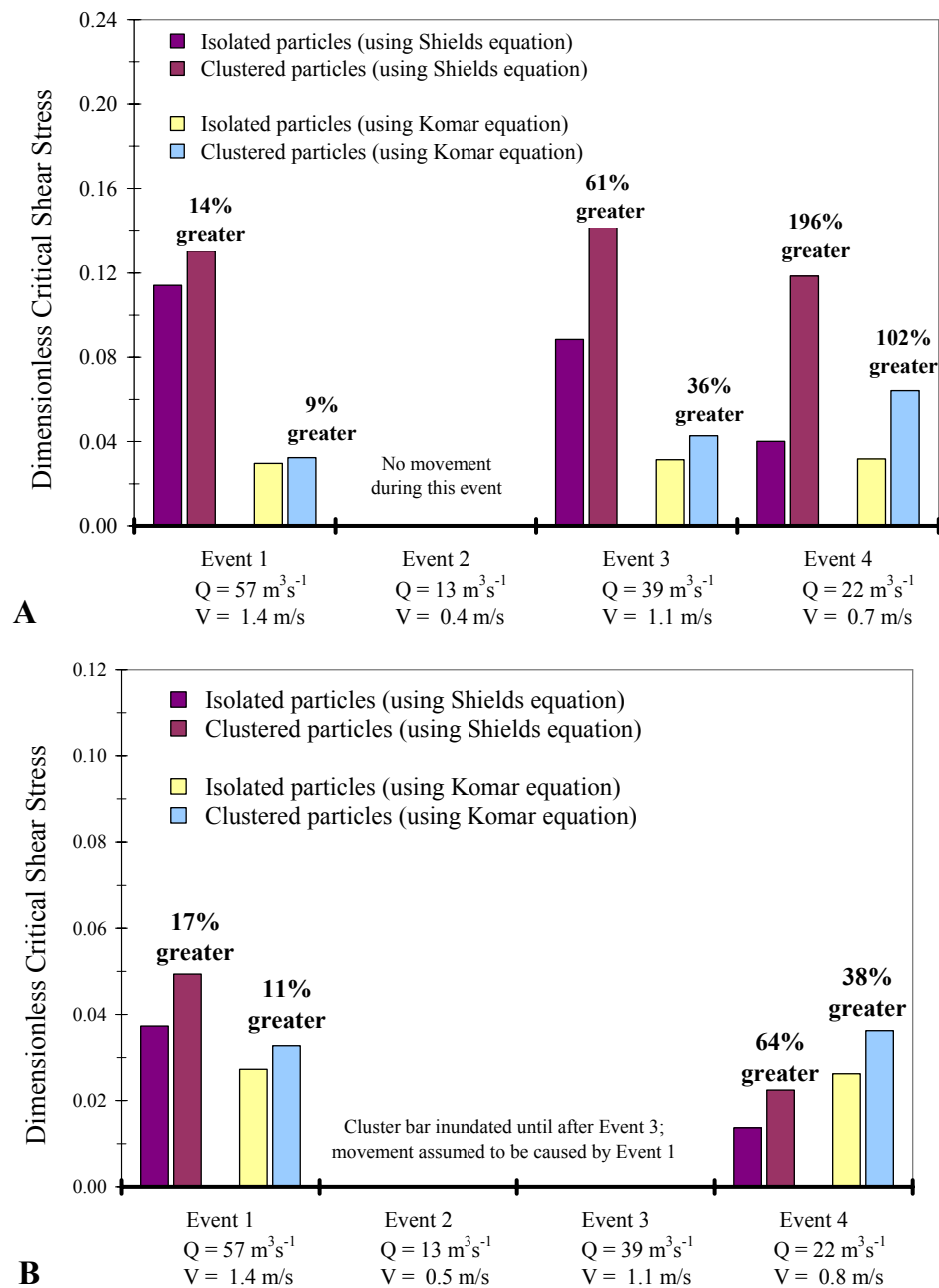


Figure 28. Critical shear stress values for largest isolated and clustered particles entrained by each flow event. Values are for site 1, plot 3 (A) and site 2, plot 1 (B). Note different scale in Part A. Percentage greater represents the percentage difference between the critical shear stress required to entrain the isolated and clustered particles. Differences were statistically significant with P values of 0.0299 using the Shields equation and 0.0125 using the Komar equation.

Statistical analyses of the differences in the critical shear stress values for entrained isolated and clustered particles were run using the Wilcoxon Rank Sum test (Wilcoxon, 1945; Mann and Whitney, 1947). Results from this test showed that the critical shear stress required to entrain clustered particles was significantly greater than for isolated particles, with a P value of 0.0299 when the Shields equation was used and 0.0125 when the Komar equation was used.

High-flow event 1. During event 1, clusters had a moderate effect on sediment transport. At site 1, the critical shear stress required to entrain isolated particles ranged from 0.046 to 0.114 as calculated using the Shields equation. Clustered particles required critical shear stresses of 0.055 to 0.130, 14%-19% greater than for isolated particles. The Komar equation yielded smaller critical shear stress values of 0.028-0.032 for isolated particles and 0.031-0.036 for clustered particles, but still a 9%-12% difference. The upper range of the critical shear stress values (0.114 and 0.130) calculated from the Shields equation are higher than expected, as Buffington and Montgomery (1997) reported a range of critical shear stress values of 0.012-0.087 based on data compiled from eight decades of incipient motion studies. Implications of these high values are discussed in the Discussion and Summary sections of this chapter.

At site 2, there were similar differences in the critical shear stress values for isolated and clustered particles during event 1. The Shields equation yielded critical shear stress values of 0.037 for isolated particles and 0.044 for clustered particles, a 17% increase, while the Komar equation yielded values of 0.027 for isolated and 0.030 for clustered particles, an 11% increase. This may seem contradictory to the conclusion

that site 2 had more stable clusters (see chapter III); however, one weakly formed cluster destroyed during event 1 (the only one destroyed) entrained two large particles that increased the mean b-axis diameter of the five largest particles entrained (7.0 cm, see Table 4), which was used in the critical shear stress equations. Removing these two particles from the five largest particles entrained would reduce the mean of the five largest particles to 6.2 cm and increase the critical shear stress values calculated for clustered particles to 0.049 (Shields equation) and 0.033 (Komar equation). Using these values would result in 33% and 20% increases in critical shear stress values for clustered particles compared to isolated particles, using the Shields and Komar equations, respectively. Therefore it can still be concluded that clusters at site 2 are more stable than at site 1, as stated in chapter III.

High-flow event 2. There was no observed movement of isolated or clustered particles during event 2 at site 1. The gravel bar at site 2 was inaccessible during this event, and minimal to no movement is assumed.

High-flow event 3. Clusters appeared to have a greater effect on sediment entrainment during event 3 at site 1 compared to event 1. The Shields equation yielded critical shear stress values that ranged from 0.042 and 0.088 for isolated particles and 0.045-0.142 for clustered particles, a 7%-89% increase. The Komar equation yielded values of 0.029-0.032 for isolated particles and 0.033-0.043 for clustered particles, a 4%-47% increase. The large range in these values is caused by the relatively small difference between the five largest entrained isolated and clustered particles at plot 2 of site 1, as noted earlier. Site 2 was inaccessible during this event.

High-flow event 4. Clusters also had a significant effect on sediment entrainment during event 4 at sites 1 and 2; the exception is plot 2 at site 1. Excluding plot 2 (which will be discussed below), the Shields equation yielded critical shear stress values of 0.023-0.040 for isolated particles and 0.043-0.119, an 81%-196% increase, for clustered particles. The Komar equation yielded values of 0.031-0.032 for isolated particles and 0.047-0.067, a 51%-102% increase for clustered particles. Because the mean of the five largest isolated and clustered particles entrained during event 4 were the same at plot 2, site 1 (see Table 4), both the Shields and Komar equations yielded a critical shear stress value of 0.036 for isolated and clustered particles. As discussed earlier, a ring cluster that included an anchor clast 10 cm in diameter was completely mobilized during event 4, causing the mean of the five largest clustered particles entrained to be 5.8 cm (Table 4). Omitting this larger anchor clast would reduce the mean of the five largest clustered particles entrained to 4 cm during event 4 and would increase the critical shear stress values to 0.053 (Shields equation) and 0.044 (Komar equation). These new values would result in 45% and 27% increases to the critical shear stress values of clustered particles compared to isolated particles, using the Shields and Komar equations, respectively.

The above mentioned increases in the critical shear stresses required to entrain clustered particles are consistent with previous field and laboratory flume experiments (Reid et al., 1992; Montgomery et al., 1996; Buffington and Montgomery, 1997; Church et al., 1998; Papanicolaou et al., 2003; Strom et al., 2004b). Reid et al. (1992) used the Shields equation to determine the critical shear stress for electrometric particles

seeded in clusters and in the open plane bed during the course of nine separate high flow events with discharges ranging from 0.4 to 7.1 m³s⁻¹. The results of Reid et al. (1992) are presented in Table 6.

TABLE 6. CRITICAL SHEAR STRESS VALUES REPORTED BY REID ET AL. (1992)

Flood date	Critical stress at entrainment of first particle		Difference* (%)	Range of critical stress at entrainment of particles	
	Plane-bed	Clustered		Plane-bed	Clustered
3/5/1981	0.015	0.017	13	0.015-0.052	0.017-0.052
3/9/1981	0.026	0.026	0	0.021-0.030	0.021-0.047
4/25/1981	0.022	0.029	32	0.021-0.073	0.027-0.073
6/1/1981	0.017	0.024	41	0.017-0.099	0.027-0.106
7/9/1981	0.039	0.036	8	0.033-0.044	0.036-0.044
9/19/1981	0.036	0.039	8	0.036-0.052	0.039-0.052
10/6/1981	0.024	0.036	50	0.024-0.045	0.036-0.045
10/20/1981	0.039	0.055	41	0.039-0.114	0.051-0.114
11/16/1981	0.024	0.029	21	0.011-0.042	0.013-0.042

Note: Plane-bed as referred to by Reid et al. (1992) = isolated particle in the present study.
 *Percentage differences were calculated by author of the present study.

Results reported by Reid et al. (1992) showed 0%-50% increases in the critical shear stresses required to entrain clustered particles. These values are slightly lower than the range found in the present study where the Shields equation was used (see Table 5 and Figures 27-28). This difference may be due to the smaller grain sizes of the seeded particles in the Reid et al. (1992) study (2.8 cm), which probably require less shear stress to be entrained. Also, because the seeded particles used in the Reid et al. (1992) study were artificially placed into the clusters or on the open-plane bed, they may have been less stable and more easily entrained. The percentage increases in critical shear stress values for clustered particles, some greater than 100% greater, found in the present study agree with those found by Church et al. (1998), Papanicolaou et al. (2003)

and Strom et al. (2004b), who each found that clusters were mobilized at twice the critical shear stress required to mobilize an isolated particle in laboratory flume experiments.

The critical shear stress values calculated from the Shields equation ranged from 0.014 to 0.144 for isolated particles and 0.022-0.142 for clustered particles within all plots at sites 1 and 2. The critical shear stress values calculated from the Komar equation were, in general, smaller, ranging from 0.026 to 0.034 for isolated particles and 0.028-0.047 for clustered particles within all plots at sites 1 and 2 (see Table 5). There was one example in which the Komar equation calculated higher values, at site 2 during event 4. These higher values are likely due to the fact that the Shields equation takes into account the average bed shear stress of each event, so that during a low flow event that entrained large particles such as event 4, values calculated by the Shields equation will be smaller because it accounts for both the small flow event and the large particle that was entrained, and thus predicts a smaller critical shear stress value for that particle. In contrast, the Komar equation only accounts for the size of the particle entrained compared to the average size of the sediment on the bed with constant coefficients.

Buffington and Montgomery (1997) reported a range of critical shear stress values, based on data compiled from eight decades of incipient motion studies from natural rivers and laboratory flumes that used various critical shear stress equations, including the Shields equation, to be 0.012-0.087. Church et al. (1998) and Reid et al. (1992) cited that critical shear stress values can be as high as 0.1 in some rivers, while

Reid et al. (1992) reported values from their study to be 0.011-0.114 (Table 6). Knighton (1998) even reported that some studies have described values as high as 0.25, although unlikely. All the values calculated by the Komar equation were well within these ranges (Table 5), suggesting accurate estimations of critical shear stress values based on field data from the present study. Some values calculated by the Shields equation were higher than 0.087 (plot 3 at site 1 for events 1, 3, and 4), suggesting that the Shields equation may be over-predicting critical shear stress values, which may be expected given the simplistic nature of this equation (Strom, 2002; Papanicolaou et al., 2003). Values derived from the Shields equation therefore provide upper-end estimates of the shear stress required to entrain both clustered and isolated particles within the study reach. These values would prove useful in determining the range of flows required to entrain similar-sized sediment within similar river systems, especially if those rivers have regulated flow regimes so that river managers can design maintenance flows that are large enough to transport regular sediment fluxes but do not create significant erosion.

In spite of possible over- or under-predictions of critical shear stress values, the equations were applied equally to isolated or clustered particles and any associated errors associated can be assumed to be systematic for both isolated and clustered particles. Furthermore, it is the percentage difference between the values that was of major interest in the present study, and whether the critical shear stress is 0.03 for isolated and 0.045 for clustered particles or 0.1 for isolated and 0.15 for clustered particles, the increase for the clustered particles is 50% in both cases.

A major component of shear stress acting on a gravel bed is the amount of water, or flow depth, flowing over the top of the gravel-bed particles. Because the Duboys equation calculates the average bed shear stress from flow depth, and the Shields equation calculates the critical shear stress based on the average bed shear stresses the varying flow depths, a possible uncertainty exists when using the average flow depth each plot. For example, an isolated particle located in a section of the plot with greater flow depths would be under greater shear stress. To test this uncertainty, the minimum and maximum flow depths of each plot, based on the largest observed flow event (Figures 19 and 21) were incorporated into the calculation of average bed shear stress and then into the critical shear stress using the Shield equation (Table 7). The critical shear stress that would be required to entrain the mean diameter of the five largest isolated and clustered particles were calculated assuming the isolated particles were located in the section of the plot with the greatest flow depth and the clustered particles were located in the section of the plot with the least flow depth. This scenario provides an estimate of the minimum possible differences in critical shear stress estimates between the clustered and isolated particles. The percentage difference between these critical shear stress values were compared to the percentage difference found using the average flow depth (see Table 5 and Figures 27 and 28). If the percentage difference between isolated and clustered particles was positive, then clusters were still considered to be delaying sediment transport, regardless of the variations in flow depths at the given plot. However, if the percentage difference between isolated and clustered particles was negative and the critical shear stress for

TABLE 7. CRITICAL SHEAR STRESS VALUES BASED ON MINIMUM AND MAXIMUM FLOW DEPTHS

Event and site/plot no.	Minimum flow depth (m)	Maximum flow depth (m)	Critical shear stress for isolated particles using maximum flow depth	Critical shear stress for clustered particles using minimum flow depth	Difference using minimum and maximum flow depths (%)*	Difference using average flow depth (%) [†]
<u>Event 1</u>						
Site 1/plot 1	0.75	0.85	0.059	0.062	4.6	19
Site 1/plot 2	0.64	0.76	0.048	0.049	0.5	19
Site 1/plot 3	0.70	0.87	0.126	0.116	-8.0	14
<u>Event 2</u>						
Site 1/plot 1	N. A.	N. A.	N. A.	N. A.	N. A.	N. A.
Site 1/plot 2	N. A.	N. A.	N. A.	N. A.	N. A.	N. A.
Site 1/plot 3	N. A.	N. A.	N. A.	N. A.	N. A.	N. A.
<u>Event 3</u>						
Site 1/plot 1	0.55	0.65	0.049	0.075	52.7	80
Site 1/plot 2	0.47	0.58	0.045	0.039	-13.7	7
Site 1/plot 3	0.56	0.68	0.107	0.142	32.6	61
<u>Event 4</u>						
Site 1/plot 1	0.31	0.41	0.027	0.038	42.8	89
Site 1/plot 2	0.26	0.43	0.038	0.023	-39.5	0
Site 1/plot 3	0.26	0.43	0.055	0.099	78.6	196

Note: No particle movement was observed during event 2, therefore no calculation was necessary.
N.A. = not applicable.

*Percentage difference between critical shear stress calculated for isolated particles using the maximum flow depths and for clustered particles using the minimum flow depths (using Shields equation). Negative values indicate that the critical shear stress for the isolated particle was greater.

[†]Percentage difference between the critical shear stresses calculated for the isolated and clustered particles using the average flow depths, as presented in Table 5 and Figures 27 and 28 (using Shields equation).

the isolated particle was greater than for the clustered particle, then clusters might not have an effect on sediment transport if the clustered particles were located in the much shallower portion of the plot.

The percentage difference between isolated and clustered particles was negative at plot 3 during event 1 and plot 2 during events 3 and 4 (Table 7). As discussed earlier,

the threshold for particle entrainment may be lower at plot 2, and therefore clusters appear to have a minimal effect on sediment transport at plot 2. Plot 3 had the largest difference in the minimum and maximum flow depths (Figure 21), but all of the clusters that were tracked were located in the deeper half of the plot (Figure 19), indicating that the worst-case scenario calculated in Table 7 underestimated the actual critical shear stress for the cluster particles in plot 3. Thus, even under the depth scenario that minimizes the difference in the critical shear stress, it can be concluded that the clusters still impact sediment entrainment.

Summary

Results from this chapter suggest that clusters at site 1 are mobilized and destroyed at flows greater than $57 \text{ m}^3 \text{ s}^{-1}$ and velocities greater than 2 m/s (event 1), and are stable at flows less than $13 \text{ m}^3 \text{ s}^{-1}$ and velocities less than 0.2 m/s at site 1 (Figure 29). Higher flow events are likely required to entrain clusters at site 2, which remained relatively stable during the entire period of study. Clusters at site 2 are larger, protrude higher above the bed, and have a wider grain-size distribution compared to site 1, caused in part by the site-specific geomorphic features and channel constrictions between the two sites. This pattern suggests that site-specific geomorphic features play an important role in cluster formation, and are a significant factor in the stability of clusters.

Flow events observed during this study were relatively low compared to historical values (Figure 29). The mean annual peak flow for this reach of the Entiat

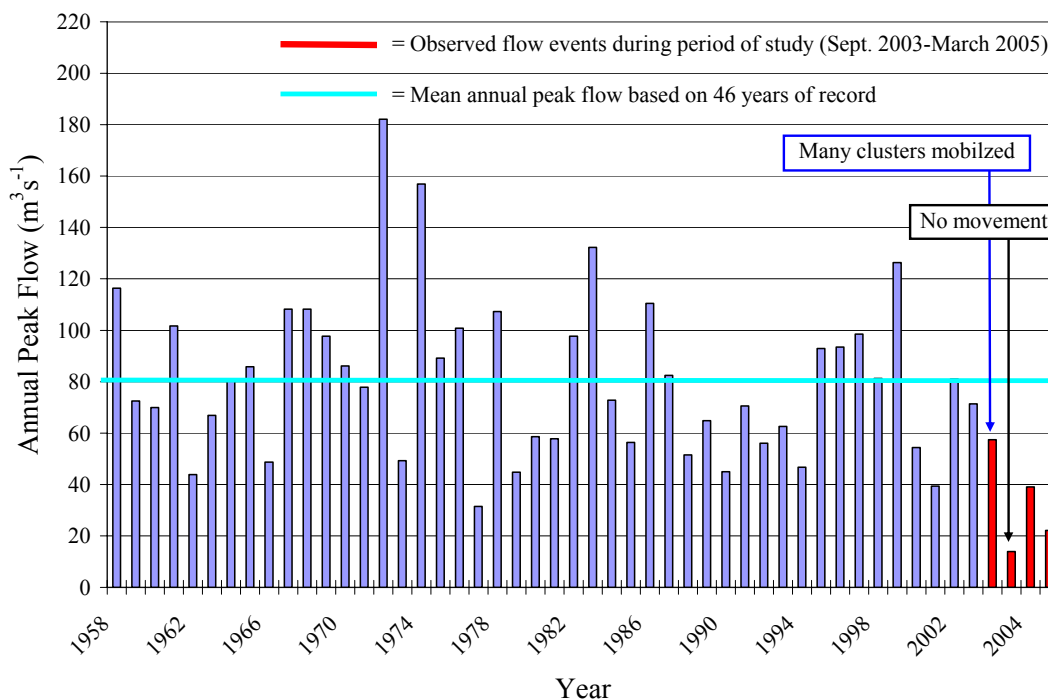


Figure 29. Annual peak flow values between sites 1 and 2 since 1958. Data adapted from U.S. Geological Survey (2005) streamflow gage located near Rkm 29 (RM 18). Time interval scale changes after 2002 from years to the date of flow events observed during this study (red bars).

River is $80 \text{ m}^3\text{s}^{-1}$, and only 14 of the last 46 years had annual peak flows less than $57 \text{ m}^3\text{s}^{-1}$ (Figure 29), thus clusters at site 1 are likely mobilized at least 2 out of every 3 years. However, it also appears that new and/or remnant clusters may form during the waning stages of high flow events, especially ones of long duration such as the yearly spring-runoff event. These results suggest that although clusters are likely destroyed or mobilized at least 2 out of every 3 years, they are also likely to be reformed that often, given that reformation occurred during the weak events observed during this study.

At site 1, which had a nearly uniform sediment-size distribution, clusters were destroyed by complete mobilization of the entire cluster and anchor clast, and by mobilization of only the clustered particles (anchor clast still in place). At site 2, which had bimodal sediment-size distribution, the only three clusters that were done so by complete mobilization of the entire cluster and anchor clast. These results suggest that the method of cluster break-up, which has been disputed in previous studies (Brayshaw, 1984; Billi, 1988; De Jong, 1991; Church et al., 1998), is likely dependent on sediment-size distribution. Clusters in a bimodal sediment-size distribution setting, with much larger anchor clasts than the particles being impeded, likely require the anchor clast to be entrained prior cluster destruction, whereas clusters in a nearly uniform sediment-size distribution setting do not need the anchor clast to be entrained prior to the clustered particles being mobilized.

No evolutionary pattern was determined for clusters in the Entiat River, as had been suggested in laboratory flume experiments (Strom, 2002; Papanicolaou et al., 2003). This lack of an evolutionary pattern is likely due to the order of flow events and the instability of clusters at site 1, and possible cluster evolution during the waning stages of flow events that cannot be determined by this field-based study. Future work is needed to fully determine the evolutionary pattern of clusters in the field during the entire duration of a flow event. However, evidence of two-particle clusters evolving into upstream triangles at site 1 was noted, which is similar to the initial formation patterns shown by the flume experiments (Strom, 2002; Papanicolaou et al., 2003).

Clusters appear to have a delaying effect on sediment transport at site 1 at flows less than $57 \text{ m}^3\text{s}^{-1}$ (event 1), based on the size differences in both the size of isolated and clustered particles entrained and the critical shear stress required to initiate their movement. At flows greater than $57 \text{ m}^3\text{s}^{-1}$, most clusters were destroyed at site 1 either by complete mobilization (including anchor clast) or by entrainment of clustered particles (anchor clast still in place). Because the mean annual flow for this reach of the Entiat River is $80 \text{ m}^3\text{s}^{-1}$, it appears that clusters have the greatest effect on sediment transport during relatively flow events in this reach of the Entiat River.

CHAPTER IV

CLUSTER CHARACTERISTICS

This chapter describes the morphology and density of clusters at sites 1 and 2. The descriptions were conducted in August of 2004, between flow events 3 and 4 (Figure 16). The purpose of this element of the study is to detail the cluster density on the gravel bars and characterize the general size and geometry of the clusters in more detail than the initial clusters, which were mainly identified and described for the purpose of tracking their evolution through a series of high flow events. In addition, detailing cluster characteristics for the Entiat River will provide a complete dataset that will add to the relatively limited data on the details of cluster characteristics (Brayshaw, 1984; Wittenberg, 2002; Strom et al., 2004a).

Methods

The methods for identifying clusters for the detailed descriptions followed those set in chapter I. Each cluster must consist of at least one anchor clast that is trapping at least two other particles and protrudes above the immediate surrounding area. The original three plots at site 1 were used to characterize the clusters. At site 2, the original plot 1 was used and a second plot was added upstream. The plot sizes were enlarged to 8-m x 8-m in size. For this part of the study, instead of identifying only the 15 most prominent clusters in each plot, as was done for the cluster evolution component, every identifiable cluster that met the predefined criteria was described within the 8 m x 8 m plots to better determine dominant cluster type, size, and density. Each cluster was marked with flagging, described and measured, and surveyed with a Total-Station laser

theodolite surveyor. The classification parameters of the clusters were similar to those used in describing the clusters tagged for tracking movement, as explained in chapter III. An additional component to these descriptions was a classification of the relative degree of development of each cluster as strong, moderate, or weak (Table 8).

TABLE 8. CLUSTER STRENGTH CLASSIFICATION CRITERIA

Strength classification	Number of particles impeded	Protrusion (cm)
Strong	5+	5+
Moderate	3-5	3-5
Weak	3	2-3

Note: The number of particles impeded is a general statement, and varied by cluster, e.g., some strong clusters only impeded three particles but were very prominent and/or exhibited strong imbrication.

Results and Discussion

Figure 30 shows the total number of each cluster type for all plots at sites 1 and 2. At both sites the upstream triangle was the most abundant cluster type, accounting for 72 of 134 total clusters (54%) at site 1 and 108 of 196 total clusters (55%) at site 2. A similar distribution was shown by the original baseline clusters identified for tracking cluster evolution in September of 2003 at site 1 (Figure 17); however, the diamond and upstream triangle each accounted for 37.5% of the total baseline clusters at site 2 (Figure 18). This difference could be a factor of the smaller sample size identified for tracking (16) for the baseline data set at site 2. No pattern could be found in the spatial distribution of each cluster morphology (Figure 31), similar to what was found for the data set used for tracking cluster evolution (chapter III, Figures 19 and 22).

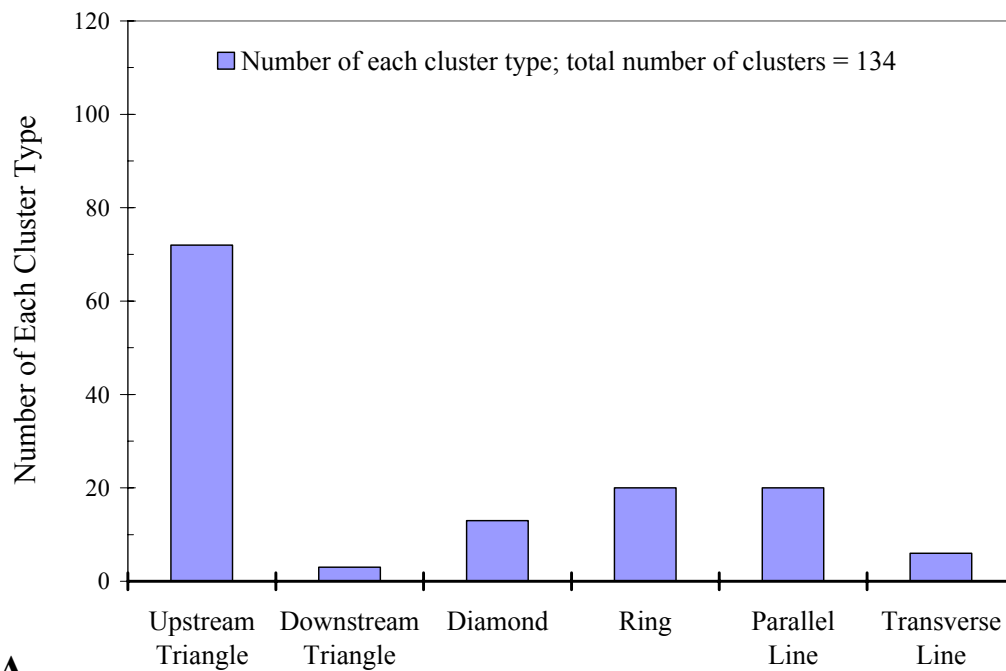
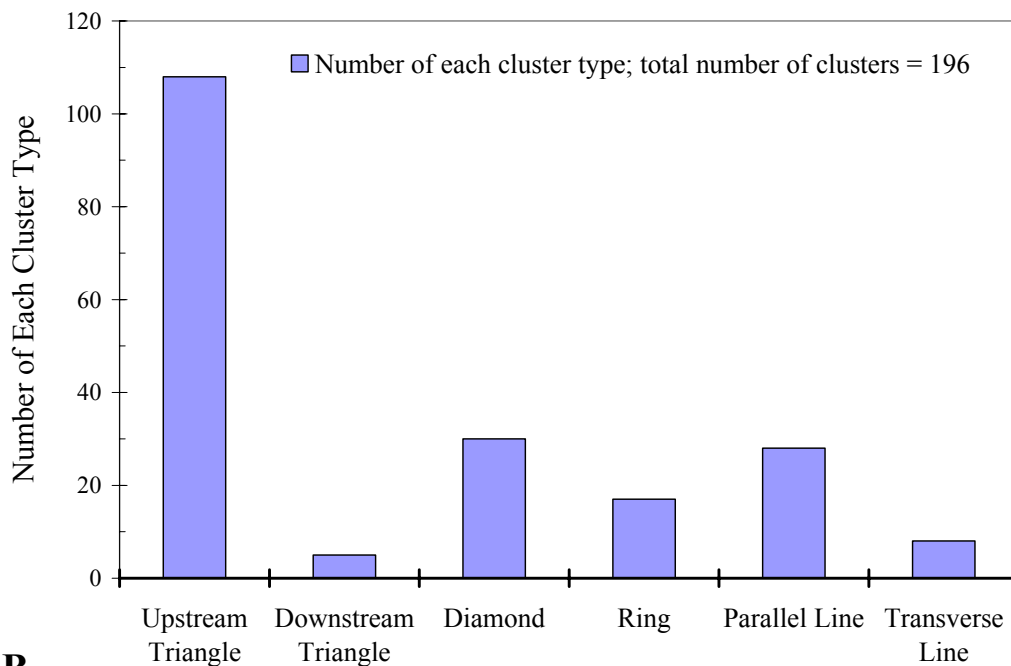
**A****B**

Figure 30. Number of each cluster type within detailed cluster plots at sites 1 (A) and 2 (B). There were three 8-m x 8-m plots at site 1 and two 8-m x 8-m plots at site 2.

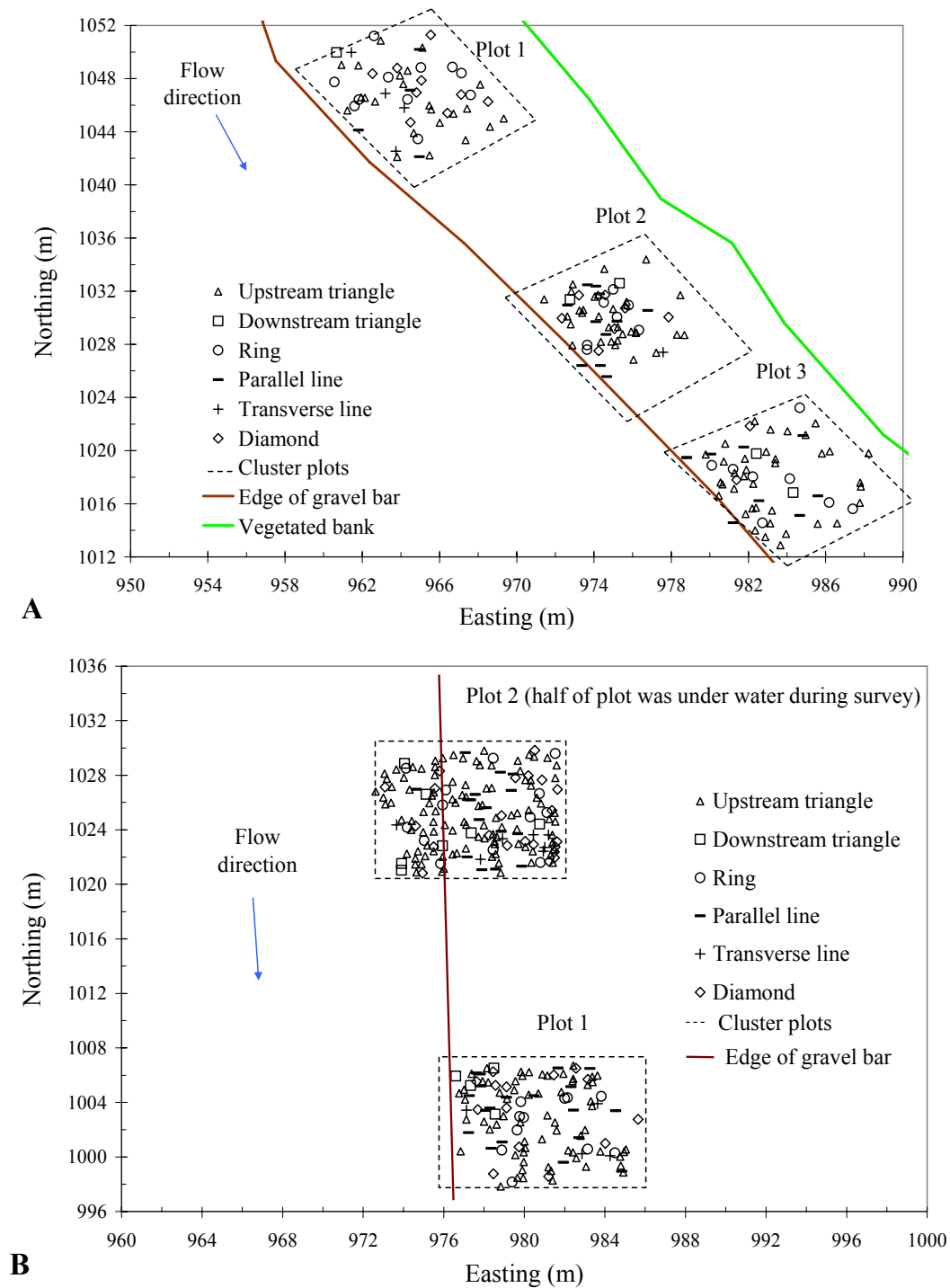


Figure 31. Spatial distribution of cluster morphologies for all plots at sites 1 (A) and 2 (B). There were three 8-m x 8-m plots at site 1 and two 8-m x 8-m plots at site 2.

Table 9 shows the density of clusters at sites 1 and 2 for each plot, and shows a mean density of 0.7 clusters/m² at site 1 and 1.5 clusters/m² at site 2. Table 10 shows the mean cluster characteristics for sites 1 and 2.

TABLE 9. CLUSTER DENSITY

Site and plot no.	Density (no./m ²)
<u>Site 1</u>	0.7*
Plot 1	0.7
Plot 2	0.7
Plot 3	0.6
<u>Site 2</u>	1.5*
Plot 1	1.8
Plot 2	1.2

*Mean cluster density for each site.

TABLE 10. MEAN CLUSTER CHARACTERISTICS FOR ENTIAT RIVER

Site no.	Mean cluster length (cm)	Mean cluster width (cm)	Mean diameter of anchor clasts (cm)	Cluster density (no./m ²)	Abundant cluster morphology
Site 1	22.0	21.0	9.0	0.7	Upstream triangle
Site 2	28.0	25.0	11.0	1.5	Upstream triangle

In general, all of the cluster types were similar in length and width at site 1 with the exception of the parallel lines (longer than wide) and transverse lines (wider than long) cluster types (Figure 32). At site 2 the clusters were slightly longer than they were wide, with the exception of the parallel lines (significantly longer than wide) transverse lines (slightly wider than long). The transverse lines are a bit peculiar; it would be expected that they should be significantly wider than long, which was not the case at

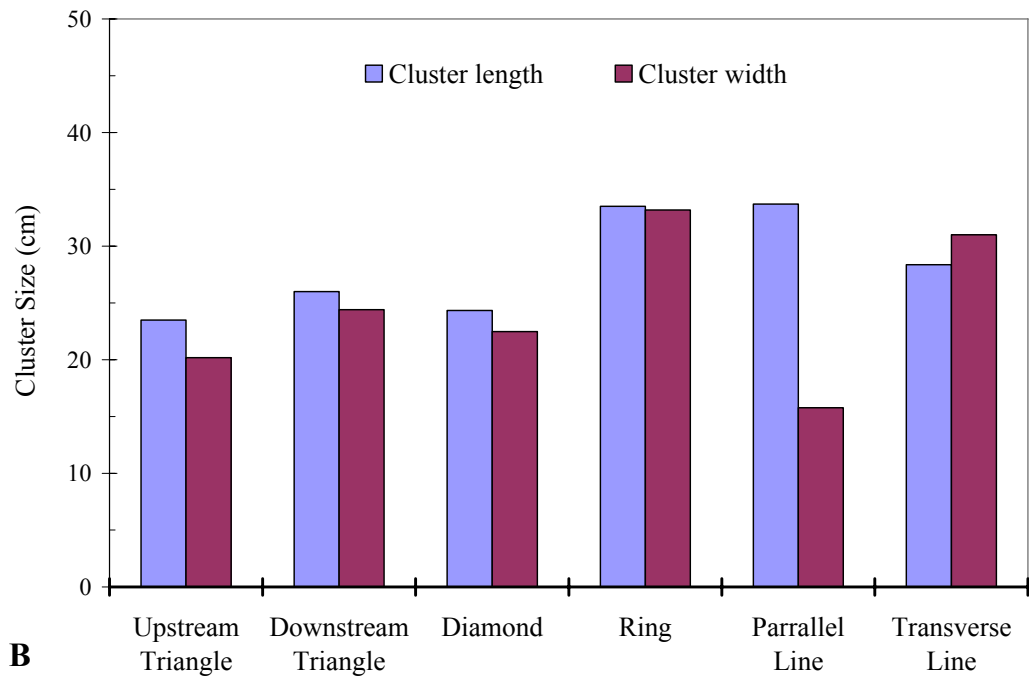
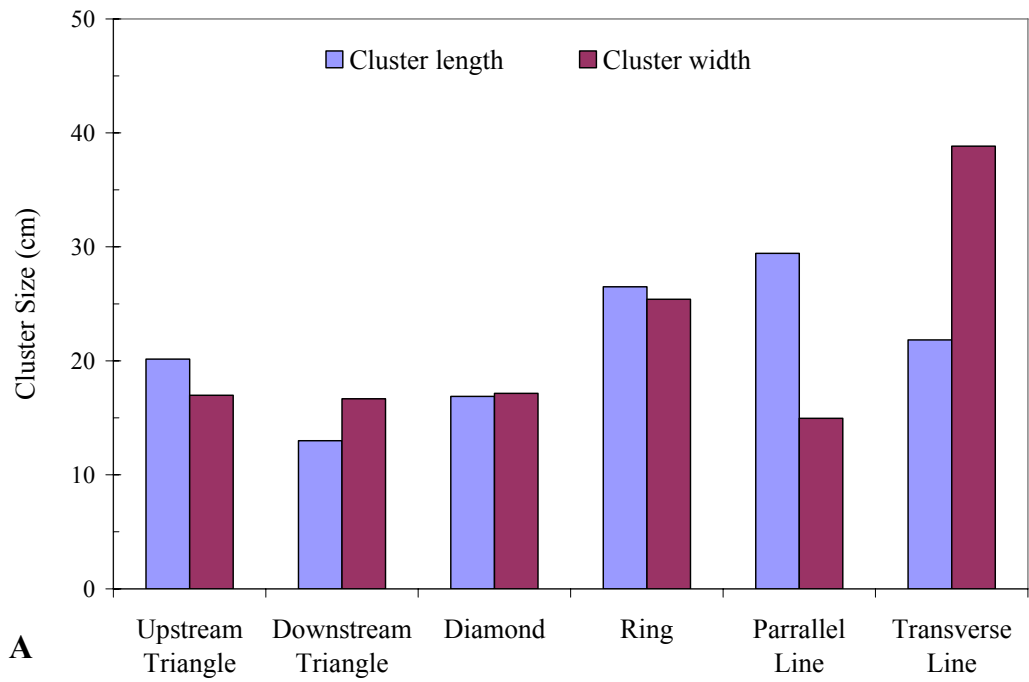


Figure 32. Average size of each cluster type within detailed cluster plots at sites 1 (A) and 2 (B).

site 2. This discrepancy is attributed to the larger anchor clasts of the transverse lines at site 2, which were wide and long because they impeded many particles in their stoss and wake, thus causing the clusters to be nearly as long as they were wide. In addition, the clusters at site 2 were larger than those at site 1, as was expected given the bimodal size distribution at site 2, which contains larger anchor clasts more prone to trap particles (Figure 10). Appendix B shows the cluster characteristics for all clusters identified.

Table 11 and Figure 33 show number of cluster types classified as strongly, moderately, or weakly developed. This random distribution of cluster development suggests that in the Entiat River each cluster type forms within each stage of development from strong, moderate, to weak and that no one cluster type predominantly forms as strong, moderate, or weak. Furthermore, this implies that there was no bias

TABLE 11. CLUSTER STRENGTH CLASSIFICATIONS

Cluster strength and site number	Upstream triangle		Downstream triangle		Diamond		Ring		Parallel line		Transverse line		Total no.
	No.	(%)	No.	(%)	No.	(%)	No.	(%)	No.	(%)	No.	(%)	
<u>All strengths</u>													
Site 1	72	N.A.	3	N.A.	13	N.A.	20	N.A.	20	N.A.	6	N.A.	134
Site 2	108	N.A.	5	N.A.	30	N.A.	17	N.A.	28	N.A.	8	100	196
<u>Strong</u>													
Site 1	10	14	2	67	0	0	1	5	8	40	2	33	23
Site 2	12	11	1	20	1	3	6	35	6	21	3	38	29
<u>Moderate</u>													
Site 1	40	56	1	33	5	38	11	55	7	35	2	33	66
Site 2	42	38	3	60	9	30	5	29	12	43	4	50	75
<u>Weak</u>													
Site 1	22	31	0	0	8	61	8	40	4	20	2	33	44
Site 2	54	50	1	20	20	67	6	35	10	36	1	12	92

Note: N.A. = not applicable.

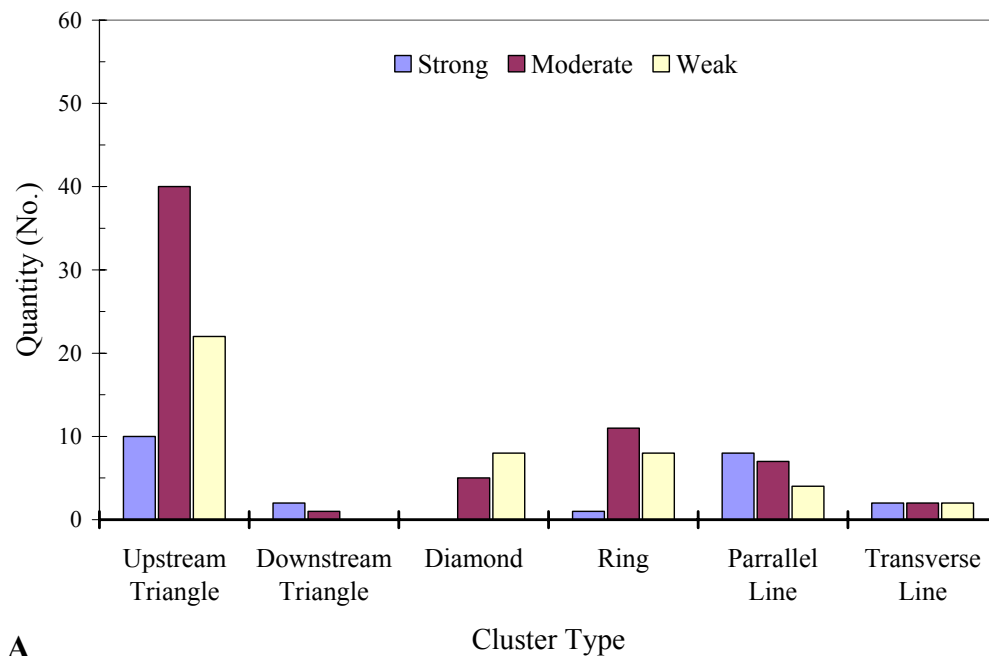
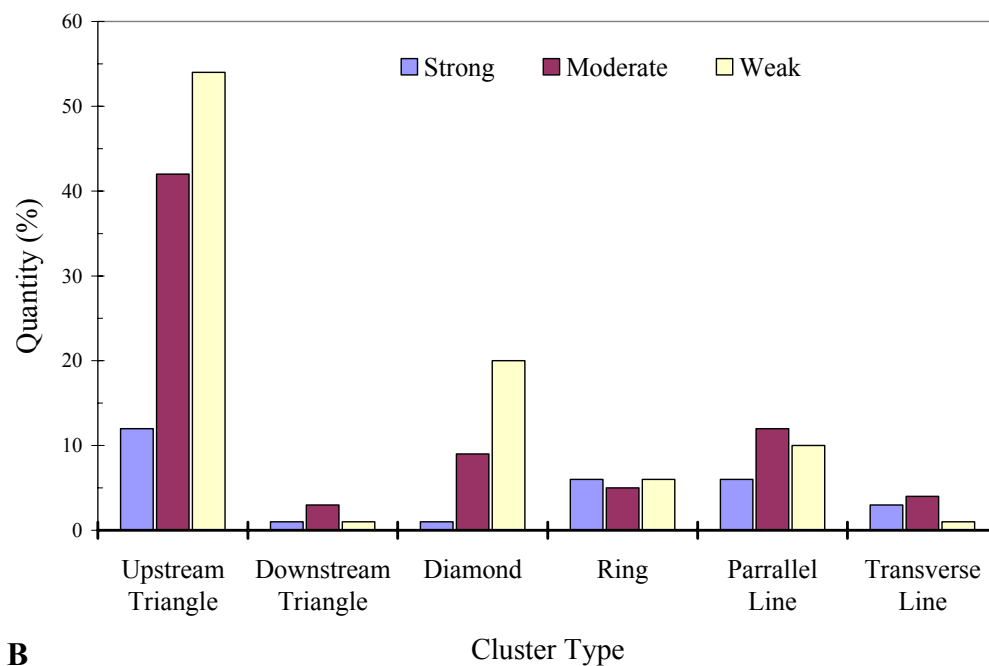
**A****B**

Figure 33. Number of each cluster type within each detailed plot at sites 1 (A) and 2 (B). There were three 8-m x 8-m plots at site 1 and two 8-m x 8-m plots at site 2.

toward identifying one type of cluster, such as upstream triangles, because it is more strongly developed than other cluster types.

Results from this component of the study validate the results found in chapter III that the upstream triangles are the most abundant cluster morphology. Furthermore, results found in chapter III and from laboratory flume experiments (Strom, 2002; Papanicolaou et al., 2003) suggested that the upstream triangle may represent the initial form in the evolutionary cycle of clusters. Data collected for this chapter were collected after event 1, which destroyed many clusters at site 1, and showed the upstream triangle to be the most abundant cluster morphology. These results suggest that clusters may be at the initial stage of formation and support results found in chapter III and from the laboratory flume experiments.

Because in the Entiat River relatively weak flow events destroy or mobilize clusters (Figure 29), clusters are being reset before they can evolve and stabilize as diamond cluster types. This conclusion is further validated by the large number of upstream triangles and low number of diamond cluster types in the Entiat River.

The difference in cluster density between sites 1 and 2 validates conclusions found in chapters II and III: clusters are more dense at site 2 due to the bimodal sediment-size distribution, caused in part by the channel constriction and increased supply of larger sediment particles from the alluvial fans and geologic outcrop upstream (Figures 8 and 9).

Comparisons with Previous Work

Previous work describing cluster characteristics in the detailed presented in the present study has been limited. Appendix C shows data from previous river systems that contained clusters. Biggs et al. (1997) compiled data from nine headwater-streams in New Zealand and found cluster densities that ranged from 0.07 per square meter to 0.28 per square meter, compared to cluster densities in the Entiat River of 0.7 per square meter (site 1) and 1.5 per square meter (site 2). Brayshaw (1984) provided detailed descriptions of the components of clusters (obstacle or anchor clast, stoss, and wake; see chapter I), and found the mean length and width of clusters, from three different streams in the England, to be 29 cm and 17 cm, respectively; slightly longer and narrower than clusters in the Entiat River. Strom et al. (2004a) and Marcell et al. (2005) provided cluster characteristic data from two locations (approximately 0.5 km apart) along the American River, WA from which Strom et al. (2004a) reported mean cluster lengths of 42 cm and cluster widths of 30 cm, respectively, while Marcell et al. (2005) reported slightly smaller clusters upstream of 35 cm (mean length) and 26 cm (mean width). Each of these data sets from the American River show clusters to be larger than those found in the Entiat River.

Only the studies of Church et al. (1998), Wittenberg (2002), Strom et al. (2004a), and Marcell et al. (2005) described the different cluster morphologies found in the field. Table 1, Appendix C shows the most abundant cluster morphology found by each of the above-mentioned studies. Church et al. (1998) found a completely different cluster type in Harris Creek, B.C., in which larger exposed grains form irregular

reticulate networks within which finer material persists. These reticulate patterns are similar to the individual clusters described in the present study, as they also impede sediment and protrude above the normal bed-surface; however, individual clusters are connected and thus form reticulate patterns that spread across the gravel bar (Church et al., 1998). These reticulate patterns were also found to delay sediment transport based on laboratory flume experiments (Church et al., 1998). In studies that described cluster morphologies similar to those described in the present study, Wittenberg (2002) found the diamond to be the most abundant cluster type in four mountain streams in the northeast UK, while Strom et al. (2004a) found both the diamond and upstream triangle to be equally abundant, and Marcell et al. (2005) reported that the upstream triangle was most abundant. These results, combined with those found in the present study, suggest that cluster morphologies created in laboratory flume experiments are valid, as Strom (2002) and Papanicolaou et al. (2003) reported cluster morphologies similar to upstream triangle and diamond clusters (see chapter III), and can thus facilitate future studies at conducted at the IIHR center which aim to simulate sediment transport processes.

Summary

Results from this chapter have shown that the upstream triangle is the most abundant cluster morphology in the Entiat River at sites 1 and 2. Clusters at site 2 were larger and more dense than at site 1, which was expected given the geomorphic constriction, alluvial fans, and bedrock outcrop downstream of site 1 and upstream of site 2 (see chapter II). Cluster morphologies were classified by relative development (strong, moderate, or weak), and there was a random distribution of cluster development

between morphologies, suggesting no bias toward identifying one cluster morphology over another.

Data and results presented in this chapter have shown cluster characteristics in the Entiat River, and have added to the limited database that details cluster characteristics. Some of this limited data set from other river systems was also discussed and is shown in Appendix C. It is apparent that clusters form under a variety of conditions, from headwater streams in New Zealand (Biggs et al., 1997), small slate-bed, flint gravel-bed, and well-rounded sandstone and limestone beds in the UK (Brayshaw, 1984), to classic snow-melt dominated, cobble to gravel-bed rivers such as Harris Creek, B.C. (Church et al., 1998), American River (Strom et al., 2004a; Marcell et al., 2005), Entiat River (present study, see also chapter II), and in four mountain streams in the UK (Wittenberg, 2002). It is also apparent that clusters simulated in laboratory flume experiments (Strom, 2002; Papanicolaou et al., 2003) are similar to those found in the field and therefore results obtained from those experiments may be applicable in natural streams.

CHAPTER V

SUMMARY AND CONCLUSIONS

This study on the Entiat River, Washington quantified the effects of sediment clusters on sediment transport and assessed the role of geomorphic features and sediment-size distributions on the formation and stability of cluster bedforms. These results were made possible due to the unique setting of sites 1 and 2 that provided a laboratory-like setting in a natural environment, due to the proximity of the sites to each other and to the real-time USGS (2005) streamflow gage, similar hydrologic regimes, and channel geometries. These similarities provided conditions that could be held “constant” while the effects of different geomorphic features and sediment-size distributions on the formation and stability of clusters could be determined. These two sites would provide ideal sites for future studies focused on isolating the effects of sediment-size distributions on other geomorphic or hydrologic processes.

The effects of clusters on sediment transport were quantified by determining the differences in the size of isolated and clustered particles entrained by a given flow event and the critical shear stress required to entrain them. The range of flows required to maintain and destroy clusters was also determined. Clusters appear to have a delaying effect on sediment transport at site 1 at flows and velocities less than $57 \text{ m}^3\text{s}^{-1}$ and 2 m/s. Flows and velocities greater than $57 \text{ m}^3\text{s}^{-1}$ and 2 m/s are likely to mobilize and destroy clusters at site 1, while flows and velocities less than $13 \text{ m}^3\text{s}^{-1}$ and 0.2 m/s are too low to alter or move clusters. Clusters have a greater effect on sediment transport at

site 2, as clusters were larger, more prominent, denser, and remained relatively stable throughout this study than at site 1. These differences in cluster characteristics at site 2 are due, in part, to the geomorphic features upstream. Minimum flow and velocity required to mobilize and destroy clusters at site 2 was not determined, but is greater than $57 \text{ m}^3 \text{ s}^{-1}$ and 2 m/s .

In general, the critical shear stress required to entrain particles was greater for particles in clusters than for adjacent isolated particles of similar sizes and shapes. Using the Shields equation the range of critical shear stress values for entrained isolated particles was 0.014-0.114, compared with 0.022-0.142 for clustered particles. For all plots, sites, and flow events the critical shear stress for clustered particles ranged from 0-196% greater than isolated particles, but in general were 40%-50% greater. The difference in critical shear stress values between clustered and isolated particles, for all plots and all flow events, were statistically significant with a *P* value of 0.0299. Using the Komar equation the range of critical shear stress values for entrained isolated particles was 0.026-0.034, compared with 0.03-0.064 for clustered particles. For all plots, sites, and flow events the critical shear stress for clustered particles ranged from 0-102% greater than isolated particles, but in general were 25%-35% greater. The difference in critical shear stress values between clustered and isolated particles, for all plots and all flow events, was statistically significant with a *P* value of 0.0125.

This study also identified some of the site-specific geomorphic features surrounding cluster formation, such as pools, riffles, sediment-size distributions, water-surface slope, and presence of alluvial fans, terraces, and bedrock outcrops, surrounding

cluster formation. Clusters formed adjacent to pools with water-surface slopes $\geq 1\%$, moderate-to-poorly sorted sediment and D_{50} and D_{100} values of 3-9 cm and 9.5-26 cm, respectively. Detailed cluster descriptions, such cluster size, morphology, densities were collected at sites 1 and 2 and compared to the limited database of field-based cluster studies.

Conflicting hypotheses on the method of cluster destruction (Brayshaw, 1984; Billi, 1988; De Jong, 1991; Church et al., 1998) was resolved, in part, by results of this study. Based on tracking of cluster evolution at sites 1 and 2, located less than 1 km apart in similar hydrologic regimes, but with very different sediment size characteristics, it appears that sediment-size distribution is a major factor in the method of cluster destruction as well as the stability of clusters. The larger, bimodal sediment-size distributions at site 2 produced larger, more prominent clusters that required the anchor clast to be mobilized prior to cluster destruction. Smaller, nearly uniform sediment-size distributions at site 1 produced smaller, less prominent clusters causing many to be destroyed by both methods of cluster destruction, with or without anchor clast mobilization. Therefore it appears that gravel bars with bimodal sediment-size distributions that exhibit clusters will require anchor clast mobilization prior to cluster destruction.

Results from this field-based study have validated laboratory flume experiments conducted by Strom (2002) and Papanicolaou et al. (2003). Cluster morphologies found in the Entiat River are similar to those simulated in the flume studies, and the delaying effect on sediment transport found in the flume studies was also supported by the results

of this study. The lack of an apparent evolutionary cycle in the Entiat River compared to the laboratory experiments may be due to the order of the flow events observed during this study, which were different than the experimentally generated smallest-to-largest flow conditions produced laboratory studies. In addition, the evolution of clusters throughout the rise and fall of an entire flow event cannot be observed in the field, and only the before and after conditions are observable. Further complicating the field-based evolutionary patterns of clusters is the fact that many clusters were destroyed at site 1 during flow events 1, 2, and 3, which may have “reset” the cluster cycle after each flow event. Future work is needed to determine if similarities exist between the evolutionary patterns of clusters in the field compared to the flume studies.

Clusters are a component of the gravel-bed of an unregulated and relatively undisturbed portion of the Entiat River, which supports an abundance of aquatic habitats and salmonid populations (Archibald, personal communication, October 18, 2004; CCCD, 2004). Active salmonid spawning was observed at nearly every cluster site during the fall of 2004, suggesting that clusters are at the very least part, if not a significant factor, of the excellent aquatic habitat found in this reach of the Entiat River.

Finally, results and methods provided in this study could have several applications to fluvial geomorphology and river restoration. First, results from this study could aid in-channel restoration projects by helping determine the stability of a gravel-bed and the ability of a channel to handle its sediment flux, based on cluster formation, stability, and evolution patterns. For example, a river that exhibits stable cluster morphologies over the course of moderate-large flood events would suggest a

relatively stable gravel bar. A river that exhibits consistent cluster mobilization without reformation might suggest an eroding gravel bar. In addition, a river such as the Entiat River that exhibits both cluster mobilization and reformation may suggest a gravel bar that is efficiently managing its sediment load by transporting sediment downstream while new sediment is being deposited from upstream. Secondly, results from this project could also aid in the design of channel maintenance flows in regulated rivers by determining the discharge, velocities, and associated shear stress values required to form and mobilize clusters, thus retaining this component of natural streams that might not only play a role in aquatic habitat, but may help avoid the development of armored or eroding channel beds. Finally, results from this study could aid further development of sediment transport experiments and numerical models by providing field-based data on cluster formation, stability, and evolution under various geomorphic features and hydrologic processes.

Future Work

Future work based on this study could include continued tracking of the original baseline clusters, including remnant anchor clasts, to determine further evolution, destruction, and/or reformation under various flow events, particularly a flow event closer to the mean annual peak flow $80 \text{ m}^3 \text{ s}^{-1}$ to determine whether the entire population is mobilized or newly deposited sediment is trapped by the remaining anchor clasts. Additional cluster sites along the Entiat River could also be investigated as part of future work, in particular in the upper and lower reaches, which exhibit different geomorphic conditions and sediment-size distributions than the middle reach where this

study was conducted. Furthermore, instream structures have recently been placed in this reach of the river to improve aquatic habitat and stream stability (CCCD, 2004), and future work could document the effects of these structures on the formation and stability of clusters.

Previous biological surveys have indicated that clusters provide refuge for benthic populations, a key ingredient of a healthy instream habitat (Biggs et al., 1997; Boelman and Stein, 1997). Another interesting and useful future study would be to further investigate the possible benefits of clusters to benthic populations.

Finally, the methods and results of this study will be compared with on-going field-based studies of cluster evolution and formation characteristics along the American River in south-central Washington state (Strom et al., 2004a; Marcell et al., 2005). Furthermore, data obtained in this field based study will be incorporated in on-going laboratory flume experiments and the development of numerical sediment transport models, e.g., Papanicolaou et al. (2004), being conducted by faculty and students at the IIHR hydrologic research center, thus advancing our current knowledge of sediment transport processes.

REFERENCES CITED

- Andrews, E. D., and Nankervis, J. M., 1995, Effective discharge and the design of channel maintenance flows for gravel-bed rivers: Geophysical monograph, v. 89, p. 151.
- Archibald, P., 2004, October 18, personal communication, Fishery Biologist, U.S. Forest Service, Entiat, Washington.
- Biggs, B. J. F., Duncan, M. J., Francoeur, S. N., and Meyer, W. D., 1997, Physical characterisation of microform bed cluster refugia in 12 headwater streams, New Zealand: *New Zealand Journal of Marine and Freshwater Research*, v. 31, no. 4, p. 413-422.
- Billi, P., 1988, A note on cluster bedform behaviour in a gravel-bed river: *Catena*, v. 15, no. 5, p. 473-481.
- Biron, P. M., Richards, K. S., Lane, S. N., Roy, A. G., and Bradbrook, K. F., 1998, Sensitivity of bed shear stress estimated from vertical velocity profiles: The problem of sampling resolution: *Earth Surface Processes and Landforms*, v. 23, no. 2, p. 133-139.
- Boelman, S. F., and Stein, O. R., 1997, Performance of instream boulder clusters in a cobble-bed river, *in* Wang, S. S., and Carstens, T., eds., *Environmental and coastal hydraulics: Protecting the aquatic habitat*: New York, American Society of Civil Engineers, p. 1049-1054.
- Brayshaw, A. C., 1984, Characteristics and origin of cluster bedforms in coarse-grained alluvial channels, *in* Koster, E. H., and Steel, R. J., eds., *Sedimentology of gravels and conglomerates*: Calgary, Canadian Society of Petroleum Geologists, p. 77-85.
- Brayshaw, A. C., 1985, Bed microtopography and entrainment thresholds in gravel-bed rivers: *Geological Society of America Bulletin*, v. 96, no. 2, p. 218-223.
- Brayshaw, A. C., Frostick, L. E., and Reid, I., 1983, The hydrodynamics of particle clusters and sediment entrainment in coarse alluvial channels: *Sedimentology*, v. 30, no. 1, p. 137-143.
- Buffington, J. M., and Montgomery, D. R., 1997, A systematic analysis of eight decades of incipient motion studies, with special reference to gravel-bedded rivers: *Water Resources Research*, v. 33, no. 8, p. 1993-2029.

- Carling, P. A., 1983, Threshold of coarse sediment transport in broad and narrow natural streams: *Earth Surface Processes and Landforms*, v. 8, no. 1, p. 1-18.
- Chelan County Conservation District [CCCD], 2004, Entiat water resource inventory Area 46 management plan. Chelan County Conservation District, Wenatchee, Washington.
- Chow, V. T., 1959, *Open-channel hydraulics*: New York, McGraw-Hill, Inc., 680 p.
- Church, M., Hassan, M. A., and Wolcott, J. F., 1998, Stabilizing self-organized structures in gravel-bed stream channels: Field and experimental observations: *Water Resources Research*, v. 34, no. 11, p. 3169-3179.
- Dal Cin, R., 1968, Pebble clusters: Their origin and utilization in the study of palaeocurrents: *Sedimentary Geology*, v. 2, p. 223-324.
- De Jong, C., 1991, A reappraisal of the significance of obstacle clasts in cluster bedform dispersal: *Earth Surface Processes & Landforms*, v. 16, no. 8, p. 737-744.
- Dey, S., 2004, Critical bed shear for initial movement of sediments on a combined lateral and longitudinal slope: *Nordic Hydrology*, v. 35, no. 2, p. 153-164.
- Elliott, J. G., 2002, Bed-material entrainment potential, Roaring Fork River at Basalt, Colorado: U.S. Geological Survey, 02-4223.
- Feldman, A. D., 1981, HEC models for water resources system simulation: Theory and experience: *Advances in Hydroscience*, v. 12, p. 297-423.
- Hammond, F. D., Heathershaw, A. D., and Langhorne, D. N., 1984, A comparison between Shields' threshold criterion and the movement of loosely packed gravel in a tidal channel: *Sedimentology*, v. 31, p. 51-62.
- Hassan, M. A., and Church, M., 2000, Experiments on surface structure and partial sediment transport on a gravel bed: *Water Resources Research*, v. 36, no. 7, p. 1885-1895.
- Hassan, M. A., and Reid, I., 1990, The influence of microform bed roughness elements on flow and sediment transport in gravel bed rivers: *Earth Surface Processes & Landforms*, v. 15, no. 8, p. 739-750.
- Hosman, K. J., 2001, Stratigraphic reconstruction of paleoflood frequencies and magnitudes, lower Deschutes River, Oregon [M.S. thesis]: Ellensburg, Central Washington University, 84 p.

- Hydrologic Engineering Center, 2002, HEC-RAS river analysis system—program user's manual: Davis, California, U.S. Army Corps of Engineers.
- Knighton, D., 1998, *Fluvial forms and processes: A new perspective*: New York, Oxford University Press, Inc., 383 p.
- Komar, P. D., 1989, Flow-competence evaluations of the hydraulic parameters of floods: An assessment of the technique, *in* Baven, K., and Carling, P., eds., *Floods: Hydrological, sedimentological and geomorphological implications*: Hoboken, New Jersey, John Wiley & Sons Ltd, p. 265.
- Komar, P. D., and Zhenlin, L., 1986, Pivoting analyses of the selective entrainment of sediments by shape and size with application to gravel threshold: *Sedimentology*, v. 33, no. 3, p. 425-436.
- Kondolf, M. G., 1995, Managing bedload sediment in regulated rivers: Examples from California, U.S.A.: *Geophysical Monograph*, v. 89, p. 165.
- Lawless, M., and Robert, A., 2001, Three-dimensional flow structure around small-scale bedforms in simulated gravel-bed environment: *Earth Surface Processes and Landforms*, v. 26, no. 5, p. 507-522.
- Mann, H. B., and Whitney, D. R., 1947, On a test of whether one of two random variables is stochastically larger than the other: *The Annals of Mathematical Statistics*, v. 18, p. 50-60.
- Marcell, J. L., Ely, L. L., and Hendrick, R. R., 2005, Evolution of sediment cluster morphologies on the American River, Cascade Mountains, WA., *in* Bay, basins, basement, and beyond: 2005 annual meetings of the Cordilleran Section of the Geological Society of American, and the Pacific Section of the American Association of Petroleum Geologists, San Jose, California.
- Maxwell, A. R., and Papanicolaou, A. N., 2001, Step-pool morphology in high-gradient streams: *International Journal of Sediment Research*, v. 16, no. 3, p. 380-390.
- Milhaus, R. T., 1973, Sediment transport in a gravel-bottomed stream [Unpublished Ph.D. thesis]: Corvallis, Oregon State University, 232 p.
- Montgomery, D. R., Quinn, T. P., Buffington, J. M., Peterson, N. P., and Schuett-Hames, D., 1996, Stream-bed scour, egg burial depths, and the influence of salmonid spawning on bed surface mobility and embryo survival: *Canadian Journal of Fisheries and Aquatic Sciences*, v. 53, no. 5, p. 1061-1070.

- Naden, P. S., and Brayshaw, A. C., 1987, Small- and medium-scale bedforms in gravel-bed rivers, *in* Richards, K., ed., *River channels: IBG special publication*, 18: Leeds, United Kingdom, Basil Blackwell, p. 249-271.
- O'Connor, J. E., 1993, Hydrology, hydraulics, and geomorphology of the Bonneville Flood, special paper no. 274: Geological Society of America, Inc., 83 p.
- O'Connor, J. E., and Webb, R. H., 1988, Hydraulic modeling for paleoflood analysis, *in* Baker, V. R., Kochel, R. C., and Patton, P. C., eds., *Flood geomorphology*: New York, Wiley-Interscience, p. 383-402.
- Papanicolaou, A. N., 2005, January 25, personal communication, Associate Professor, sediment dynamics, watershed sedimentation, and hydrodynamics, Department of Civil and Environmental Engineering, Iowa Institute of Hydraulic Research-Hydroscience & Engineering, University of Iowa, Iowa City.
- Papanicolaou, A. N., and Schuyler, A., 2003, Cluster evolution and flow-frictional characteristics under different sediment availabilities and specific gravity: *Journal of Engineering Mechanics*, v. 129, no. 10, p. 1206-1219.
- Papanicolaou, A. N., Strom, K., Schuyler, A., and Talebbeydokhti, N., 2003, The role of sediment specific gravity and availability on cluster evolution: *Earth Surface Processes and Landforms*, v. 28, no. 1, p. 69-86.
- Papanicolaou, A. N., Bdour, A., and Wicklein, E., 2004, One-dimensional hydrodynamic/sediment transport model applicable to steep mountain streams: *Journal of Hydraulic Research*, v. 42, no. 4, p. 357-375.
- Reid, I., Frostick, L. E., and Brayshaw, A. C., 1992, Microform roughness elements and the selective entrainment and entrapment of particles in gravel-bed rivers, *in* Billi, P., Hey, C. R., and Tacconi, P., eds., *Dynamics of gravel-bed rivers*: Hoboken, New Jersey, John Wiley & Sons Ltd, p. 253-275.
- Strom, K., 2002, *Microforms in gravel bed rivers* [M.S. thesis]: Pullman, Washington State University, 94 p.
- Strom, K., Papanicolaou, A. N., Billing, B., Ely, L. L., and Hendrick, R. R., 2004a, Characterization of particle cluster bedforms in a mountain stream, ASCE/EWRI World Water and Environmental Resources Congress, Anchorage, Alaska (15, May).
- Strom, K., Papanicolaou, A. N., Evangelopoulos, N., and Odeh, M., 2004b, Microforms in gravel bed rivers: Formation, disintegration, and effects on bedload transport: *Journal of Hydraulic Engineering*, v. 130, no. 6, p. 554-567.

- Teisseyre, A. K., 1977, Pebble clusters as a directional structure in fluvial gravels: Modern and ancient examples: *Geologia Sudetica*, v. 12, no. 2, p. 79-89.
- U.S. Geological Survey [USGS], 2005, Real-time stream gaging station no. 12452800, Entiat River near Ardenvoir, Washington, U.S. Geological Survey. <http://waterdata.usgs.gov/wa/nwis/uv?12452800>
- Washington State Department of Ecology, 2005, Geographic Information System (GIS) services. Washington State Department of Ecology, March 2005. [http:// www.ecy.wa.gov/services/gis/maps/maps.htm](http://www.ecy.wa.gov/services/gis/maps/maps.htm)
- Wilcoxon, F., 1945, Individual comparisons by ranking methods: *Biometrics Bulletin*, v. 1, p. 80-83.
- Wittenberg, L., 2002, Structural patterns in coarse gravel river beds: Typology, survey and assessment of the roles of grain size and river regime: *Geografiska Annaler, Series A: Physical Geography*, v. 84, no. 1, p. 25-37.
- Wolman, M. G., 1954, A method of sampling coarse river-bed material: *American Geophysical Union Transactions*, v. 35, p. 951-956.

APPENDIXES

Appendix A

Entrained Isolated and Clustered Particle Data

TABLE A1. FIVE LARGEST ENTRAINED ISOLATED AND CLUSTERED PARTICLE SIZES AT SITE 1, PLOT 1

Event no.	Entrained particle size	
	Isolated (cm)	Clustered (cm)
<u>Event 1</u>	7	6
	7	5.5
	6	5.5
	6	5
	6	5
<i>Mean</i>	6.4	5.4
<u>Event 2</u>	N.D.	N.D.
	N.D.	N.D.
<i>Mean</i>	N.D.	N.D.
<u>Event 3</u>	7	5
	7	4.5
	6.5	4
	6	4
	6	3
<i>Mean</i>	6.5	4.1
<u>Event 4</u>	9.5	6
	7	4
	6	3
	6	3
	5.5	2
<i>Mean</i>	6.8	3.6
<i>Note: N.D. = no data.</i>		

TABLE A2. FIVE LARGEST ENTRAINED ISOLATED AND CLUSTERED PARTICLE SIZES AT SITE 1, PLOT 2

Event no.	Entrained particle size	
	Isolated (cm)	Clustered (cm)
<u>Event 1</u>	9	8
	8	7
	8	7
	7.5	6.5
	7.5	5
<i>Mean</i>	8.0	6.7
<u>Event 2</u>	N.D.	N.D.
	N.D.	N.D.
<i>Mean</i>	N.D.	N.D.
<u>Event 3</u>	7	7
	7	6.5
	6.5	6
	6	6
	6	5
<i>Mean</i>	6.5	6.1
<u>Event 4</u>	6	10
	6	5
	6	4
	5.5	4
	5.5	5.8
<i>Mean</i>	5.8	5.8
<i>Note: N.D. = no data.</i>		

TABLE A3. FIVE LARGEST ENTRAINED ISOLATED AND CLUSTERED PARTICLE SIZES AT SITE 1, PLOT 3

Event no.	Entrained particle size	
	Isolated (cm)	Clustered (cm)
Event 1	8	7
	7	7
	7	6
	7	6
	7	5.5
<i>Mean</i>	7.2	6.3
Event 2	N.D.	N.D.
	N.D.	N.D.
<i>Mean</i>	N.D.	N.D.
Event 3	9.5	5
	9	4.5
	7.5	4
	6	4
	5	3
<i>Mean</i>	7.4	4.1
Event 4	9.5	6
	7	4
	6	3
	6	3
	5.5	2
<i>Mean</i>	6.8	3.6
<i>Note: N.D. = no data.</i>		

TABLE A4. FIVE LARGEST ENTRAINED ISOLATED AND CLUSTERED PARTICLE SIZES AT SITE 2, PLOT 1

Event no.	Entrained particle size	
	Isolated (cm)	Clustered (cm)
Event 1	10	9
	8.5	7
	8	7
	7.5	6
	7	6
<i>Mean</i>	8.2	7
Event 2	N.D.	N.D.
	N.D.	N.D.
<i>Mean</i>	N.D.	N.D.
Event 3	N.D.	N.D.
	N.D.	N.D.
<i>Mean</i>	N.D.	N.D.
Event 4	10	6
	10	5.5
	8.5	5
	8	5
	7	5
<i>Mean</i>	8.7	5.3
<i>Note: N.D. = no data.</i>		

Appendix B

Cluster Characteristic Data

TABLE B1. CLUSTER CHARACTERISTICS AT SITE 1, ENTIAT RIVER

Plot no./ cluster no.	Cluster morphology	Number of anchors*	Size of anchor axes			Cluster size		Cluster strength
			Long (cm)	Intermediate (cm)	Short (cm)	Length (cm)	Width (cm)	
<u>Plot 2</u>								
1	Dw	1	13	10	8	15	24	m
2	Di	1	20	11	8	18	11	m
3	U	1	10	8	3	16	12	m
4	U	1	13	11	9	19	15	w
5	P.L.	3	7	6	4	30	20	s
6	U	1	18	7	5	23	7	m
7	R	5	9	5	5	35	30	s
8	U	1	16	9	7	15	16	m
9	U	1	20	10	8	31	20	w
10	U	1	12	9	4	22	17	v.w.
11	U	1	18	10	5	39	18	w
12	U	5	13	7	5	30	29	w
13	Dw	1	18	11	6	18	19	w
14	R	4	9	5	2	21	21	m
15	U	1	12	11	7	20	20	w
47	U	3	8	6	3	38	14	m
48	Di	1	13	10	7	18.5	15	w
49	U	1	10	6	3	24	13	m
52	U	2	7.5	4	2.5	14	19	m
54	P.L.	5	11	7	4	46	19	s
58	U	2	6.5	3	2.5	26	21	m
66	P.L.	3	6	5.5	5	36.5	17	w
67	Di	1	13	5.5	4	10	15	w
68	U	1	15	7	3	21	26	s
69	P.L.	4	11	6	3	23	11	m
69a	U	2	5	5	2	14	13	w
70	R	4	8	6	3	19	15	m
73	U	5	4	5	2	15	14	v.w.
74	U	1	8	6	4	20	10	m
76	U	1	10.5	7	5	27	10	m
78	P.L.	3	8	6	2	23	11	w
79	U	1	11	6.5	3	30	15	m
80	R	4	5	6	3	15	16	m
81	P.L.	4	4.5	4	3	18	17	w
83	Di	1	10	8	7	15	12	m

TABLE B1. (continued)

Plot no./ cluster no.	Cluster morphology	Number of anchors*	Size of anchor axes			Cluster size		Cluster strength
			Long (cm)	Intermediate (cm)	Short (cm)	Length (cm)	Width (cm)	
84	U	1	14	5.5	5.5	22	18	m
85	R	5	5	4.5	3	17	17	w
86	P.L.	1	7	6	2	29	11	s
87	P.L.	3	13	7.5	3	38	16	s
89	U	1	8.5	5	3	18	17	m
90	U	1	15	4	3	15	15	w
91	U	1	10	7	5	17	12	m
92	Di	1	16	5.5	5	14	17	w
93	U	1	7	4.5	2.5	18	19	m
94	R	5	7	6.5	3	40	24	m
95	U	1	10	7.5	6	14	12	m
96	P.L.	1	8	6.5	3	33	12	m
97	P.L.	1	3.5	3.5	3	34	11	s
98	Di	1	10	9	5	16	13	w
99	U	2	11	4.5	2.5	25	27	m
100	U	1	12.5	6	4	21	14	m
101	U	1	14	7.5	3.5	18	23	m
102	U	2	8	6	4	12	21	w
103	Di	1	11	6.5	6	19	16	w
104	U	1	12	7	6	18	19	s
105	T.L.	3	9	5.5	3	17	31	s
107	U	1	16.5	9	4	17	16.5	m
108	U	1	6.5	3.5	2	13	16	m
109	P.L.	1	9.5	5	4	23	12	s
110	U	1	12	7	5	22	24	s
111	U	1	14	7.5	6	15	14.5	m
<u>Plot 3</u>								
16	R	6	13	7.5	4	29	25	m
17	U	1	21.5	11	7	20	11	m
18	Dw	3	17	7	4	30	19	v.w.
19	P.L.	3	10.5	10	5	41	15	m
20	U	1	13.5	10.5	5	12	10.5	m
22	P.L.	3	10	6	5	31	17	s
21	U	1	20	11	5	21	20	w
23	U	1	12	8	4.5	13	14	v.w.
24	R	5	8	6.5	4	23	18	s
25	U	1	12	8	3	11	15	w
26	U	1	11	8	5	14	14	m
27	U	2	12	9.5	6	21.5	14	v.w.
28	U	1	6.5	5	2	25	19	v.w.
29	U	1	10.5	6.5	3	17	12	v.w.
30	U	1	11	8	5	16	11	v.w.

TABLE B1. (continued)

Plot no./ cluster no.	Cluster morphology	Number of anchors*	Size of anchor axes			Cluster size		Cluster strength
			Long (cm)	Intermediate (cm)	Short (cm)	Length (cm)	Width (cm)	
120	P.L.	2	12	7	4	29	14	s
121	U	1	7.5	5.5	2.5	17	12	m
122	P.L.	3	8	5.5	3	20	7	w
123	U	1	13	7.5	5	11	15	w
124	P.L.	2	7	6	2.5	32	18	s
125	Di	1	14	8	6	18	16	m
126	U	1	12	5.5	5	20	15	m
127	R	2	10	5	4	18	21	w
128	U	1	9	6	3	18	12	w
129	U	2	14	8	6	29	24	v.w.
130	U	1	9	5	2	17	12	w
131	P.L.	1	8	6	1.5	24	9	m
132	U	1	21	8	7.5	22	25	m
133	Dw	1	13	8	6.5	15	17	s
134	R	5	6.5	6	4	27	35	m
135	U	1	10	6	5	20	12	w
136	U	1	7	6.5	3	17	10	w
137	R	5	6.5	5.5	3	30	23	w
138	U	3	5.5	5	3.5	23	16	m
139	U	1	11	6.5	3	21	16	m
140	U	1	9	3.5	2	25	14	m
141	U	1	9	5	4.5	37	25	m
142	U	1	8	6.5	3	27	18	s
143	P.L.	2	11	9	6	31	12	s
144	U	2	5.5	3.5	2	19	16	w
145	U	1	15	7	4.5	25	18	s
146	Dw	1	17	7.5	5	12	19	s
147	R	4	6.5	5	3	18	24	w
148	U	1	9	5	2	19	13	m
149	U	1	10	5	3	13	14	m
150	U	1	12	7	5	24	15	s
151	U	1	14	7.5	3.5	27	22	w
152	R	4	6	3.5	2	20	28	w
153	P.L.	2	7.5	5.5	3	37	17	m
154	T.L.	3	7	6	4	20	21	v.w
155	U	1	10.5	6	5	16	15	m
156	R	7	7	4	2	26	21	m
157	U	2	8	6	4	19	20	s
158	U	1	6	5.5	3.5	19	13	m
159	U	1	6	4	2.5	14	12	s

TABLE B1. (continued)

Plot no./ cluster no.	Cluster morphology	Number of anchors*	Size of anchor axes			Cluster size		Cluster strength
			Long (cm)	Intermediate (cm)	Short (cm)	Length (cm)	Width (cm)	
160	U	1	6.5	6	3	22	21	m
161	U	3	11.5	9	4.5	18	27	s
162	R	4	8	4	2	17	27	w
163	U	2	10	5	4	23.5	23	m
164	U	1	14	5	3	14.5	15	m
164a	Dw	1	12	7	6.5	12	14	m
165	U	1	12	8	4	15	18	m
<u>Plot 1</u>								
31	Dw	1	16	8	5	12.5	18.5	w
32	Di	2	14	8.5	4.5	22	16	m
33	U	1	11	7.5	4.5	22.5	16	s
34	U	3	13	8.5	7	30	14	m
35	P.L.	4	11	5	3	25	14	m
36	Dw	1	26	12	10	29	26	v.w.
37	U	1	15.5	8.5	5	11.5	15.5	w
37a	U	4	15.5	8.5	5	47.5	15.5	m
38	Di	4	11.5	7	3.5	29.5	26.5	m
39	R	1	19	10	5	23	21	w
40	R	5	12	8.5	4	36.5	27	m
41	U	4	8	7.5	5	28	27	m
42	U	1	17	11	6.5	30	21	w
43	Di	1	11.5	7.5	6	15	15	w
44	U	1	13	9.5	7	23	17	m
45	R	7	10	5	4	23	22.5	m
175	R	3	13	8	7	36	22	w
176	U	1	11.5	5	3.5	17	15	m
177	T.L.	4	5	4.5	4	23	35	m
178	R	3	12	6.5	5.5	37	33	m
179	U	1	15	10	8	23	23	w
180	P.L.	3	10	6	4	31	12	m
181	Di	1	12	8.5	6	16	23	w
181a	Di	1	9.5	8	5.5	15	15	w
182	U	3	6.5	5	3	20	19	m
183	U	1	16.5	8	3	34	21	w
184	T.L.	4	15	8	3	38	65	s
185	U	1	11	4.5	4	17	18	w
186	U	1	11.5	6.5	4	21	13	w
187	R	4	8	5	3.5	25	19	m
188	R	5	8	7	5	32	37	w
189	U	2	9.5	5	4	21	20	w
190	P.L.	3	10	5	3	3	47	m

TABLE B1. (continued)

Plot no./ cluster no.	Cluster morphology	Number of anchors*	Size of anchor axes			Cluster size		Cluster strength
			Long (cm)	Intermediate (cm)	Short (cm)	Length (cm)	Width (cm)	
191	T.L.	4	13	8	5	18	63	w
192	R	3	9	8	4	24	35	s
193	R	3	10	6.5	5	30	22	m
194	R	4	9	7	3.5	38	26	m
195	U	1	14	6	5	15	18	w
196	R	3	9	5	4	23	23	m
197	Di	1	19	8	4.5	19	23	m
198	U	2	8.5	5.5	3	19	18	w
199	U	1	6	4	2	20	10	m
200	Di	1	18	9	4	16	20	w
201	U	1	11	6	4.5	14	13	w
202	U	1	9	8	7	23	14	m
203	U	1	7	5	2	15	11	m
204	Di	1	18	7	3	20	23	m
205	U	1	13	8	7.5	27	16	m
206	R	7	10	9	4	38	40	m
207	T.L.	3	11	5	3.5	15	18	m
208	U	1	14	9	6	25	20	m
209	P.L.	3	12	7	6	41	21	m
210	U	1	7	4	2	17	12	w
211	U	2	9	7	5	30	19	w
212	U	1	10.5	6.5	6	22	17	m
213	U	1	24	9.5	6.5	23	28	s
214	Di	1	9	9	6	23	15	m
201	U	1	11	6	4.5	14	13	w

Note: Clusters 1-45 were part of original cluster evolution dataset. Dw = downstream triangle, Di = diamond, U = upstream triangle, P.L. = parallel line, R = ring, T.L. = transverse line, m = moderate, w = weak, s = strong, v. w. = very weak.

*For clusters that had more than one anchor clasts, the average size of the anchors is presented.

TABLE B2. CLUSTER CHARACTERISTICS AT SITE 2, ENTIAT RIVER

Plot no./ cluster no.	Cluster morphology	Number of anchors*	Size of anchor axes			Cluster size		Cluster strength
			Long (cm)	Intermediate (cm)	Short (cm)	Length (cm)	Width (cm)	
<u>Plot 1</u>								
1	U	2	16.5	9	8.5	20	24	m
2	Di	1	35.5	18	10	34	40.5	s
3	Di	1	31	24	9	52	37	w
4	Di	1	42.5	37	10	52	45	m
5	Di	1	23.5	17	7	30	23.5	s
6	U	1	19	13	10.5	33	18	m
7	Di	1	40	29.5	15	58	44	m
8	U	1	9	7	4	14	12	w
9	P.L.	3	10	8	5	34	10	m
10	R	4	15	10.5	5	24	27	w
11	P.L.	2	11	7.5	5	31	17.5	s
12	U	2	18.5	12.5	6.5	31	26.5	w
13	U	1	20.5	11.5	4	37.5	20.5	s
14	R	4	8	6.5	4	24	29.5	w
15	U	1	12.5	9	5	30	21.5	s
16	U	1	8.5	7	4	15	9	m
17	P.L.	1	6.5	3	2	23	8	m
18	U	1	15	8	3.5	23	16	s
19	U	1	7	6	3	9	7	w
20	R	4	8.5	7.5	5.5	28	28	s
21	T. L.	1	9	6.5	3	17	9	m
22	U	1	13	8	5	15	13	w
23	U	1	16	4.5	4	24	16	s
24	T. L.	1	9	4.5	4	20	12	s
25	R	3	12	8	4	31	35	w
26	U	2	21	16	10	4	46	s
27	U	1	24	18	10	30	24	w
28	U	1	12.5	9	8	24	15	s
29	P.L.	1	10	7	4.5	23	10	s
30	U	1	16	12.5	10	18	16	w
31	Di	1	25	15	16	35	22	w
32	U	1	20	16	7	28	26	m
33	U	1	8	5	5	19	18	m
34	U	3	12	8	5	26	15	m
35	U	2	8	6	3.5	22	19	m
36	U	1	14	10	5	38	21	w
37	R	6	10	9	5	48	35	s
38	U	2	15	10	6	30	38	s

TABLE B2. (continued)

Plot no./ cluster no.	Cluster morphology	Number of anchors*	Size of anchor axes			Cluster size		Cluster strength
			Long (cm)	Intermediate (cm)	Short (cm)	Length (cm)	Width (cm)	
39	Di	1	24	20	19	32	24	w
40	U	1	25	19	11	44	38	m
41	U	1	16.5	15.5	9	33	33	m
42	U	1	27	16	9	40	27	m
43	P.L.	1	20	15	8	52	15	m
44	R	4	16	9	4	38	64	m
45	U	1	20	14	8	31	28	s
46	U	1	17	13	13	30	20	s
47	U	1	15	14.5	10	24	20	w
48	Di	1	24	15.5	7	28	24	m
29a	U	1	11	10.5	4.5	24	20	m
49	P.L.	3	21	10	5	53	25	s
50	U	2	13	7	6	31	30	s
51	R	4	15	9	4	31	48	w
52	U	1	15	11	5	20.5	18	w
53	U	1	15.5	8	6	16	23	m
54	U	2	14.5	19.4	18.0	35	28.5	s
55	U	1	17	10	9	30	17	m
56	P.L.	7	10	7	5	44	13	s
57	P.L.	3	8	7	15	19	10	w
58	U	1	13	9	9	13	13	v.w.
59	U	2	19.3	15.9	4.5	16	23	w
60	Di	2	22	13.5	4	21	26	w
61	U	2	8.5	6.5	2.5	15	18	w
62	U	1	13	6	5	19	16	m
63	Di	1	23.5	9.5	9	19	23.5	w
64	P.L.	3	10	7	5	30	14	m
65	R	2	6	3	3	19	22	w
66	T.L.	2	10	8	7.5	17	36	m
67	U	1	14	10	4.5	21	18	m
68	U	1	22	14	7	46	27	m
69	R	6	14.5	12	9	76	34	s
70	R	4	11.5	6	5	28	17	w
71	U	1	6	6	4	20	14	w
72 + 73	R	6	14	10	5	58	47	s
74	U	2	7	5	2	19	20	w
75	U	1	13	11	7	29	17	m
76	U	1	15	12	7	35	19	m
77	P.L.	4	16	12	10	58	18	s
78	U	1	16	15	6	38	30	m
79	U	1	23	20	13	46	38	w

TABLE B2. (continued)

Plot no./ cluster no.	Cluster morphology	Number of anchors*	Size of anchor axes			Cluster size		Cluster strength
			Long (cm)	Intermediate (cm)	Short (cm)	Length (cm)	Width (cm)	
78	U	1	16	15	6	38	30	m
79	U	1	23	20	13	46	38	w
80	T. L.	2	20	14	11	45	25	w
81	P.L.	1	23	16	8	30	27	w
82	P.L.	1	15	12	5	40	20	m
83	P.L.	1	9	9	4	23	9	w
84	DW	1	17	13	10	22	22	w
85	U	1	23	17	8	27	33	v.w
86	Di	3	12	11	6	30	42	w
87	U	2	16	13	9	38	30	m
88	P.L.	1	14	11	7	25	24	w
89	U	1	15	7	4	23	23	s
124	U	2	19.5	16.5	15	27	40	w
123	P.L.	3	20	13	10	50	20	w
122	U	1	20	18	10	33	36	m
121	Dw	1	24	14.5	9	26	24	m
125	U	1	18	10	9	28	30	m
126	Dw	1	22	17	15	31	31	m
127	U	1	17	15	8	23	20	v.w
128	P.L.	4	11	10	5	23	26	w
120	R	1	14	10	6	27	23	w
119	P.L.	1	10	9	6	24	13	v.w
90	R	3	12	8	4	21	20	w
91	U	2	8	6	4.5	16	22	m
92	U	1	10	7	4	18	12	w
93	P.L.	1	12	6	4	38	17	m
94	U	2	13	10	7	29	33	m
95	P.L.	6	10	8	4	46	17	m
96	U	1	13.5	10	9	18	17	m
97	U	1	10	10	6	19	17	m
98	U	1	9	8	3.5	25	14	m
99	Di	1	9	8	7	21.5	11	m
100	U	1	10	9.5	4.5	17	16	w
100	U	1	10	9.5	4.5	17	16	w
101	U	2	7.5	6	3	16	20	m
102	U	1	11	9.5	8	18.5	16	w
103	P.L.	1	10	11	8	40	15	w
104	Di	2	8.5	4.5	4	19	18	w
105	U	1	17	7	5.5	12	17	w
106	U	1	15	8	6	17	14	w
107	P.L.	1	6	3	2	25	8	w

TABLE B2. (continued)

Plot no./ cluster no.	Cluster morphology	Number of anchors*	Size of anchor axes			Cluster size		Cluster strength
			Long (cm)	Intermediate (cm)	Short (cm)	Length (cm)	Width (cm)	
108	Di	1	16	10	9	25	24	m
109	U	1	23	18	7	28	27	w
110	U	1	12	8	7	25	17	m
111	U	1	15	8	4.5	16	17	w
112	U	1	24	14	10	32	29	w
113	U	1	6	5	3	19	15	w
114	U	1	20	13	3	24	27	w
115	Di	1	23	21	13	27	21	w
116	Di	1	20	16	10	25	36	w
117	U	1	26	21	9	38	33	m
118	U	2	10	8	5	21	20	m
129	P.L.	5	20	13	7	86	24	s
130	U	1	28	25	13	56	33	m
131	Dw	1	24	15	8	22	24	m
132	Di	1	23	9	8	29	31	m
<u>Plot 2</u>								
1	U	1	9	7	4	19	13	w
2	Di	1	11	10	3.5	15	11	w
3	U	1	7	5	3.5	21	9	w
4	R	4	12	8	5	36	33	m
5	Di	1	13.5	10	4	20	15	v.w.
6	Di	1	15	10	11	23	17	w
7	U	1	10	5	3	17	12	w
8	Di	1	10	8	3	17	24	w
9	T.L.	3	10	8.5	2	42	22	m
10	T.L.	3	9	7	4.5	35	25	m
11	U	1	12	11.5	6	17	16	w
12	U	1	19	11	9	17	25	v.w.
13	P.L.	1	7	5.5	5	19	12	m
14	U	1	11	10	5	26	17	m
15	P.L.	1	9	5	4	18	13	w
16	U	1	6	4.5	4	16	14	m
19	U	1	12	10	7	13	14	v.w.
20	U	2	13	7	3.5	15	27	m
21	R	5	12	7.5	4	27	32	s
22	U	1	14	8	5	24	14	w
23	Di	1	20	11.5	4	23	24	m
24	U	1	12	8	5	25	24	w
25	U	2	6	4	3.5	19	22	s
26	Di	1	24	18	14	48	46	s

TABLE B2. (continued)

Plot no./ cluster no.	Cluster morphology	Number of anchors*	Size of anchor axes			Cluster size		Cluster strength
			Long (cm)	Intermediate (cm)	Short (cm)	Length (cm)	Width (cm)	
27	Di	1	20	9	7	23	20	m
28	U	1	17	10	6	22	18	m
29	Di	1	12	8	4	20	17	w
30	U	2	7	3.5	2	28	19	s
31	T.L.	6	13	10	5	30	92	s
32	P.L.	3	11	9	4	30	20	m
33	U	2	9	5.5	3.5	25	23	m
34	T.L.	3	10	5	2	21	27	s
35	U	1	14	8	3.5	18	16	w
36	U	2	9.5	5.5	4	25	17	w
37	Di	1	14	6	5	16	13	w
38	U	1	13	8.5	5	22	17	m
39	P.L.	3	8	7	6	29	22	m
40	U	1	9	7	4	17	9	w
41	P.L.	4	15	12.5	8.5	46	48	s
42	Dw	1	18	17	9	29	21	s
43	U	1	14	10	7	31	12	w
44	U	1	18	9	8	17	22	w
45	U	3	4	2	1	15	15	w
46	Di	1	10	7	6	19	17	w
47	R	4	13	9	4	35	30	m
48	U	1	10	8	3	24	17	w
49	U	1	10	9	7	15	13	m
50	U	1	19	10	6	27	22	w
51	U	2	5	4	2	19	15	w
52	Di	1	15	6	3	19	15	w
53	U	2	7	5.5	2	20	18	m
54	P.L.	3	7	6.5	2	22	13	w
55	U	2	8	5	3.5	16	17	w
56	U	1	16	11	4	27	19	m
57	U	1	8	7	3	24	15	w
58	P.L.	3	8	5	6	22	10	m
59	U	2	9	6	4	18	21	s
60	R	4	8	6	4	29	27	m
61	Di	1	19	10	9	22	20	m
62	U	1	12	6	5	18	12	w
63	Di	2	14.5	9	5	29	27	m
67	U	2	9	6.5	4.5	27	19	m
68	U	1	9	7	5	23	9	w
69	U	1	8	7	5	16	11	w

TABLE B2. (continued)

Plot no./ cluster no.	Cluster morphology	Number of anchors*	Size of anchor axes			Cluster size		Cluster strength
			Long (cm)	Intermediate (cm)	Short (cm)	Length (cm)	Width (cm)	
70	Di	1	12	9	6	22	21	m
71	U	1	22	11	3	26	24	w
72	Di	1	15	12	8	26	14	w
73	P.L.	3	11	7	4	23	12	m
74	P.L.	4	9	7	4	25	18	s
75	U	1	9.5	7	5	26	9	w
76	R	3	10	8	5	27	23	m
77	U	1	12	7.5	4	23	20	m
78	U	1	10	8	4	26	16	m
79	U	1	10	6	4	17	12	w
80	U	1	18	9	5	21	20	m
81	Di	1	17	12	5	20	21	w
82	U	1	9	8	3	18	12	w
83	U	1	10	8	4	19	17	m
84	R	3	7.5	5.5	4	23	21	w

Note: Clusters 1-45 were part of original cluster evolution dataset. U = upstream triangle, Di = diamond, P.L. = parallel line, R = ring, T.L. transverse line, Dw = downstream triangle, m = moderate, w = weak, s = strong, v.w. = very weak.

*For clusters that had more than one anchor clasts, the average size of the anchors is presented.

Appendix C

Compilation of Previous Cluster Characteristic Data

TABLE C1. PREVIOUS FIELD-BASED STUDIES FEATURING CLUSTER CHARACTERISTICS										
Source and river system	Type of river	D_{50} (cm)	Mean channel width (cm)	Slope	Mean annual peak flow ($m^3 s^{-1}$)	Cluster length (cm)	Cluster width (cm)	Mean diameter of anchor clasts (cm)	Cluster density (no./ m^2)	Abundant cluster type
Brayshaw, (1984)										
Wye, UK	S.B.	2.3	9.0	N.D.	N.D.	24.5	17.1	N.D.	N.D.	N.D.
Turkey Brook, UK	F.B.	1.5	2.5	N.D.	N.D.	13.2	9.2	N.D.	N.D.	N.D.
Widdale Beck, UK	W.R.	5.2	10.0	N.D.	N.D.	48.1	23.1	N.D.	N.D.	N.D.
Biggs et al., (1997)										
North Kowai, NZ	H.W.	3.7	4.8	0.028	0.38*	N.D.	N.D.	29.9	0.075	N.D.
Woodshed, NZ	H.W.	1.2	7.4	0.005	0.03*	N.D.	N.D.	29.1	0.089	N.D.
Timber, NZ	H.W.	2.5	4.9	0.041	0.26*	N.D.	N.D.	26.5	0.078	N.D.
West Kowai, NZ	H.W.	6.4	4.9	0.018	1.13*	N.D.	N.D.	33.8	0.172	N.D.
Bowyers, NZ	H.W.	2.4	9.4	0.015	0.67*	N.D.	N.D.	45.4	0.214	N.D.
Kyeburn, NZ	H.W.	6.9	0.3	0.019	0.09*	N.D.	N.D.	21.2	0.167	N.D.
Rough, NZ	H.W.	4.9	4.8	0.040	0.31*	N.D.	N.D.	32.5	0.279	N.D.
Slaty, NZ	H.W.	6.4	12.7	0.006	0.01*	N.D.	N.D.	30.0	0.067	N.D.
Camp, NZ	H.W.	1.3	9.4	0.014	0.62*	N.D.	N.D.	33.2	0.068	N.D.
Victoria, NZ	H.W.	8.3	5.0	0.054	0.45*	N.D.	N.D.	40.0	0.165	N.D.
Granity, NZ	H.W.	5.3	1.6	0.050	0.18*	N.D.	N.D.	26.8	0.079	N.D.
Sams, NZ	H.W.	6.9	6.1	0.025	0.20*	N.D.	N.D.	33.4	0.138	N.D.
Reid et al., (1992)										
A. Frijoles, NM	G.B.	0.072	24.0	0.018	2.8	N.D.	N.D.	N.D.	N.D.	N.D.
Farma River, Italy	G.B.	6.4	19.0	0.009	N.D.	N.D.	N.D.	N.D.	N.D.	N.D.
Seale's Brook, Quebec	G.B.	7.5	N.D.	0.050	5.9	N.D.	N.D.	N.D.	N.D.	N.D.
Turkey Brook, UK	F.B.	1.5	3.3	0.006	7.1	N.D.	N.D.	N.D.	N.D.	N.D.

TABLE C1. (continued)

Source and river system	Type of river	D_{50} (cm)	Mean channel width (cm)	Slope	Mean annual peak flow ($m^3 s^{-1}$)	Cluster length (cm)	Cluster width (cm)	Mean diameter of anchor clasts (cm)	Cluster density (no./ m^2)	Abundant cluster type
<u>Wittenberg, (2002)</u>										
Chirdon Burn, UK	S.M.	8.0	N.D.	0.009	60	N.D.	N.D.	28.5	N.D.	Diamond
Eggleshope Beck, UK	S.M.	6.5	N.D.	0.015	6	N.D.	N.D.	N.D.	N.D.	Diamond
Harwood Beck, UK	S.M.	7.8	N.D.	0.020	17	N.D.	N.D.	N.D.	N.D.	Diamond
Harthope Beck, UK	S.M.	8.1	N.D.	0.010	37	N.D.	N.D.	N.D.	N.D.	Diamond
<u>Strom et al., (2004a)</u>										
American, US-site 1	S.M./ G.B.	4.7	N.D.	0.004	45.4	42	30	N.D.	N.D.	Diamond/ upstream triangle
AMERICAN, US-SITE 2	S.M./ G.B.	6.1	30.0	0.003	45.4	35	26	12	N.D.	Upstream triangle
<u>This study</u>										
Site 1	S.M./ G.B.	3.8	18.0	0.007	80.0	22.0	21.0	9.0	0.7	Upstream triangle
Site 2	S.M./ G.B.	5.9	17.0	0.009	80.0	28.0	25.0	11.0	1.5	Upstream triangle

Note: S.B. = slate-bed river, F.B. = flint-bed river, W.R. = well-rounded gravel-bed river, H.W. = headwater stream, G.B. = gravel-bed river, S.M. = snow-melt dominated river, N.D. = no data.